UNIVERSITA' DEGLI STUDI DI TORINO

DEPARTMENT OF MEDICAL SCIENCES

PhD PROGRAMME IN EXPERIMENTAL MEDICINE AND THERAPY

CYCLE: XXXVI

THESIS TITLE: PRESENCE, COMPOSITION, AND NEUROINFLAMMATORY CORRELATES OF THE CEREBROSPINAL FLUID VIROME IN ANTIRETROVIRAL-TREATED PEOPLE WITH HIV ACROSS DIFFERENT METAGENOMIC PIPELINES

THESIS' AUTHOR: DR. MATTIA GIOVANNI CARLO TRUNFIO

SUPERVISOR(S): PROF. GIOVANNI DI PERRI, PROF. ANDREA CALCAGNO

PhD PROGRAMME CO-ORDINATOR: PROF. PASQUALE PAGLIARO

ACADEMIC YEARS OF ENROLMENT: 2020-2021, 2021-2022, 2022-2023, 2023-2024

CODE OF THE SCIENTIFIC DISCIPLINE: MED/17 – INFECTIOUS DISEASES

Index

Background

1. Human Virome in Health and Disease: focus on the Central Nervous System

Human beings are holobiont organisms: each individual hosts a variety of living bacteria, virus, fungi, and archaea, collectively known as microbiota. In this complex homeostatic ecosystem, predatory interactions coexist with cooperative dynamics [1].

Glossary

Microbiota = the assemblage of genomes of microorganisms (bacteria, viruses, fungi) detected in a defined ecosystem (e.g., skin, CSF).
Microbiome = the assemblage of genomes of microorganisms found in the whole human body.
Virome = the viral component of the (human) microbiome.
Phageome = the viral component of the (human) virome represented by bacteriophages.
Bacteriome = the bacterial component of the human microbiome.
We will use -biome and -biota interchangeably, unless otherwise specified.

Less known than the bacteriome, virome is the most diverse and abundant collection of human symbionts. It mainly consists of bacteriophages (estimated to be 10^{16} within each human host) - the most common being lysogenic families of the orders *Caudovirales, Tubulavirales,* and *Petitvirales* [2,3]. In lower proportions lytic phages and eukaryotic viruses (e.g., *Herpesviridae* and *Polyomaviridae*) are also permanent members of the “human ecological niche” [2]. Virome is enriched during life, affected by age, health, and immune status, and by genetic and environmental determinants, and shows relatively stable intra-individual composition overtime and a good extent of inter-individual variability [2].

Most of our knowledge about virome comes from the gut, due to translational approaches from bacteriome research and the easiness of sampling. More recently, the human virome of other body compartments has received more attention, including niches historically thought to be sterile: modern molecular techniques have found viral communities inhabiting the respiratory and urinary tract, the blood-stream, and notably the central nervous system (CNS) [2,4,5].

As the concept of “normal” microbiome is evolving, we are getting more familiar also with the existence of a “normal” or “balanced” virome, where multidirectional interactions between viruses and bacteria contribute to shape the resident microbial consortia along with the host immune system [2,3,6,7]. Consistent associations between virome composition and human health have been found, such as shifts in the phageome observed in inflammatory and autoimmune diseases [8,9]. Nevertheless, the causality remains elusive. Plausible hypotheses consider health and disease as the resulting sum of interactions within and

between microbial consortia that modulate immune responses to disease-specific internal and external triggers [10,11].

A high-risk high-reward challenge is to understand whether human virome is involved in CNS inflammatory disorders, neurodegenerative processes, or in modulating cognitive functions and mood [8,9,12]. Fingerprint patterns of gut microbiome are linked with major depressive disorders and response to antidepressants [13]. Similarly, specific *Caudovirales-Microviridae* ratio in the gut of humans, mice, and drosophila runs in parallel to cognition by possibly hijacking the bacterial host metabolism and resulting in different performance at executive functions and memory [14]. To date, most of the research linking microbiome and the CNS is by far driven again by investigations on the human gut and bacterial consortia. The idea of a gut-brain axis has been proposed to explain the several associations between gut microbiome composition and mental health outcomes (e.g, depression, neurodegenerative disorders, cognitive performance) in PWH [15–19] and in those without [20–25]. In both the populations, evidence suggest that the gut bacteriome can affect brain functions through: 1) inflammation of the CNS through chronic low-level stimulation of the innate immune system by structural bacterial components (e.g., lipopolysaccharides) and bacterial translocation through increased intestinal permeability; 2) dysfunctional adaptive immune response due to molecular mimicry (e.g., immune cells reacting to bacterial antigens that mimic antigens produced by the human body); 3) transfer of gut bacterial signals between the enteric nervous system and the brain through the vagus nerve; 4) gut bacteria production of hormones, neurotransmitters, and metabolites that may either directly or indirectly affect the brain [15–17]. However, virome is a direct controller of the microbiome composition, through predation and co-adaptation, and has its own immunomodulatory properties and effects [7,26]. Therefore, addressing only the bacterial component of gut microbiota may be too limited to fully understand mechanisms and functions of the gut-brain axis. Secondly, the existence of a cerebrospinal fluid (CSF) virome in healthy individuals has been described for the first time only in the 2019 [4], but since then no study has ever been performed to assess whether and how this local ecosystem can affect the CNS.

2. Human Virome, HIV infection, and the Central Nervous System

In the fifth decade of the HIV pandemic, the immune phenotype of people with HIV (PWH) is successfully no longer represented by severe immune deficiency. Thanks to antiretroviral therapy (ART), people engaged in HIV-care do not develop overt clinical manifestations caused by co-infecting opportunistic microbes. Rather than an immune deficiency disease, treated HIV infection has shifted into an immune dysregulation condition. In fact, compared

to the general population, the achievement of an optimal quality of life for PWH is threatened by chronic inflammation, immune activation, and immune senescence that persist at higher levels compared to people without HIV despite viral suppression [27,28]. All these come along with increased incidence of cardiovascular and malignancy events, mood and cognitive disorders, and complex syndromes such as frailty [29–33].

In this regard, other chronic infections (e.g., *Herpesviridae*, HBV, HCV) fuel immunological phenomena largely overlapping those observed in HIV infection, and the additive effects of viral co-infections upon HIV-associated immune dysregulation is robustly acknowledged [34–36]. However, the lens has been so far focused on eukaryotic viruses only, and the role of the whole virome in shaping HIV infection and its interactions with the immune system has never been investigated. Previous studies have described how human virome (mostly in the gut and blood) changes by HIV progression [37–40], as it is a passive bystander at the mercy of the overbearing retrovirus. Following the advancement in discoveries on human virome, multidirectional interactions between HIV and other members of the human ecosystem (e.g., prokaryotic viruses -e.g. bacteriophages- and human endogenous retroviruses) are also biologically plausible.

The clinical presentation of HIV infection in the CNS has changed substantially since the pre-ART era, and amidst all, the progression to AIDS dementia drastically fell [41]. Despite this incredible success, the present epidemiology still strikes the eye. The global prevalence of mild asymptomatic or mildly symptomatic HIV-associated neurocognitive disorders (HAND) worryingly ranges between 20 and 50% [42]. Even more worryingly are the reports of up to 58% increase in risk of dementia of any type in older PWH on ART compared to matched HIV-negative controls without HIV [43–45].

The pathogenesis of HAND is heterogeneous, resulting in a complex spectrum of phenotypes. Extensive research has been devoted into understanding whether HIV infection causes accentuated and/or accelerated brain ageing [46]. However, after accounting for the direct effect of the virus, ART toxicity, normal and accelerated or accentuated aging, and comorbidities (e.g., cerebrovascular injury, drug use, CNS opportunistic infections), none of the best disease models has been able to explain the entireness of pathogenesis of such a complication, and conflicting results have also been provided for each of the proposed contributing etiologies according to clinical settings, confounding factors, and variables investigated [46–57]. Meanwhile, a relevant contribution of inflammation in major and minor depressive disorders is rising from recent data in the general population [58–60], and a relevant causative role of inflammation in HIV-associated depression has also been

described [61], and overall, among the mechanisms underlying both HAND and HIV-associated depression, CNS inflammation is the stronger by evidence.

Activated B cells can reinforce CNS inflammation by producing immune globulins intrathecally [62]. The exact antigenic drivers have been poorly identified, and HIV represents about only 5% of the targets [62]. Chronic viral infections have been candidate triggers in other neuroinflammatory disorders, and data in PWH support the role of CMV and EBV CNS reactivation [63,64]. In this context, also bacteriophages can induce plasma cells to secrete anti-bacteriophage-specific immunoglobulins [3,6]. Whether changes in CSF virome following HIV infection or HIV-induced perturbations in the immune system could help at explaining why, even under viral suppression, PWH may experience abnormal intrathecal synthesis and neurocognitive deficit is worthy of efforts, considering the repeatedly reported association between elevated synthesis of immune globulins within the CSF and poorer neurocognition [62,65]. Of high relevance, the additive risk of brain injury, depression, or cognitive impairment in the presence of specific co-infections (eukaryotic viruses) was reported in the general population [66–70], and now it is also following in PWH [52,63,64,71].

A simplistic representation of the major pathways involved in neuro-HIV is depicted in Fig.1, together with examples of mechanisms acted by human bacteriophages that could intertwin with HIV physiopathology in the CNS.

Figure 1. Pathological features and mechanisms of HIV infection of the central nervous system and potential contributions of bacteriophages in shaping neuroHIV.

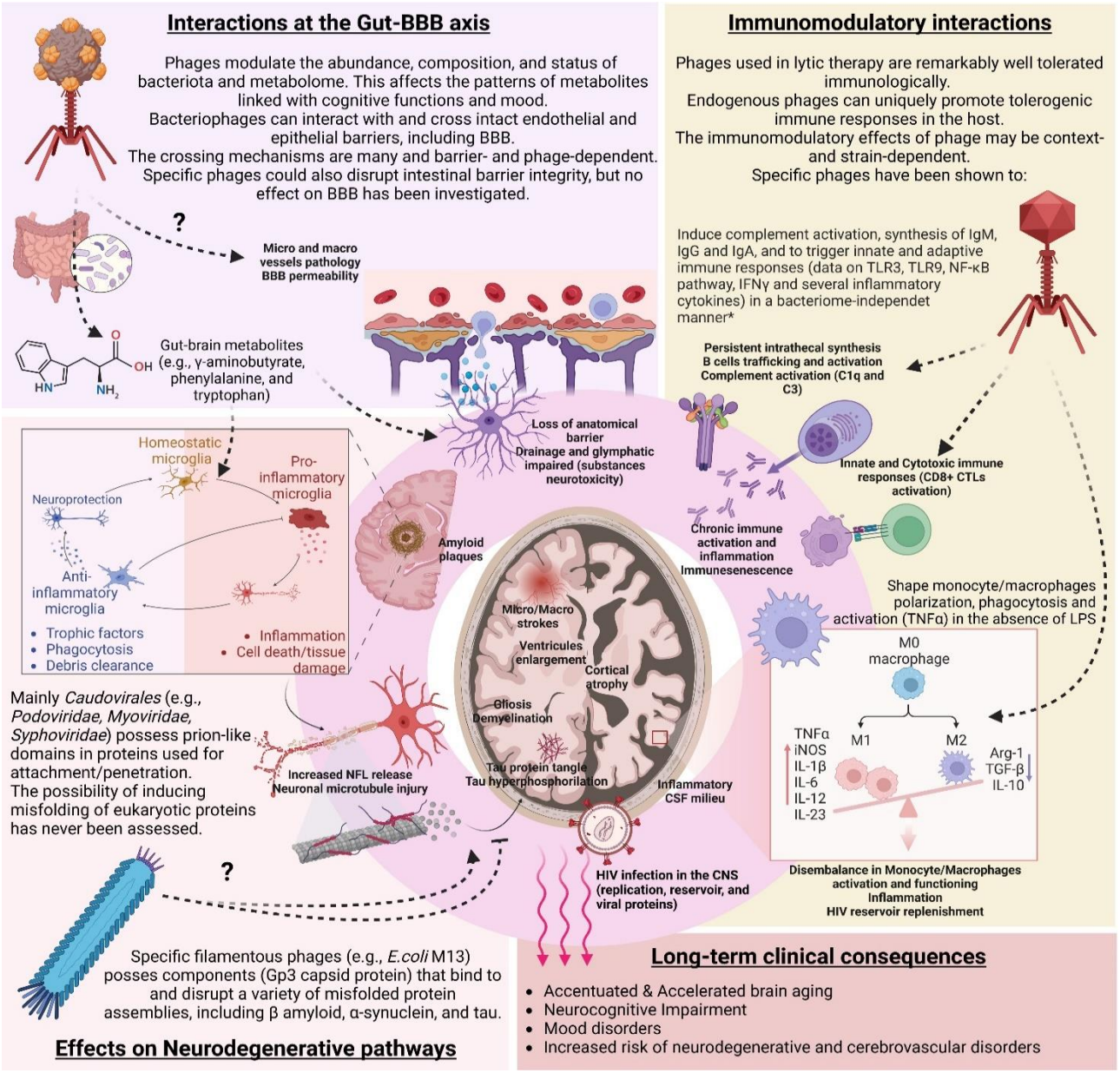

The core of the figure shows common and rarer consequences of treated (e.g., amyloid plaques deposition, increased gliosis, tauopathy, altered intrathecal synthesis and persistent immune activation, blood-brain barrier (BBB) permeability, astrocytosis, cerebral vessels pathology, mood, and cognitive disorders) and untreated HIV infections in the CNS (e.g., cortical atrophy, ventricles enlargement, demyelinating pathology, macrophages and CD8+ T cell infiltrates, dementia). The yellow box summarizes immunomodulatory properties of phages that may act on immune pathways involved in neuro-HIV. The violet box summarizes possible interactions between phages and HIV-mediated processes through the gut-BBB axis: mainly by enhanced mixture of blood and CSF microbiome and by the modulation of microbial translocation (in abundance and composition) and of gut peptides and substances produced by gut bacteriome that can easily pass through leaking barriers and can affect the functions of CNS cells. The pink box summarizes what are to date hypothesized mechanisms of interactions between phages and neurodegenerative processes (protein misfolding on a prion-like domino effect and deposition of protein tangles). Of note, studies assessing the potency and direction of the effects of phages on all the presented mechanisms are mainly in vitro or in animal models and the overall strength of evidence is weak; the same potency and direction may change between species and strains of phages and according to their relative abundance. Therefore, each candidate intersection between HIV and phages activity requires in human confirmation and could result in either enhancement or counteract of HIV activity. From Trunfio M. et al, manuscript under preparation.

3. Interactions between HIV and other viruses

Interactions between eukaryotic viruses and HIV have been reviewed elsewhere [34,35]. For example, robust evidence links the presence of some *Herpesviridae*, namely EBV and CMV, to larger HIV reservoir size and increased chronic inflammation [36,72]. Antigen-driven clonal selection and expansion of CD4+ T cell subsets harboring integrated HIV DNA represents one of the possible main mechanisms underlying this association [73].

Most interactions between HIV and viruses are mediated by the immune system: downregulation of MHC, induction and interference with cytokine signaling, expression of virus-encoded chemokine homologs and receptors, inhibition of apoptosis, and altered activation of the complement among the others [34,35]. Bacteriophages modulate all these mechanisms *in vitro* and *in vivo*, and can activate pathogen-associated molecular pattern molecules, such as Toll-like Receptor 9 (TLR9) and TLR3 [2,3,6]. Agonists for both these sensing receptors are under investigation in clinical trials for HIV cure since they showed moderate latency reversing effect and regulatory activity on HIV replication [74]. The divergence in responses to latency reversal agents between HIV reservoirs of different body compartments is multifactorial and not completely unraveled; whether a contribution to this difference is provided also by distinct inhabiting microbiomes should be considered in the light of the expanding possibilities in phage supplementation and therapy.

Likewise, no investigation on the contribution of the entire virome upon the HIV reservoir in its establishment and maintenance as ever been pursued, despite non-human data suggest links. By shaping CD4+ and CD8+ T cell activation, gut microbiota can condition the infectivity outcome of HIV exposure in primary human lamina propria cells in vitro [75]. Similarly, different susceptibility to SIV infection following the same intrarectal exposure has been documented in rhesus macaques and was correlated with different pre-exposure profiles of activation of rectal mucosa CD4+ T cells and differences in gut microbiota [76]. Even if both the studies assessed only the bacteriome of the gut, behind this it can be differences in gut virome as its role in bacteriome homeostasis is pivotal. In human, innate immunity can mediate natural resistance against HIV, and the key role of TLR9 activation and of the downstream production of antiviral factors in individuals that remain seronegative after HIV exposure has been described [77]. Short- or long-term trans-activation of TLRs that follows changes in local virome could represent an intersection point with unknown effects on HIV infectivity, replication, and persistence.

Collectively, these data support the biological plausibility of the conceptual model shown in Figure.2: when HIV is introduced in a new microbial niche, immediate outcomes (e.g., cell

infection, integration, inflammation) differ according to many variables, which include the immunological milieu shaped by the microbiome residing locally. Different ecosystems would result in different outcomes. As the infection progresses and ART is introduced, the characteristics of HIV reservoir and of chronic inflammation and immune activation could also be shaped by these same determinants (being therefore better defined as virome-associated inflammation, rather than HIV-associated inflammation).

Figure 2. The human virome of different body compartments can behave as distinct viral ecosystem with dynamic relationships within and between niches.

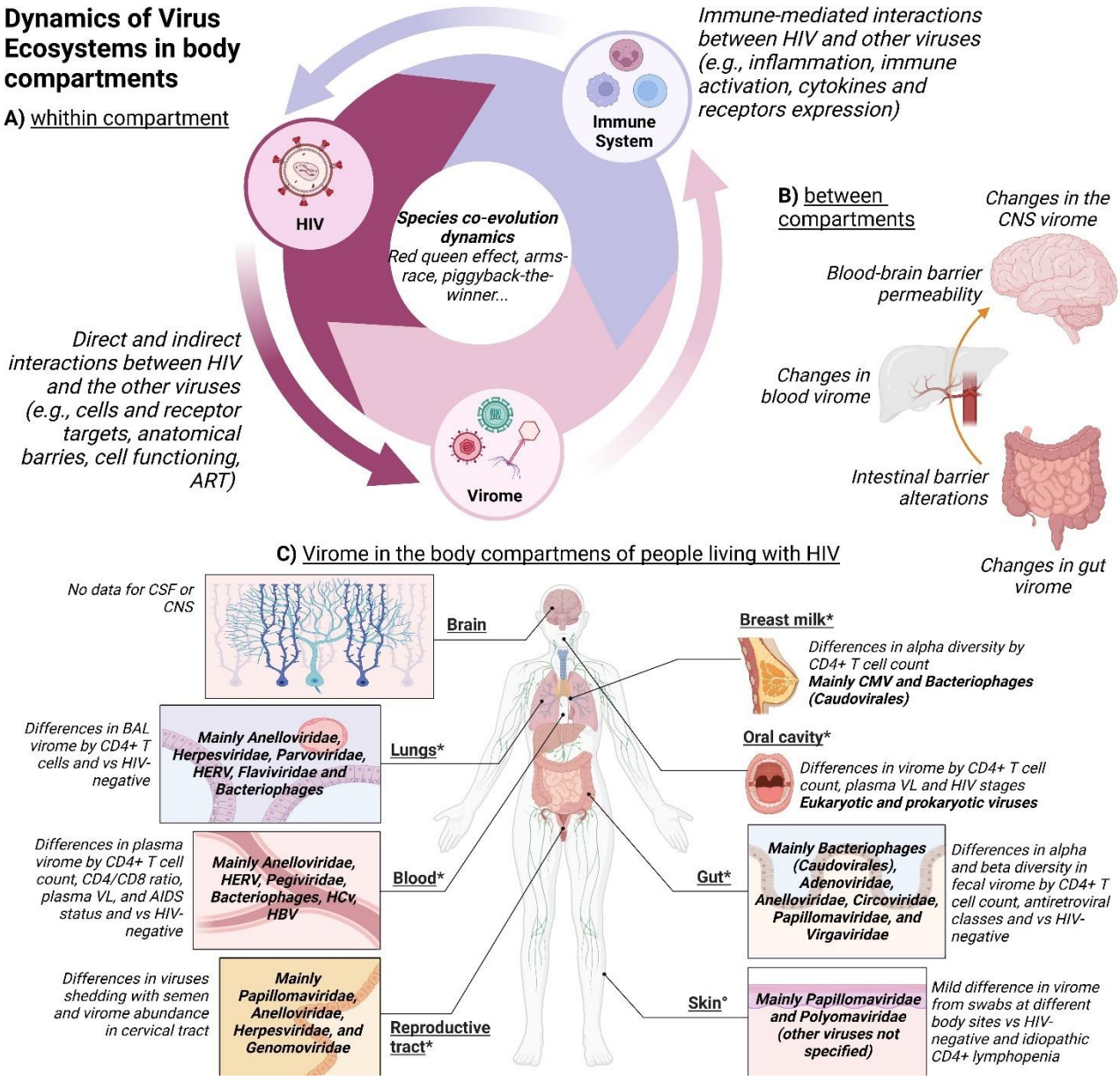

Section (A) shows the dynamic cycle that can take place between any each new virus (e.g., HIV) entering the ecosystem constituted by the balanced crosstalk between host immune system, local and trafficking cells and the virome. The interactive cycle is a model for both primary and chronic HIV infection, and can be read either way: from the newly introduced HIV affecting the immune system, and thereby the composition and abundance

of the virome, to this last one affecting the immunological (e.g., presence and composition of T and B cell subsets and their activation, macrophages abundance and functioning, activation of TLRs and other PAMPs) and non-immunological milieu (e.g., expression of (co-)receptors and proteins, metabolic activity, activation of transcriptional pathways, integrity of anatomical barriers) that will shape the adaptation of HIV in the body compartment. Once a balance will be reached, every change (e.g., ART introduction, new infections, progression to AIDS) will shape the cycle of interactions between these three major players. Section (B) highlights the fact that, despite each body compartment represents a microbiological niche with its own features and rules (in composition and relationships), each niche relates to the others and can be affected by processes that start outside, such as the link between gut, blood and CNS microbiome mediated by intestinal and BBB integrity. Section (C) summarizes all the available data on the virome composition and its changes by HIV-related parameters in the different body compartments of PLWH. Legend: ART, antiretroviral therapy; CNS, central nervous system; CSF, cerebrospinal fluid; VL, HIV viral load; BAL, bronchoalveolar liquid; HERV, human endogenous retroviruses; TLRs, Toll-like Receptors; PAMPs, Pathogen-associated molecular pattern molecules; BBB, blood-brain barrier; PLWH, people living with HIV. From Trunfio M et al., manuscript under preparation.

Tailored studies in cohorts of participants with primary HIV infection can investigate these hypotheses since the very beginning and to delve into the possibility of divergent evolutions of HIV virulence, persistence, and reactivation according to the local microbial landscape overtime. Finally, all these processes are molecular predictors of non-AIDS events. Therefore, the second step to validate our model would be the investigation of a possible role of different microbiome niches (in terms of abundance, composition, and changes overtime in CSF, blood, fecal etc. samples) in the development of clinical outcomes such as HAND, mood disorders, or cerebrovascular events.

4. Viral co-evolution: a Carroll's modern story

An additional field of research where the interplay between HIV and body microbial ecosystems may gain consideration is the study of HIV populations genetic divergence and compartmentalization.

Evolutionary theories from animal kingdoms have been previously translated to HIV infection to explain *quasispecies* selection, immunological escape, and development of ART resistance [78]. However, modern updates of the classical Neo-Darwinian model, such as the Red Queen theory (Figure 3), have been rarely considered [79], despite they may fit with recent discoveries from sequencing and co-evolutionary phenomena in the presence of co-infecting viruses, and with the fact that HIV successfully fixes mutations that provide it with survival advantages [80].

The Red Queen hypothesis encompasses many evolutionary theories that champion biotic interactions, a seemingly paradoxical challenge if applied to abiotic organisms such viruses, and briefly states that in all ecosystem omnipresent competitive interactions exist among taxonomic groups; these are continually changing, but they do not get relatively better in a competitive sense overtime, such that there is a zero-sum expectation (meant as,

evolutionary adaptive mutations happen, but when weighted with those of the other components of the same ecosystem, the net benefit is null and each component has always the same risk of extinction of the others) [81].

Subsequent modifications to the original theory have been made (Figure 3), and the work of Brockhurst et al. proposed different subtypes of interactions [82]: the “Chase Red Queen” involves several interacting component populations of different species, each evolving in varying directions due to distinct selective pressures and supposes that across the range of co-evolving species, the respective populations respond in different ways to the biotic milieu they experience [81,82]. As some of these populations will seek to escape co-occurring populations through the evolution of novelty, diversity within populations becomes reduced but divergence between populations increases as they spread across a multidimensional phenotypic space (Figure 3) [81,82].

Figure 3. Evolution of paradigms of microbial diversity

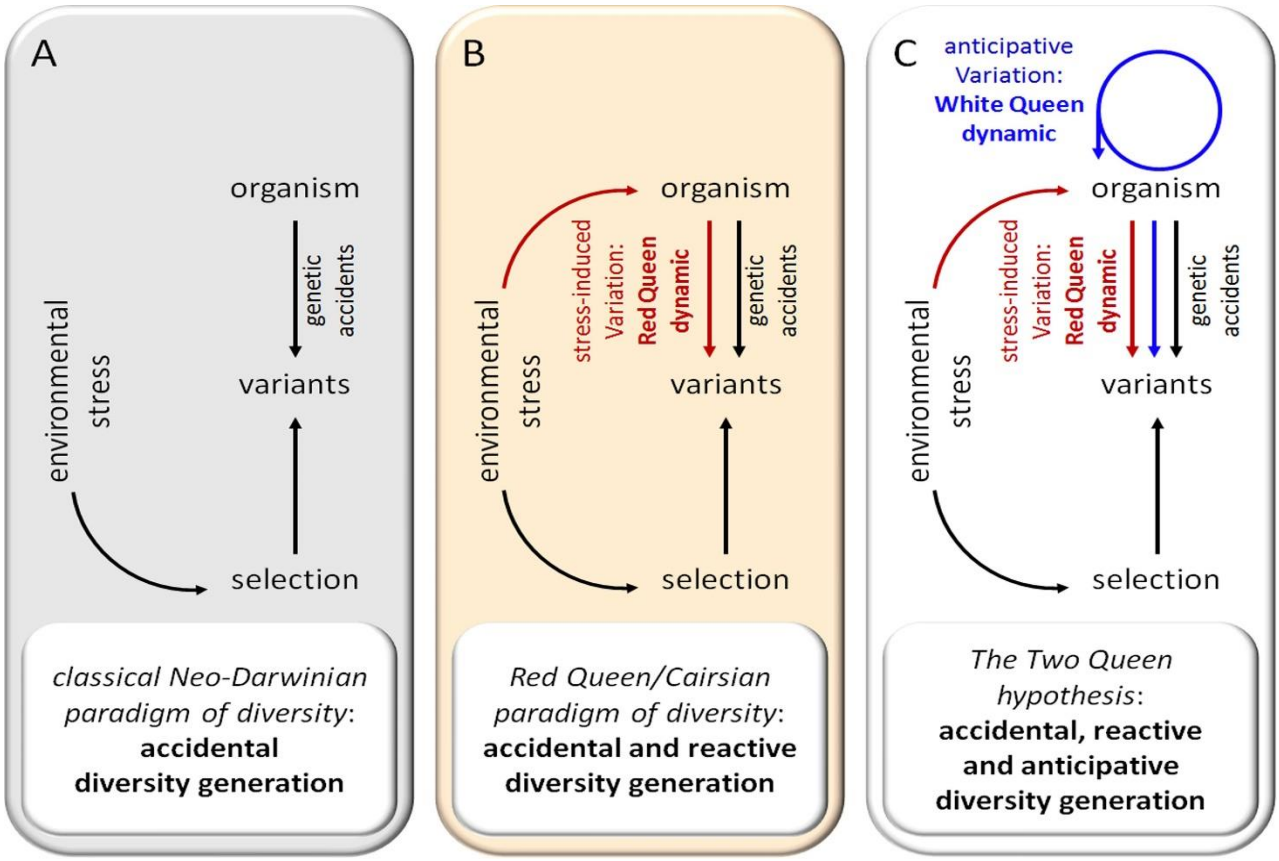

From Muraille E. Diversity Generator Mechanisms Are Essential Components of Biological Systems: The Two Queen Hypothesis. Front Microbiol. 2018 Feb 13;9:223. doi: 10.3389/fmicb.2018.00223 [83].

Many assumptions should be clarified before a direct translation of the above simplified presentation of this model into virus biology (e.g., how to consider *quasispecies* and strains, what is the reference to define evolutionary advantage), however we depicted in Fig.4 how

the “Chase Red Queen” model could resemble when applied to describe HIV-microbiome interactions.

Figure 4. The “Chase-Red Queen” paradigm of diversity for HIV evolution: integration of the role of human virome and bacteriome

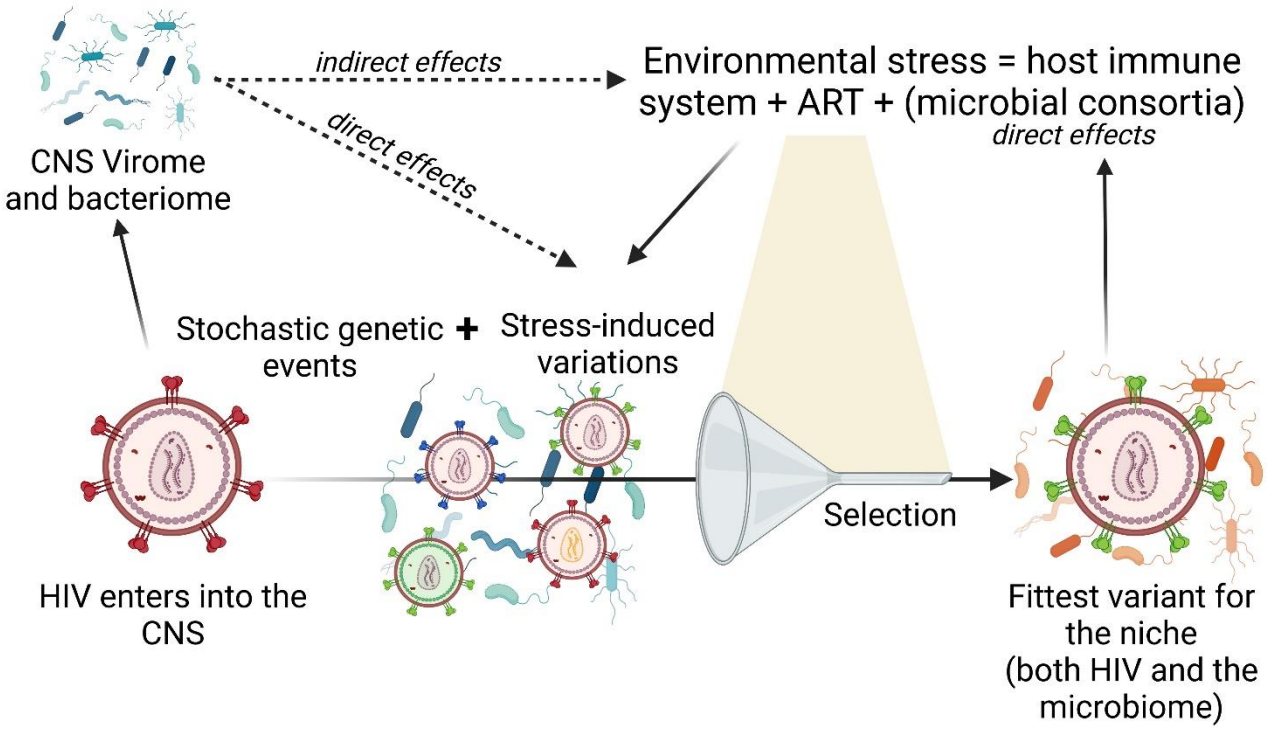

The Red Queen theory introduces a second source of dynamic evolution, the diversity generation reactive to environmental stressors (e.g., immune mediate-selective pressure) to the classical Neo-Darwinian paradigm of diversity based on accidental diversity generation (e.g., the stochastic errors introduced by the reverse transcriptase activity or recombinational strand transfer events for HIV). While there is consolidated evidence for this model when environmental stressors are represented by HIV-specific immune responses and antiretroviral drugs, no study has to date investigated possible additional effects (e.g., through modulation of the immune system, or proteins/receptors interactions) on HIV genetic evolution, divergence, and selective pressure made by distinct microbial niches in different body compartments. Co-evolution and diversification of the other components of the ecosystem is also expected by the same bidirectional mechanisms that shape HIV diversity. From Trunfio M. et al, manuscript under preparation.

The interest in straining such model stems from two major observations:

1. Recent data in people with primary HIV infection shows that following single transmission/founder virus infection, as most cases, major and minor HIV variants sequenced in blood and CNS (and other body compartments when assessed) are identical [84,85], while the proportions of minor variants differ between compartments in multiple transmission/founder viruses infections [85], suggesting initial selection bottleneck only in case of pre-existent genetic variability available for such a competition. At the end of this journey, post-mortem data described an extremely high diversity not only between body compartments, but also within: e.g., inter-regional and intra-regional diversity and specific HIV subpopulations in different brain areas, and bidirectional

transition events of HIV clones between distinct cerebrum lobes [86,87]. Even after considering variability in ART penetration [88], and the obvious differences in resident and trafficking cells between distinct brain areas [86], the wide heterogeneity of HIV clones within the same tissue of a unique individual demands that further factors should be accounted to explain it.

2. Data from individuals with hepatitis co-infection suggest that the compresence of either HCV or HBV and HIV can reciprocally affect selection pressure, type of genetic selection (diversifying vs purifying), and number of mutations per specific sites in the genome of the companion virus [89–93]. The differential genetic pressure and evolution in specific genes upon coinfection could be a strategy of adaptation to a different replicative environment, the result of direct interaction between HCV and HIV proteins-genes, or the result of different immunological landscapes between mono- and co-infections. While there is biologically plausible ground, more and larger studies should be designed to address all the relevant confounding factors (e.g., ART exposure and adherence, immune responses) before concluding for a direct or an immune-mediated interaction, or for both.

Understanding how HIV populates tissues throughout the human body and the drivers and mechanisms of divergence and compartmentalization is crucial for the development of strategies to clear or otherwise lock down these distinct reservoirs. In this regard, establishing whether an evolutionary model can fit and then which one better describes the HIV-microbiome interplay in the body ecosystems would help with addressing relevant questions: does the variety in human viromes participate in the genetic fate and compartmentalization of HIV in each body compartment? Do the differences between human viromes contribute to initial bottleneck selection that determines which HIV variant will eventually become the major one in each tissue? Could the changes of virome overtime affect the long-term evolution of HIV in a body-compartment-specific base?

5. Next-Generation sequencing, HIV, and other viral infections

Over the past few years, advancements in next-generation sequencing (NGS) technologies and bioinformatics tools have revealed a great variation in the viral population found across the human body and have greatly improved the detection and characterization of viral sequences in biological samples coming from different compartments, also those previously considered to be sterile [4,94]. A summary of the evidence on human virome in different

body compartments of PLWH is shown in Figure 2 (panel C), even though most of the studies used different NGS approaches, significantly limiting their comparability.

Current technologies for the study of virome rely on NGS techniques, and particularly on shotgun metagenomic, which is an untargeted sequencing of all the genomic material extracted from a sample [2,95,96]. This approach overcomes some of the main limitations of classic virus-detection methods, as it greatly enhances the chances to identify and characterize known microorganisms, but can also detect unexpected pathogens and unknown viruses, too divergent from those already isolated/characterized to be recognized by standard techniques [97,98].

Although viral metagenomics has made it possible to understand the complexity and richness of human virome, including bacteriophages and other virus populations, some challenges remain in the detection of viral sequences in CSF samples, mainly due to the low abundance of viral nucleic acids in the CNS.

One of the main obstacles of virome detection is the presence of host DNA and RNA, which represent a significant proportion of the nucleic acids recovered from the CNS (making up for about 99% of all material) [99]. This problem might be overcome by increasing the sequencing depth, which usually reflects in higher sequencing costs [100]. However, viral nucleic acids might also be enriched implementing measures acting pre or during sequencing. In the first case, the increase of the relative concentration of viral particles can be obtained by filtration and centrifugation steps, as well as by host DNA depletion [101–103].

Moreover, viral enrichment might also be performed at the sequencing level, through the use of viral primers and probes that can retain specific viral reads, and discard all the remaining reads [104,105]. This approach might result up to 1000-fold increase in the number of viral reads [106], but the main limitation is that it leads to the enrichment of only the known virome, whereas it hampers the detection and discovery of new viral pathogens. All these approaches are helpful, because they allow to better discriminate viruses from the background noise, mostly consisting of host and bacterial DNA [103,107].

Even with the implementation of protocol adjustments, other challenges remain in the use of NGS for the study of virome. One of these is represented by the production of large amount of bioinformatic data, that requires high storage capacity, computing power and the acquisition of computer skills and bioinformatic expertise.

Another challenge is posed by the unavailability of comprehensive viral databases. In fact, the most common approach in shotgun metagenomic analysis is represented by the

taxonomic classification of reads by alignment to reference databases [108,109]. Unfortunately, a large proportion of the sequencing data have no match in public viral databases, as they are still far from being complete or comparable to those of bacteria, limiting the accuracy of reference-based approaches [110]. A more accurate reconstruction of human virome will surely derive from the functional characterization of viruses through traditional techniques, which will progressively update and refine currently available databases [111–115].

Nonetheless, some alternative reference-free approaches are also used in metagenomics, including the assembly of complete or draft genomes in the so-called metagenome assembled genomes [116–118]. This approach allows the recovery of unknown viruses that are not present in reference databases but suffers from the presence of taxa with low coverage [119].

The choice of the sequencing technology for the shotgun metagenomic may also represents another challenging step. This is particularly true regarding read length, as short read, and long read approaches have different advantages and limitations. In fact, short reads technologies (e.g., Illumina) have usually lower sequencing costs and result in higher sequencing throughputs with lower error rates, but, due to the limited read length (usually not higher than 300 bp) are not able to resolve repeat regions and to discriminate DNA from related microorganisms. Another limitation also occurs in assembly methods, as they can result in discontinuous and chimeric assemblies, thus hampering genomic context analysis [120]. Long reads technologies (e.g., PacBio and Oxford Nanopore Technology), on the other hand, are more performing in assembling complex genomes, including difficult regions like repeats and large structural variations, allowing for genomic context analysis [120]. As downsides, even with the advent of new sequencing kits, the error rates are higher than those of short reads technologies, while in the case of PacBio also the sequencing throughput is also not comparable.

The large variety of bioinformatic tools and approaches represents another critical step double-edged sword: on one hand, it gives rise to different ways of looking at data, with the extrapolation of increasingly amount of information; on the other hand, the lack of standardization, both in NGS techniques and bioinformatic analyses, might hamper the ability to efficiently compare results across different platforms and studies [121]. This is particularly true also when considering contamination, which is a common problem in NGS analyses [122,123]. Depending on how contaminations are considered and filtered out, different findings may arise. Even in CSF, contamination cannot be ruled out due to the

collection during lumbar puncture (from skin to CSF) and processing of samples. This problem can be addressed using multiple solid negative controls in every step of sequencing, and through the use of extensive and constantly updated databases containing all the background microorganisms, that are commonly detected in body compartments and arising from laboratory contamination [124].

6. Clinical relevance of the human virome in HIV infection

Human virome is gaining momentum, but knowledge remains decades behind similar studies on human bacteriome. In light of the recent appreciation of the complexity of microbial consortia, for which new components are daily updated, the scientific community should consider causation in a broader ecosystems' context where intra-host variability, health and diseases, external triggers, and microbial strains and communities are all important. Efforts have been invested to find etiopathology connections between bacteriome and human disease, and we now decelerate in recognizing that an upstream player could be relevant as well, being human virome the puppeteer of bacterial consortia through commensalism, parasitism, and predation.

The extremely vast variety of virome composition and of its immune properties, and possible interactions with HIV, with the host and with the bacteriome, leaves open the possibility that not all these combinations would lead to additive unfavorable effects on health outcomes, as previously observed for few eukaryotic viruses [35].

The raising interest and advancements in phage therapy to treat cancer, multi-drug resistant bacterial infections, and chronic diseases (e.g., NAFLD) will soon expand our knowledge on a large proportion of species constituting human virome as well as the available options of specific phage cocktails, which administration in human already proved to be safe and well tolerated [125,126]. Similarly, initial attempts in engineering phages to treat neurodegenerative disorders have been performed [127,128], and clinical trials on grooming microbiome through phage therapy are also ongoing [126], with potential applications also in cognitive and mood disorders of PWH [129].

Finally, there is a strong need for a standard and highly reproducible metagenomic procedure that can be easily upscaled for virome sequencing and analysis by the scientific community. The development of a shared protocol could allow to in-depth characterize viral composition in different clinical and anatomical settings, including challenging body compartments like CSF where the virome signatures remain elusive.

In this evolving landscape, confirming or discrediting new hypotheses and models that describe a role for human viromes in the development and in shaping the clinical phenotypes of mental health outcomes of PWH will inform on possible additional determinants of HIV pathology in distinct human body compartments. It will also inform on the clinical feasibility and utility of targeting human virome (and bacteriome) in HIV eradication/cure strategies, in boosting responses to latency reversal agents, or in shaping inflammation, immune activation, and microbial translocation.

Study Rationale

The advent of next generation sequencing (NGS) has unleashed a microbiological revolution, discovering an underworld of new microbes and candidate etiologies for disorders formerly lacking acknowledged triggers [94]. Body compartments previously considered sterile, such as the CSF, have been found to harbor a plethora of apparently harmless microbes and viruses [4]. Concomitantly, despite ART has significantly modified the prognosis of PWH, the burden of HIV-associated comorbidities (such as neurocognitive and mood disorders) remains relevant, and it has even increased [130]. This epidemiology is mostly due to immune-activation and inflammation that persist at elevated level despite viral suppression [61,131]. However, chronic inflammation is just the downstream epiphenomenon of several processes that remain poorly understood. In this regard, the role of co-infections in HIV-associated comorbidities has gained attention. In specific regard to the CNS, as example, Alzheimer-like neurodegeneration seems more common in PWH with HSV-1 compared to HSV-1-seronegative PWH [71], EBV co-infection can affect blood-brain barrier integrity, intrathecal inflammation, and the cognitive performance [64,132], and worse neurocognitive performance has been associated with higher humoral responses against CMV [63]. Considering the recent discovery of a human CSF virome [4], many other viruses within the brain, not routinely detected by clinical investigations, may modulate similar processes, and eventually contribute to divergent mental health outcomes in PWH.

Based on the evidenced so far reviewed, we have hypothesized the following disease model for CNS inflammation, neurodegeneration, and mental health outcomes (cognitive performance and depression) in PWH: Figure 5.

Figure 5. Complimentary hypothesis models of the neuropathogenesis of HIV infection that recognize a role for the CSF virome.

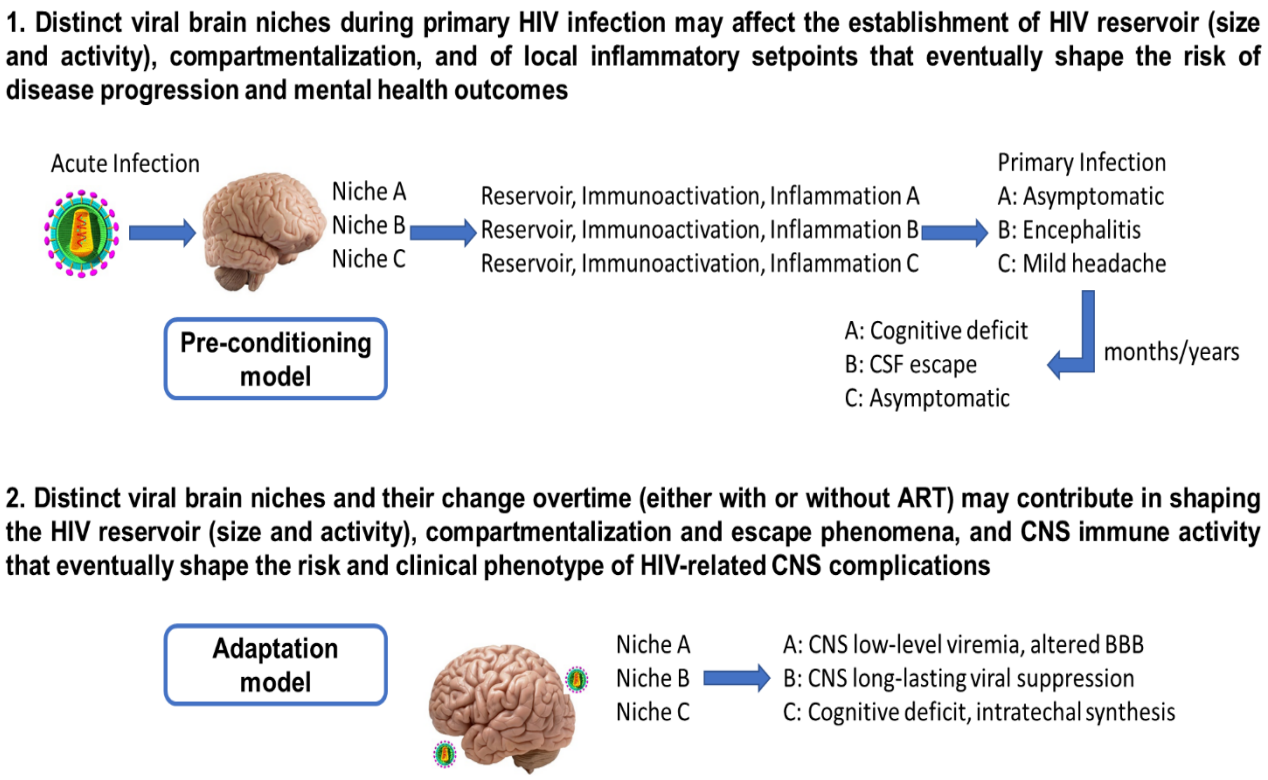

Within the framework of the "Adaptation" model that can be addressed with the data we had collected, we hypothesized that: 1) the CSF virome of PWH on suppressive ART is not sterile and its composition depends on a complex combinations of variables (e.g., BBB permeability); 2) Different characteristics of CSF virome are associated with distinct levels of local immune activation and inflammation; 3) The prevalence of depression and cognitive impairment is affected also by the characteristics of the CSF virome (e.g., α diversity, type and abundance of prevalent *spp*). These hypotheses will be investigated through three common methods for taxonomy attribution, as no assumption was strong enough to select the best approach, and, mainly because of the lack of an international consensus in virome pipelines, we want to compare the variability in the findings when either contigs or reads are used.

Methods

1. Study Design

We performed a pilot cross-sectional study of CSF virome of 81 adult PWH with plasma HIV-RNA <200 cp/mL on triple 2NRTI-based antiretroviral therapy. CSF samples from participants with HIV infection have been collected and stored between January 2010 and September 2019 at the Unit of Infectious Diseases, Amedeo di Savoia hospital, Torino (Italy), and retrospectively analyzed through metagenomic sequencing for virome detection with the following objectives:

Primary objective:

- To describe the presence and composition (observed species, α and β diversity) of the CSF virome of adult PWH on suppressive ART.

Secondary objectives:

- To evaluate demographic (e.g., age, sex), laboratory (e.g., CSF biomarkers of inflammation, immune activation, blood-brain barrier permeability, and intrathecal synthesis), and HIV-related characteristics (e.g., CD4+ T cell count, length of HIV infection) associated with the presence and composition of CSF virome.
- To evaluate whether the presence and/or composition of CSF virome is associated with depressive mood and neurocognitive impairment in a subgroup of participants that underwent neurocognitive evaluation.

Both the primary and secondary objectives were performed in replicates according to two distinct pipelines for NGS sequencing and library preparation. The two pipelines were chosen as they represent the two most common alternative NGS methods currently used in studies on human virome: 1) taxonomic assignment based on contigs 2) taxonomic assignment based on reads.

Inclusion Criteria: WB-confirmed HIV infection, age ≥18 years, plasma HIV-RNA<200 cp/mL, being on standard triple NRTI-based therapy (2 NRTIs + a third drug among protease inhibitors, integrase strand-transfer inhibitors, or non-nucleoside reverse transcriptase inhibitors), availability of ≥1 mL of stored (-80°C) CSF collected through lumbar puncture (LP), and signed informed consent for the preservation and use of the CSF samples for future analyses at the time of LP.

Exclusion Criteria: having major confounding for neurocognitive evaluation or CSF biomarkers levels prior or at the time of LP (e.g., CNS disorders or infections, untreated

psychiatric conditions, language barriers, cerebrovascular events, head trauma), substance/alcohol abuse in the year before LP, any contraindication to LP.

The sampling frame of CSF samples retrospectively selected for the study was represented by all the CSF samples collected and stored between 2009 and 2020 at Unit of Infectious Diseases; the criteria of sample selection were based on the inclusion and exclusion criteria of the study, and on the following: CSF samples had to belong to subjects for whom the whole panel of CSF biomarkers for this study had been already tested, had to belong preferentially to subjects with neurocognitive evaluation, a preferential selection based on sex at birth to allow for a significant contribution of female subjects.

A control group of 11 HIV-negative adult participants was also enrolled between March and June 2023. Controls were tested for HIV-1/2 infection through screening hospital serology, had to undergo spinal anesthesia for surgical indications, and had to have a negative medical history for immunological disorders (e.g., acquired, iatrogenic or genetic immune deficits, current cancer, immuno-rheumatological diseases), for CNS disorders (e.g., neurodegenerative disorders, CNS infections, psychiatric conditions) and for current infections. Controls were prospectively enrolled by the Unit of Emergency medicine, Reanimation and Anesthesia at the Maria Vittoria hospital, Torino (Italy), and they signed an informed consent for the NGS analysis of 1.5 mL of CSF collected during spinal anesthesia. The research was performed in accordance with the Declaration of Helsinki and has been approved by the Comitato Etico Interaziendale A.O.U. Città della Salute e della Scienza di Torino, A.O. Ordine Mauriziano di Torino, A.S.L. Città di Torino (protocol n.285/2022); all participants provided written informed consent.

2. Clinical Assessment and CSF biomarkers

Standardized assessments were performed to collect data on demographics, HIV disease characteristics, biomarkers, and medical diagnoses. At the time of LP, all participants underwent standardized physical examination. CSF samples were collected, processed immediately for CSF biomarkers, and from 1 to 2 mL were stored at -80°C within 1 hour of collection. At the time of LP, CSF was analyzed for:

1. CSF biochemistry (CSF cells, glucose, and protein).
2. CSF total tau (tau), 181-phosphorylated tau (ptau), and β-amyloid 1–42 fragments (Aβ42) by immunoassay (Innogenetics, Ghent, Belgium, EU); values were considered abnormal based on manufacturer's thresholds suggested for the general population: when: tau > 300 pg/mL (age ≤50 years), >450 pg/mL (age 51–70 years), or >500 pg/mL (age > 70 years); ptau > 61 pg/mL; Aβ42 < 500 pg/mL.

3. CSF Neopterin and S100β by commercial immunoassays (DRG Diagnostics, Marnurg, Germany, and DIAMETRA Srl, Spello, Italy, respectively); values were considered abnormal based on manufacturer's thresholds suggested for the general population: neopterin > 1.5 ng/mL; S100β > 380 pg/mL.
4. Blood-brain barrier integrity through CSF to serum albumin ratio (CSAR, CSF albumin mg/L/serum albumin mg/L); normal if <6.5 in subjects aged <40 years and <8 in older subjects.
5. Intrathecal synthesis by Tourtelotte, Tibbling, and IgG index according to age-adjusted Reibergrams [133].

HIV RNA was quantified in plasma and CSF by reverse-transcription polymerase chain reaction (Roche Amplicor, lower limit of quantitation 20 copies/mL). PCR for EBV DNA, CMV DNA, and JCV DNA were performed in CSF through in-house standardized PCR.

3. Mood and Cognitive assessment

A subgroup of PWH (n=64) underwent a comprehensive battery of neurocognitive tests within 6 months from the LP. Raw cognitive scores were converted to demographically corrected standard scores (T scores) by referencing to normative standards which correct for effects of age, education, sex, and ethnicity. Seven cognitive abilities were assessed by 13 specific tests (see Table 1): verbal/language, attention/working memory, executive functions, memory (learning and recall), speed of information processing, visuospatial sensory and perception, and motor functions. Participants were classified as per HIV-associated Neurocognitive Disorders (HAND) categories according to Frascati's criteria [134] and by binary categorization of presence/absence of cognitive impairment. The Lawton Instrumental Activities of Daily Living scale (IADL) [135] was used to assess the impact of neurocognitive impairment on daily life and differentiate between symptomatic and asymptomatic impairment, as recommended [134].

Table 1. Cognitive domains and neurocognitive tests.

Cognitive domain	Tests
Attention/Working memory	Trail Making Test Part B Stroop Color Interference and Error Test
Speed and mental Processing	Digit Symbol test Trail Making Test Part A
Short- and long-term memory	Delayed recall of the Rey-Osterrieth complex figure Disyllabic words serial repetition test Corsi block-tapping test Prose memory story Digit span forward test
Verbal Fluency/Language	Semantic and phonemic verbal fluency
Executive functions	Frontal Assessment battery
Motor Functions	Groove Pegboard test for the dominant and non-dominant hand
Visuospatial Sensory and Perception	Copy of the Rey-Osterrieth complex figure

Depressive mood was assessed in a subgroup of PWH (n=71) through the Beck Depression Inventory II (BDI-II) [136,137]. This 21-item self-administered scale measures the existence and severity of symptoms of depression. Each item corresponding to a symptom of depression is scored on a scale of 0-3 in a list of four statements arranged in increasing severity, and eventually each score is summed to give a single score for the BDI-II. Cut-off score guidelines for the BDI-II have been validated for the general population, commonly applied by studies on PWH [138,139], and given [136,137]: a total score of 0–13 is considered minimal range depressive mood, 14–19 is mild, 20–28 is moderate, and 29–63 is severe.

4. Metagenomic analyses

4.1 Sample preparation and nucleic acid extraction

Prokaryotic and eukaryotic viruses in CSF were firstly enriched by isolation and purification of virus-like particles (VLPs). This purification was performed through a filtration process that takes advantage of the smaller dimension of viruses with respect to eukaryotic and prokaryotic cells. CSF samples were initially filtered with 0.45 μm polyethersulfone filters (Merck millipore) to retain most of the bacteria and cellular contaminants and then with 0.22 μm polyethersulfone filters (Merck millipore) capable of enriching viruses.

The resulting filtrate (approximately 200-400 μl of sample) was used for nucleic acid extraction using the QIAamp MinElute Virus Spin Kit (Qiagen, Hilden, Germany), according

to the manufacturer's instructions. Both the concentration and the quality of the extracted nucleic acids were measured by the Nanodrop. Three blank samples were processed in parallel with CSF samples to document the contamination background.

4.2 Amplification and sequencing

100 ng input of purified nucleic acids was used for virome amplification and sequencing following a modification of the QIAseq® Single Cell RNA Library Kits with Unique Dual Indexes protocol.

Briefly, a first reverse transcription, amplification and cDNA production were performed from total viral nucleic acids (RNA plus DNA) to obtain a pool of cDNA. The cDNA obtained from the previous step was first subjected to enzymatic fragmentation and then used for libraries preparation by using the QIAseq Single Cell RNA Amplified cDNA. The produced libraries were purified with QIAseq Beads and validated using the High Sensitivity D1000 ScreenTape system on a Bioanalyzer (Agilent Technologies) and quantified using a High Sensitivity Double Stranded DNA kit on a Qubit Fluorometer (Thermo Fisher Scientific). Normalized indexed DNA libraries were then loaded onto an Illumina High Output Flow cell cartridge v.2.5, and sequenced using the NextSeq 550 instrument (Illumina, San Diego, CA, USA) with 2×150-bp paired-end reads.

Three different runs containing 27 CSF samples from HIV-1 positive individuals each were performed. A fourth run containing the 11 CSF samples from HIV- negative individuals and the eight sample repetitions was performed. In each run, the blank samples processed in parallel were included.

4.3 Virome characterization

Demultiplexed raw reads were trimmed for adapter and quality (Phred score > 28) and deduplicated using Fastp (v0.23.2) [140]. The final read quality was assessed by FastQC (v0.11.9) and MultiQC (v1.12) [141,142]. All reads mapping to the human (GRCh38) were removed from all samples using bbsplit (BBTools, https://sourceforge.net/projects/bbmap/). The remaining clean reads were transformed back to paired end reads using reformat (BBTools). Taxonomy was assigned using Kraken 2 (v2.1.2) [109] and visualized by Krona (v2.8.1) [143], while Bracken (v2.7) [144] was used to estimate family abundance.

Taxonomy assignment by reads: only reads classified as viral (taxonID 10239) were retrieved, using the 'extract_kraken_reads.py' script of the KrakenTools suite (v1.2, https://github.com/jenniferlu717/KrakenTools). The final taxonomy assignment was obtained by: 1) supporting each viral taxon with at least two unique reads, independently from Kraken

confidence score; 2) supporting each viral taxon with at least two unique reads with a Kraken confidence score >0.50, as previously suggested [145,146]. Species observed from the blanks were removed from all samples.

Taxonomy assignment by contigs: Only reads classified as viral (taxonID 10239) were retrieved, using the 'extract_kraken_reads.py' script of KrakenTools suite (v1.2, https://github.com/jenniferlu717/KrakenTools), and *de-novo* assembled using metaSPAdes (v3.14.1) [147] in paired-read mode with default settings. The obtained contigs were filtered for length ≥300bp using reformat from bbtools and then queried against a nucleotide viral sequences collection retrieved from the National Center for Biotechnology Information (NCBI) Reference Sequence Database (RefSeq, 8416 sequences, downloaded on 26/09/2022) using Nucleotide BLAST (blastn) with an e-value of at least $1x10^{-10}$ and a percentage identity of at least 70%. Only contigs matching viral species were considered. Species observed from the BLAST search of the contigs assembled from the blanks (without length filtering) were removed from all samples.

Eukaryotic and non-eukaryotic viral species and their genome coverage were visualized through a heatmap constructed using the ggplot2 (v3.3.6) and pheatmap (v1.0.12) R packages [148].

The filtered Bracken report output files were used to generate a BIOM-format table using the kraken-biom python package (v1.0.1, https://github.com/smdabdoub/kraken-biom), with option –fmt json. The biom-format package (v2.1.12) [149] was then used to add sample metadata to the BIOM table, which was then loaded into R studio. The alpha (Observed, Shannon and Simpson) and beta (Bray-Curtis) diversities of the viral species, together with PcoA analysis were performed using the phyloseq (v1.40.0, on Bioconductor) [150] and Vegan (v2.6.2) R packages, while plots were generated using ggplot2 (v3.3.6) R package [148].

5. Statistical Analyses

Data are presented as median (interquartile range, IQR), mean (standard deviation, SD), and absolute number (proportion, %) according to type and distribution of the variables. Plasma and CSF HIV RNA and other non-normally distributed variables were log10-transformed to reduce skewness.

Virome composition was described through α diversity (the within-specimen diversity): number of observed species, Shannon, and Simpson index. The last two indexes are used to measure different but complimentary features of α diversity. Shannon emphasizes the richness component of diversity, which refers to the number of different taxon types present

in the samples; the greater the number of taxon types (at every taxonomic level, e.g., genus, class, or phylum), the more diverse the biological sample in terms of richness. On the other hand, Simpson emphasizes the evenness component of α diversity, which refers to the relative percentage of taxa distributed amongst the different taxon types. The more equitable this distribution, the more diverse the sample in terms of evenness.

The difference (distance) in the diversity of taxa between two or more samples in a whole pool of samples that define the "ecosystem" is β diversity (the between-specimen diversity). Differences in β diversity (as Bray-Curtis' dissimilarity - based on occurrence and abundance of taxa -, and as Jaccard distance - based on presence/absence of taxa -) were investigated with Permutation Based Analysis of Variance (PERMANOVA) with Adonis function and Principal Coordinate Analysis (PCoA) using the phyloseq and Vegan R packages for β diversity.

To define potential differences in CSF virome composition and in virome presence/absence against selected parameters, Kruskal Wallis H test, Mann-Whitney U test, or Chi squared test were used as appropriate.

Based on the distinct results from the two methods of taxonomic assignment (e.g., in number of positive samples and of identified species) specific analyses were also performed. For assignment based on contigs, binary logistic regressions were performed. For assignment based on reads, Pearson's correlations, linear regressions (with unadjusted and adjusted beta coefficients, β), and unsupervised two-step cluster analysis were used. The clustering approach was pursued to remove any potential bias introduced by the clinical cut-offs required for the other analyses and was based on a quantitative composition of different macro-categories of viruses (relative abundance of reads of prokaryotic, non-human eukaryotic and human eukaryotic viruses), as determinant of clustering; a fourth cluster was represented by participants with no detectable CSF virome; the continuous variables were normalized by square root transformation due to their positive skewed non-normal distribution and standardized for the log-likelihood distance measure approach of clustering. The fit statistics was based on Schwartz Bayesian criteria.

Logistic and linear regressions were used exploratorily for associations between either presence or composition of CSF virome and the variables of interest; multivariable models were built including univariable significant variables and covariates with presumed biological relevance regardless of univariable significance. In case of perfect distribution or nonconcave convergence after data transformation, Firth penalized methods was applied to force an exact computation of the estimated effect (odds ratio, OR). Multicollinearity was

assessed for each model but it did not require to be addressed as the variance inflation factor (VIF) for each included variables was always <5 (threshold for problematic collinearity [151]).

Analyses were performed and plots were generated using the ggplot2 R package in R Studio and through SPSS Statistics v.28 (IBM Corp., NY, USA).

Results

1. Study Population

We enrolled 81 participants with HIV infection (PWH). As shown in Tab.1, PWH were mostly white (93.8%) male (71.6%) of middle age. The distribution of HIV acquisition routes was evenly distributed (about one third each) as male who have sex with other males (MSM), heterosexual, and past intravenous drug users (pIDU).

The 17.3% and the 25.9% of PWH had detectable HIV RNA in blood and in CSF despite being all on ART, and the range of viral load among PWH with detectable viremia was 23-125 in blood and 20-133 cp/mL in CSF. Current immunological status was good (median CD4+ T cell count and CD4/CD8 ratio of 460 cells/μL and 0.7, respectively), and 63.0% was diagnosed with AIDS in the past.

Table 1. Demographic and clinical characteristics of the study population.

PWH (n=81)	
Age, years	49.8 (±11.3)
Male sex, n	58 (71.6%)
White race, n	76 (93.8%)
Risk factor, n ***MSM*** ***Heterosexual*** ***pIDU***	 27 (33.3%) 24 (29.6%) 30 (37.0%)
Plasma HIV RNA<20 cp/mL, n ***Plasma HIV RNA, cp/mL°***	67 (82.7%) 45 (32-62)
CSF HIV RNA <20 cp/mL, n ***CSF HIV RNA, cp/mL°***	60 (74.1%) 48 (29-62)
CSF viral escape, n ***CSF HIV RNA, cp/mL****	14 (17.3%) 48 (27-57)
Current CD4+ T cell count, cells/μL	460 (323-681)
Current CD4+ T cell count, %	29 (20-35)
Current CD4+/CD8+ ratio	0.7 (0.5-1.1)
CD4+ T cell count nadir, cells/μL	168 (50-275)
Past AIDS episodes, n	51 (63.0%)
Est. duration of HIV infection, years	12 (3-19)
ART regimen, n ***PI-based*** ***NNRTI-based*** ***INSTI-based***	 32 (39.5%) 21 (25.9%) 28 (34.6%)

*°Among participants with plasma/CSF HIV RNA >lower limit of quantification of 20 copies/mL; *Among participants with CSF viral escape. Legend: PWH, people with HIV; MSM, males who have sex with other males; pIDU, past intravenous drug users; CSF, cerebrospinal fluid; ART, antiretroviral therapy; PI, protease inhibitors; NNRTI, non-nucleoside reverse transcriptase inhibitors; INSTI, integrase strand-transfer inhibitors.*

The 11 participants without HIV infection (controls without HIV, CWH) were also mainly white (100%) male (90.9%) of middle age, and mildly older compared to PWH (57 vs 50 years, p=0.083), as shown in Tab.2.

CWH underwent spinal anesthesia for orthopedic surgery (3 for femur fractures or coxarthrosis and 2 for meniscus injury), urology surgery (1 transurethral resection of the prostate and 1 varicocelectomy), or abdominal surgery (2 hernioplasty, 1 intervention on hemorrhoids, and 1 polyps' removal). Among the comorbidities of potential interest, one CWH had psoriatic arthritis and obesity, one had Hodgkin lymphoma in the past and currently diabetes mellitus, and one had monoclonal gammopathy of uncertain significance.

Table 2. Demographic and clinical characteristics of controls without HIV.

HIV-negative controls (n=11)	
Age, years	57.0 (±18.6)
Male sex, n	10 (90.9%)
White race, n	11 (100%)
Reason for spinal anesthesia, n ***Orthopedic surgery*** ***Urology surgery*** ***Abdominal surgery***	 5 (45.4%) 2 (18.2%) 4 (36.4%)
Relevant comorbidities, n ***Diabetes mellitus*** ***Obesity*** ***Gastrointestinal disorders*** ***Past cancer*** ***Past Tonsillectomy/Adenoidectomy*** ***Past Appendectomy/Cholecystectomy***	 1 (9.1%) 1 (9.1%) 1 (9.1%) 1 (9.1%) 2 (18.2%) 2 (18.2%)

CSF biomarkers of inflammation, immune activation, intrathecal synthesis, tauopathy, β amyloid, and BBB permeability in PWH and CWH are shown in Tab.3. All participants had <5 cells/mL in their CSF, except for two PWH that showed 7 and 40 cells/mL (without other signs or biomarkers indicating CNS or peripheral infections). The prevalence of BBB impairment was similar between PWH and CWH, possibly due to the older age of CWH and the good viro-immunological status of PWH; instead, intrathecal synthesis was observed only in PWH (25.9% vs 0%, p=0.063).

Overall, abnormal values of CSF biomarkers were uncommon in PWH (each altered in <10% of the study population), except for neopterin (marker of monocyte-macrophages activation) that was increased in 15% PWH.

By standard PCR assays, traces of EBV (42, <100, <100, and 164 EBV DNA cp/mL) and JCV (16 and <100 JCV DNA cp/mL) were detected in four and two CSF samples from PWH, respectively. None of the samples tested resulted positive for CMV DNA (Tab.3).

Table 3. CSF characteristics and biomarkers in PWH and in CWH.

	PWH (n=81)	CWH (n=11)	p
CSF leukocytes, cells/mL	0 (0-0)	0 (0-0)	*NS*
CSF protein, mg/dL	46 (34-53)	51 (35-55)	*NS*
CSF glucose, mg/dL	59 (55-64)	61 (58-63)	*NS*
BBB impairment, n	18 (22.2%)	2 (18.2%)	*NS*
CSAR	5.5 (4.0-7.2)	6.6 (4.6-7.7)	*NS*
Intrathecal synthesis, n	21 (25.9%)	0 (0%)	*0.0631*
Tourtelotte	0.33 (0-6.9)	-	-
Tibbling	0.6 (0.4-0.8)	-	-
IgG index	0.34 (0.24-0.48)	0.36 (0.26-0.39)	*NS*
CSF total tau, pg/mL	135 (47-213)	-	-
Increased, n	6 (7.4%)		
CSF 181-ptau, pg/mL	36 (30-47)	-	-
Increased, n	7 (8.6%)		
CSF βA42, pg/mL	897 (679-1081)	-	-
Consumed, n	5 (6.2%)		
CSF neopterin, ng/mL	0.58 (0.34-1.10)	-	-
Increased, n	12 (14.8%)		
CSF S100β, pg/mL	127 (85-186)	-	-
Increased, n	4 (4.9%)		
Detectable CSF EBV DNA, n	4/73 (5.5%)°	-	-
Detectable CMV DNA, n	0/73 (0%)	-	-
Detectable JCV DNA, n	2/57 (3.5%)*	-	-

°EBV DNA range 42-164 cp/mL; JCV DNA range 16-99 cp/mL; Legend: PWH, participants with HIV; CWH, controls without HIV; CSF, cerebrospinal fluid; NS, non-significant at α level >0.1; BBB, blood-brain barrier; CSAR, CSF-to-serum albumin ratio; EBV, Epstein Barr virus; CMV, Cytomegalovirus; JCV, John Cunningham virus.

Sixty-four PWH (79.0%) underwent neurocognitive evaluation, and 71 (87.6%) were evaluated for depressive mood (see Tab.4). Prevalence of any degree of cognitive impairment was high (60.9%), due to inherent selection bias linked with the sampling frame of the study (participants enrolled in studies on HIV infection of the CNS). In line with the modern phenotype of HIV-associated neurocognitive disorders, most of the participants with impairment were diagnosed with asymptomatic neurocognitive impairment (ANI; 48.4%). Depressive mood was also common (32.4%), mostly mild, and in line with prevalence data reported for other modern populations living with HIV [152].

Table 4. Cognition and depressive mood in PWH.

PWH (n=64)	
Education, years	8 (8-13)
Neurocognitive impairment, n	39 (60.9%)
Frascati categories, n	
No impairment	25 (39.1%)
ANI	31 (48.4%)
MND	6 (9.4%)
HAD	2 (3.1%)
PWH (n=71)	
BDI-II score	10 (3-17)
Depression category, n	
None-minimal (<14)	48 (67.6%)
Mild (14-19)	13 (18.3%)
Moderate (20-28)	5 (7.0%)
Severe (≥29)	5 (7.0%)

Legend: PWH, people with HIV; ANI, asymptomatic neurocognitive impairment; MND, mild neurocognitive disorders; HAD, HIV-associated dementia; BDI-II, Beck depression Inventory II.

2. CSF Virome composition

Sequencing returned a total of 1953.05 million reads of mean length of 149 nucleotides and a median of 15.69 (IQR: 10.77-24.24) millions reads per subject. After quality filtering and removal of human-host reads, a total of 173.71 million non-human reads for 1.15 (0.56-2.11) million per subject were retained. After the blank reads' removal, a total of 16,395 viral reads for 38 (10-102) reads per subject were retained. When the confidence score >0.50 was applied, the number of total reads decreased to 14,083 for 6 (0-36) reads per subject, while after contigs reconstruction, the number of total reads was 3,574 for 35 (23-97) reads per participant (Figure 1).

2.1 Contigs-based method: taxonomic composition of CSF virome

When only viral reads combined in contigs ≥300 nucleotides (nt) were considered, results could not be retrieved for 78 samples, because all sequences detected were removed as background/contaminant species following filtering (Figure 1 and Table 5). Thus, a total of 14 samples (belonging to 11 PWH and 3 CWH) characterized by a median (IQR) number of 35 (23-97) reads were included in the analysis. To confirm these results, 8 samples were processed twice. No virome was detected in all pairs of repeated samples, except for one sample (470), where a CrAssphage could be identified only in the first experiment (Figure 2, Panel C).

Figure 1. Number of viral reads before and after reconstructions.

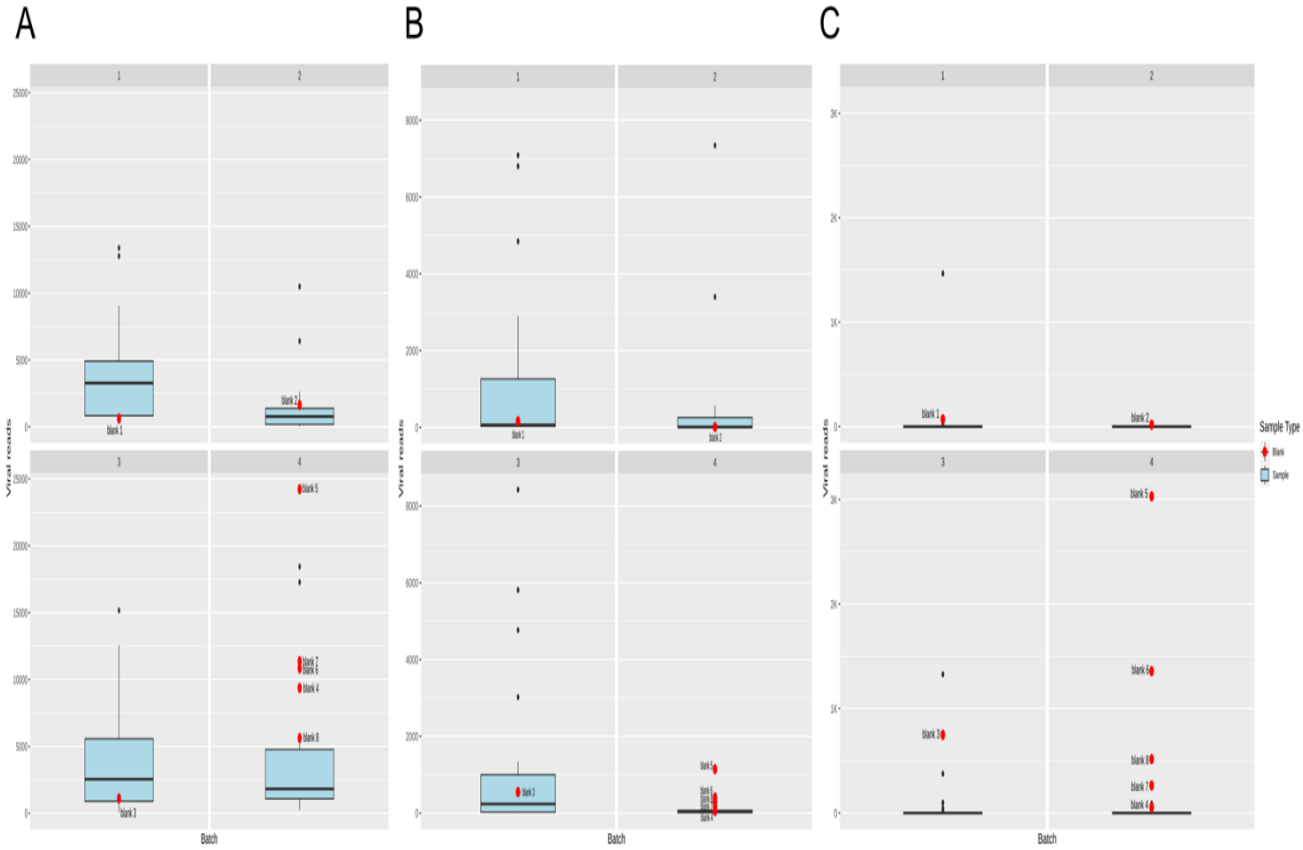

A) Number of reads assigned to viral species independently by confidence score, read count, and abundance. B) Number of reads assigned to viral species by a confidence score >0.50, independently by read count and abundance. C) Number of reads assigned to viral species after contigs assembly. Blank samples are in red.

Figure 2. Reads number in the 8 CSF samples processed twice.

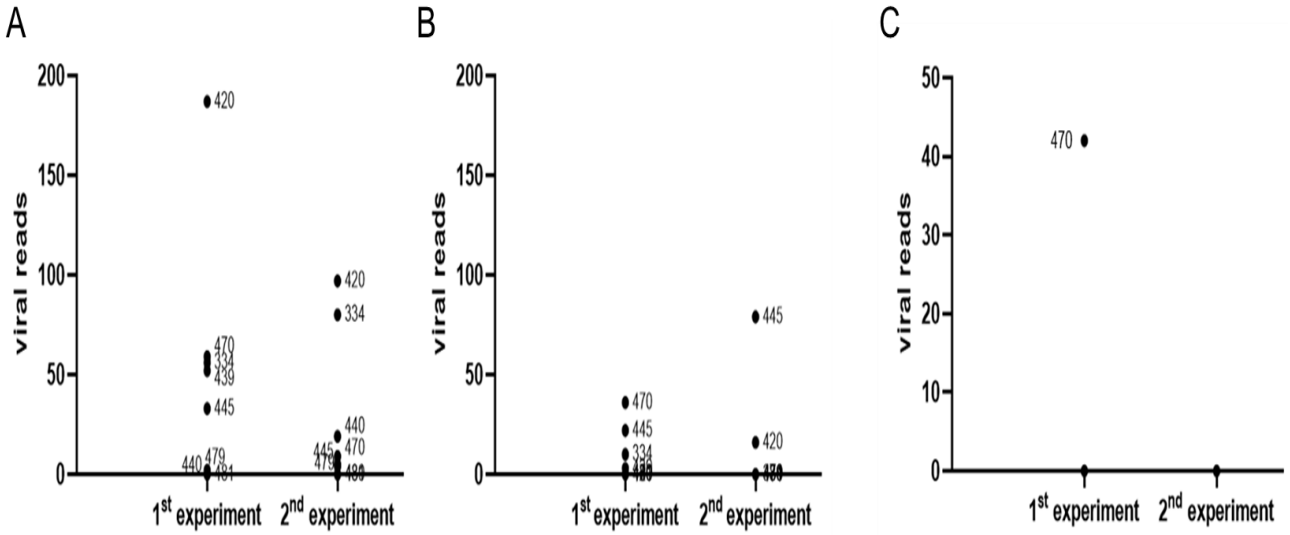

A) Number of reads assigned to viral species independently by confidence score in repeated samples. B) Number of reads assigned to viral species by a confidence score >0.50 in repeated samples. C) Number of reads assigned to viral species after contigs assembly in repeated samples.

Table 5. Contaminant viral species detected in the blank samples and removed from the study samples.

Blank	Virus Family	N of reads	N of contigs	Conting bp length	BLAST	Blast Identity (%)
1	Coronaviridae	26	3	68 (55-94)	Severe acute respiratory syndrome coronavirus	100 (100-100)
	Myoviridae	121	17	158 (115-221)	Synechococcus phage	85.56
	Podoviridae	59	2	99, 63	Caudoviricetes sp.	92.9 (88.9-94.9)
	Retroviridae	41	9	209 (223-223)	Equine infectious anemia virus*	100 (100-100)
	Siphoviridae	11	4	228 (210-243)	Propionibacterium phage Cutibacterium phage	81-99
2	Autographiviridae	56	4	204 (161-243)	Ralstonia phage	71.4 (70.8-72.6)
	Genomoviridae	29	2	190, 159	Genomoviridae sp.	83.9 (80.9-84.7)
	Microviridae	10	3	216 (177-239)	Microviridae sp. Gokushovirinae	80.9 (79.2-86.6)
	Myoviridae	1145	22	172 (144-205)	Aeromonas phage	97.2 (97.1-97.2)
	Siphoviridae	119	36	163 (113-178)	Gordonia phage	83.2 (81.8-88.6)
3	Retroviridae	748	61	90 (68-109)	Equine infectious anemia virus*	100 (100-100)
4	Myoviridae	8600	9	145 (134-158)	Bacillus phage	84.4-85.3
	Retroviridae	53	5	176 (90-223)	Equine infectious anemia virus*	100 (100-100)
	Siphoviridae	529	5	171 (155-173)	Lactococcus phage	93.6 (88.1-96.8)
5	Circoviridae	2663	3	127 (119-1919)	Cyclovirus	79.7 (74.0-82.8)
	Myoviridae	21140	4	151 (149-175)	Vibrio phage	90.5
	Retroviridae	428	46	104 (71-120)	Equine infectious anemia virus*	100 (100-100)
6	Myoviridae	7699	8	181 (145-194)	Bacillus phage	94.3 (93.4-94.8)
	Retroviridae	1131	52	103 (72-126)	Equine infectious anemia virus*	100 (100-100)
	Siphoviridae	319	8	1363 (135-188)	Lactococcus phage	90.8 (90.4-91.7)
7	Herelleviridae	72	2	296, 279	Bacillus phage	80.5 (78.4-86.0)
	Myoviridae	10808	9	135 (132-153)	Vibrio phage	90.2
	Podoviridae	22	4	162 (150-217)	Caudoviricetes sp	73.7 (71.6-75.0)
	Retroviridae	152	12	96 (68-124)	Equine infectious anemia virus*	100 (100-100)
	Siphoviridae	230	15	185 (158-243)	Propionibacterium phage Cutibacterium phage	71-89
8	Myoviridae	4809	8	140 (136-163)	Vibrio phage	91.3
	Podoviridae	164	5	164 (110-172)	Podoviridae sp	82.1
	Retroviridae	370	43	98 (66-117)	Equine infectious anemia virus*	100 (100-100)
	Siphoviridae	107	8	1232 (80-224)	Propionibacterium phage Cutibacterium phage	91-99

**Equine infectious anemia virus is contained in the reagents used to prepare genome libraries, and it was detected in 7 out of 8 blanks. Legend: N, number; bp, base pairs.*

We identified 8 unique human eukaryotic viruses, 2 plant eukaryotic viruses, and 6 unique bacteriophages/prophages that constituted the virome community in 3/11 (27.2%) CWH and 11/81 (13.6%) PWH (Figure 3). Among the 8 human eukaryotic viruses detected, the dsDNA *Herpesviridae* family was represented by EBV and HHV6, present in one participant each, with 1,467 and 376 reads respectively (genome coverage of 2.64% and 8.85%,

respectively). We also found evidence of Torque-Teno-virus and HPV, in one and two participants, with 44, 23, and 26 reads, respectively (genome coverage of 11.83%, 5.68% and 8.62%, respectively). Of note, these last two DNA viruses have been already identified in metagenomic analyses of CSF samples belonging to patients with suspected CSF infection or neurological disorders [153–156], albeit not being included in routine diagnostics of CSF samples. The only eukaryotic RNA virus identified was HCV, found in one sample with 98 reads and a genome coverage of 8.03% (the participant was also HCV-positive according to routine serology). The presence of HCV in CSF was already described because of the virus carriage in this compartment by HCV-infected leukocytes [157]. The *Poxviridae Molluscum contagious virus*, the *Human Mastadenovirus C* and the *Gemycircularvirus HV-GcV2* - three eukaryotic DNA viruses already described in human samples including CSF [158–160] - were also detected in the CSF of 3 CWH (reads number: 27, 23 and 64; genome coverage of 33.7%, 1.78%, and 0.16%).

Figure 3. Heatmap of the CSF virome profile in PWH and CWH.

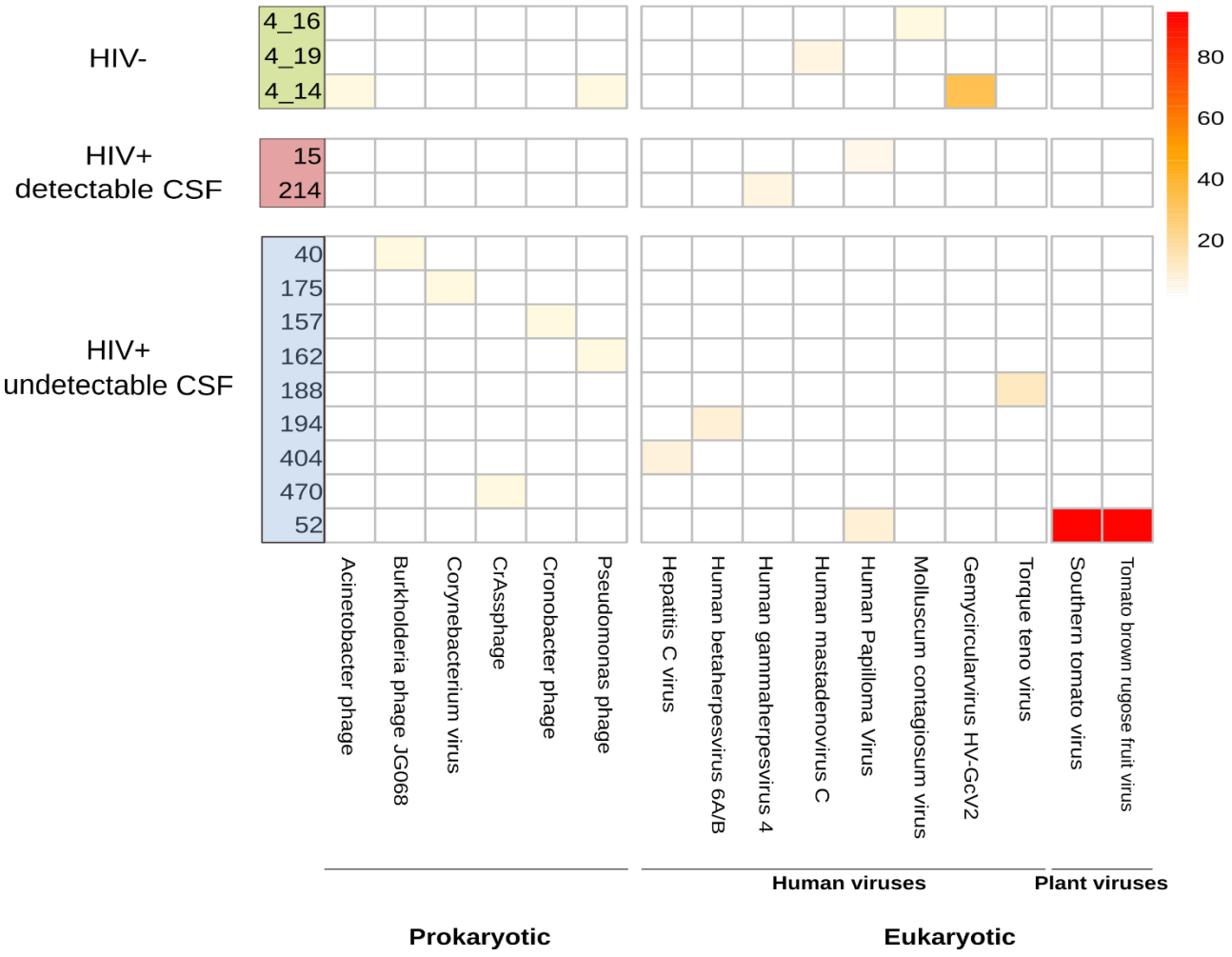

Each row represents a sample, and each column represents the percentage of the virus genome recovered. The samples are grouped into HIV negative and HIV positive samples. HIV positive samples were further split into detectable and undetectable HIV RNA in CSF.

Bacteriophage/prophage genomes were also recovered from 6 samples, all HIV-positive and with detectable HIV in CSF except for one HIV-negative sample, albeit with lower genome coverage.

Taxonomic classification failed to identify HIV-1 (in all the 21 CSF samples with detectable HIV RNA), EBV (in 3 out of 4 PCR-positive samples) and JCV reads (in both the 2 PCR-positive samples). This could be explained by the fact that most samples did not have evidence of their genome in CSF, while the remaining had only traces of HIV, EBV or JCV viral load (always below the 150 copies/mL). Noteworthy, previous studies investigated the limit of detection of HIV-1 RNA in CSF through metagenomics and found it to be ~10^2 copies/mL [95,161,162].

2.1.1 Diversity against HIV status and other characteristics

To determine potential differences in virome composition between PWH and CWH, α and β-diversity were examined. In the α diversity analysis, despite the CSF viral communities of PWH did not statistically differ from CWH, the comparison of values between the two groups, very limited in size (11 vs 3), reported lower α diversity in CSF samples from PWH when measured either by the Shannon diversity index (0.00 [0.00-0.21] vs 0.00 [0.00-0.92], p=0.928), Simpson index (0.00 [0.00-0.10] vs 0.00 [0.00-0.48], p=0.928), and Observed species (1[1-2] vs 1 [1-4], p=0.928; Figure 4).

Figure 4. Observed, Shannon and Simpson α diversity indexes of the viral communities against HIV status.

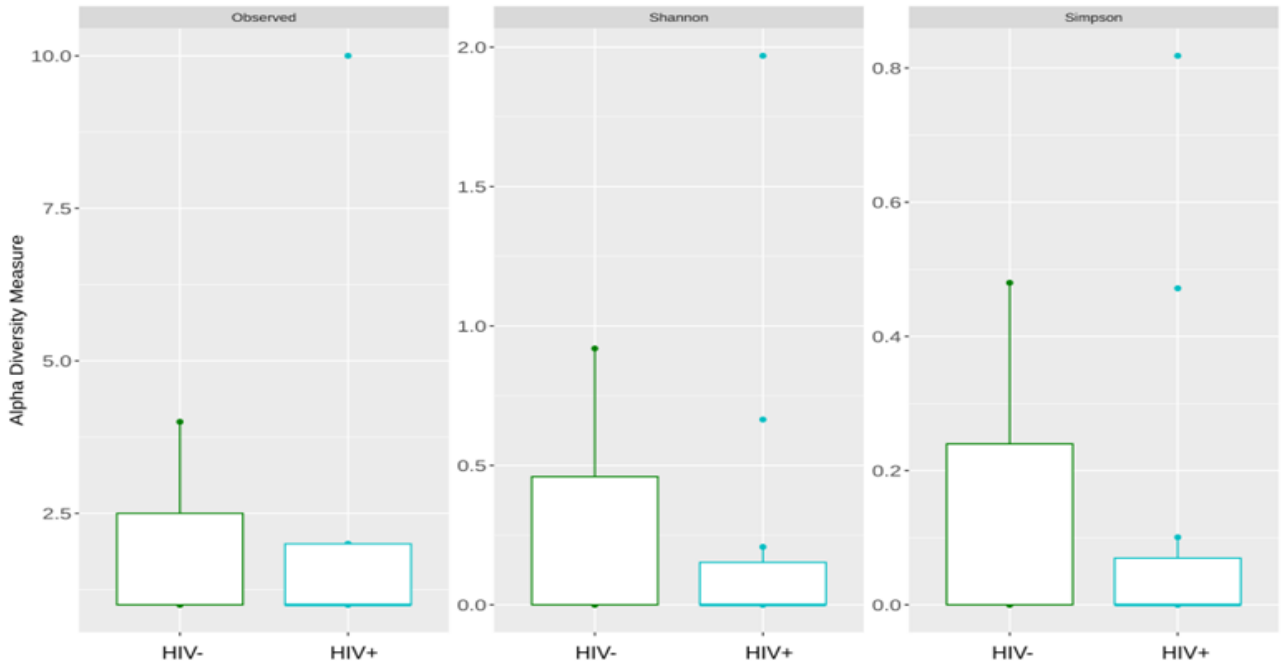

Differences in alpha diversity were investigated with Mann-Withney (11 PWH vs 3 CWH) for all the three indexes.

To characterize β diversity, we calculated Bray-Curtis and Jaccard distances and visualized the output using principal coordinate analysis (PCoA; Figure 5). Here, a considerable overlap between specimens from PWH and CWH was observed, without a clear definition of clusters. This overlap in community composition was confirmed statistically via Adonis (p=0.1.00). No differences in β diversity were detected against demographic, clinical, and HIV-related parameters.

Figure 5. Representation of β diversity in CSF samples by HIV status.

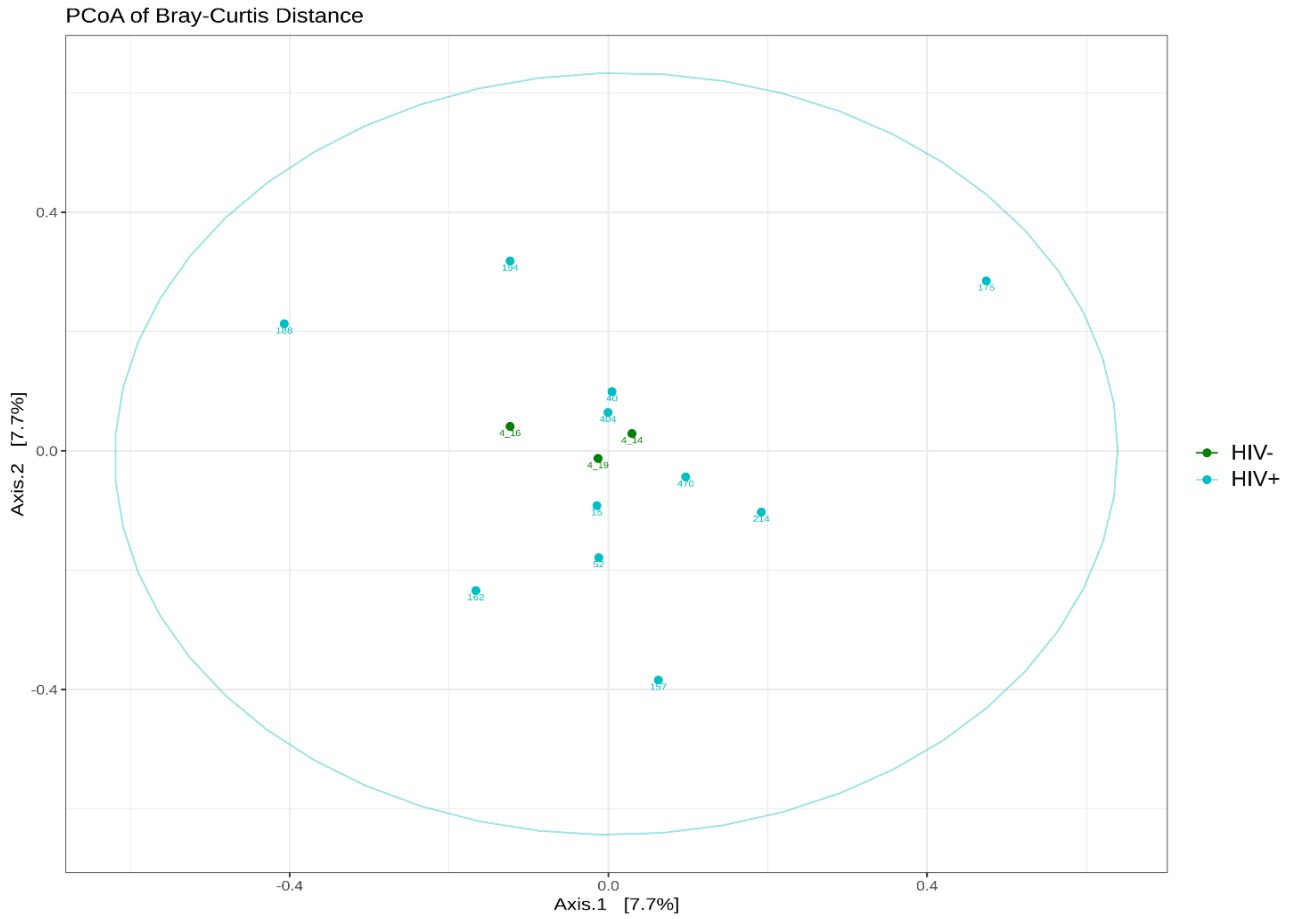

Representation of beta-diversity based on Bay Curtis and Jaccard distances. Each dot represents a sample. Differences in beta diversity (Bray-Curtis and Jaccard distances) were investigated with Permutation Based Analysis of Variance (PERMANOVA) with Adonis function.

2.1.2 Presence of detectable CSF virome

We investigated whether demographic, clinical, and HIV-related characteristics differ between participants with versus without detectable CSF virome according to the contigs-based results. No characteristic was associated with the presence of CSF virome except for sex at birth. Specifically, detectability of CSF virome was more frequent in female participants compared to males: in the whole study population (n=92), 25.0% of female participants had detectable CSF virome versus 11.8% of male participants (p=0.121); among

PWH (n=81), 26.1% of female participants had detectable CSF virome versus 8.6% of male participants (p=0.039).

Figure 6. Prevalence of detectable CSF virome by Sex at birth.

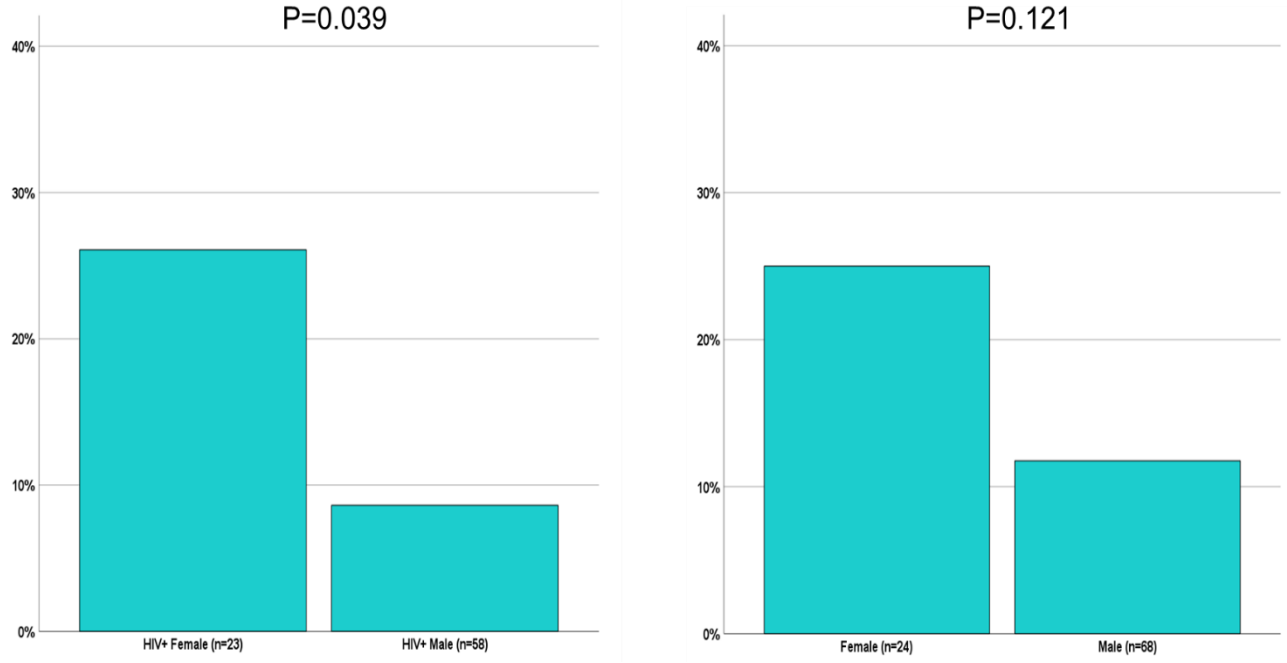

After adjusting for age, ethnicity, HIV status, and CSAR, female sex at birth remained significantly associated with higher likelihood of detectable CSF virome in the whole study population (aOR 3.9 [1.2-14.8], p=0.038) and in PWH only (aOR 4.9 [1.2-19.4], p=0.025). Further adjustments for HIV acquisition route and CD4+ T cell count in PWH did not affect the association (aOR 6.6 [1.4-30.6] for female versus male sex, p=0.017).

2.2 Reads-based method: taxonomic composition of CSF virome

When the taxonomy assignment was obtained by supporting each viral taxon with at least two unique reads, independent of Kraken confidence score, virome was detected in 78 (96.3%) PWH and 11 (100%) CWH. Bacteriophages accounted for the 71% of total viral reads and were detected in 87 subjects (median, IQR number of reads: 27 [9-69]), and *Siphoviridae* constituted the most abundant phage community (number of reads per sample 13 [5-29]; Figure 7). In addition to a significant presence of bacteriophages, we identified several sequences for eukaryotic human DNA and RNA viruses, and eukaryotic invertebrate, animal, and plant viruses, which accounted for the 17% and 12%, respectively, of the total viral reads and were detected in 44 (number of reads 11 [6-38]) and 47 subjects (number of reads 10 [4-18]), respectively (Figure 7).

Figure 7. CSF virome composition among positive samples (n=89) using the taxonomy assignment by reads without cut-offs.

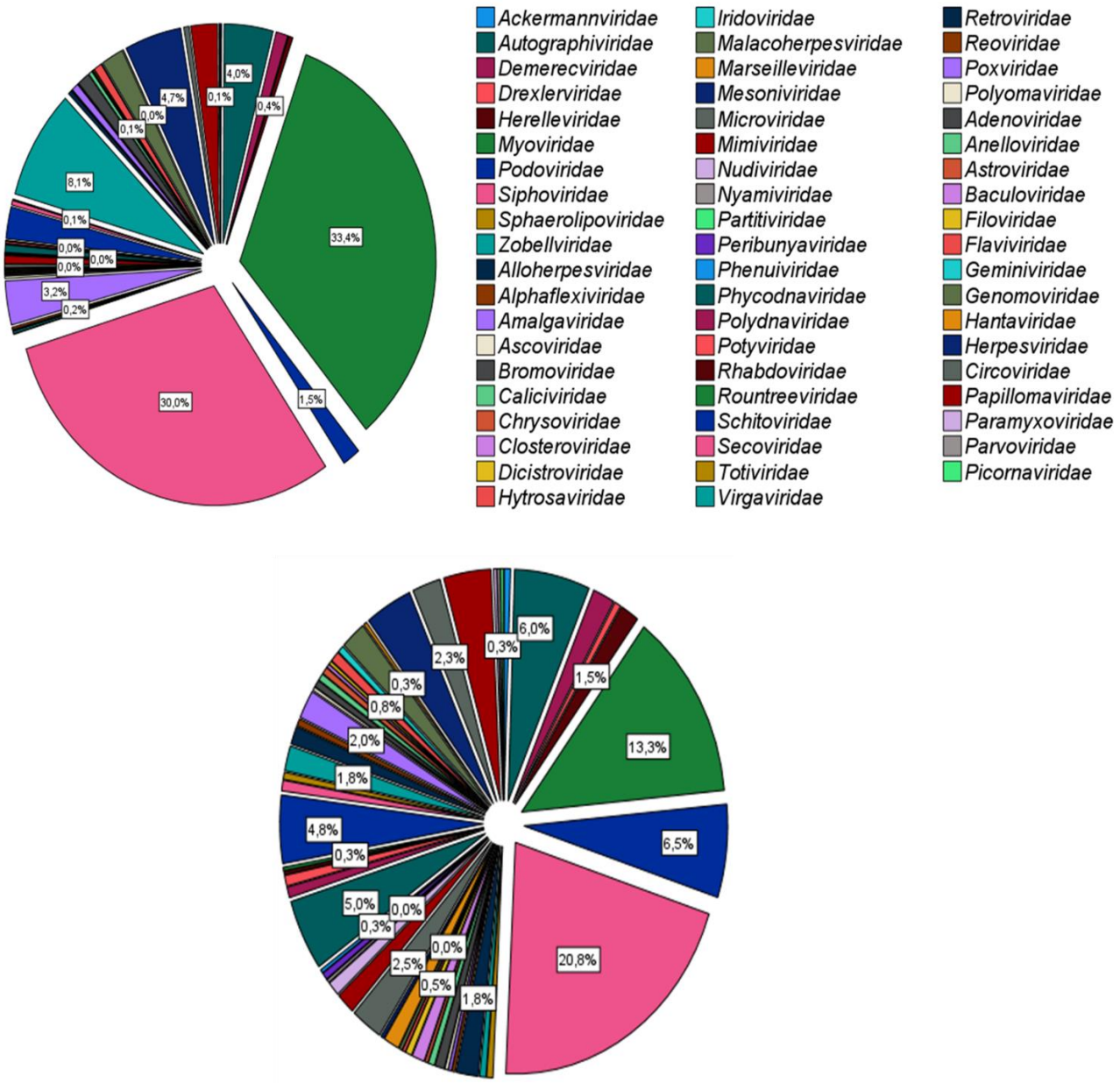

Two unique reads per taxon were considered without cut-offs. The upper pie reports the relative abundance in number of viral reads among the CSF samples positive for at least one viral read (n=89; of which 78 PWH and 11 CWH): 66.4% of all the reads were attributable to Myoviridae and Siphoviridae (bacteriophages). The lower pie chart shows the proportion of samples positive for each identified viral taxon (family level): 20.8% were positive for Siphoviridae, followed by 13.3% for Myoviridae and 6.5% for Podoviridae (all the three bacteriophages).

Figure 8. CSF virome composition among positive samples (n=47) using the taxonomy assignment by reads with the Kraken cut-off.

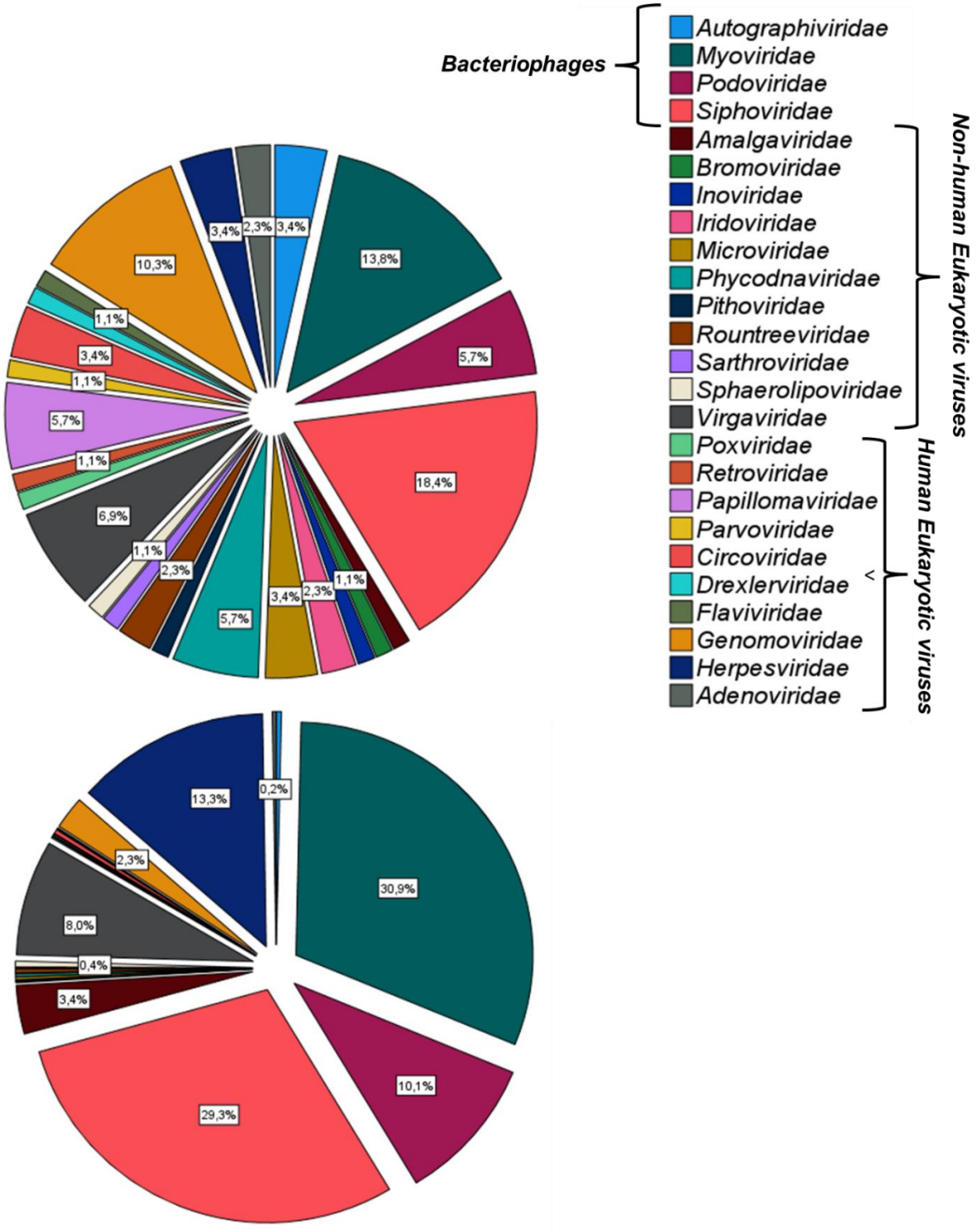

Two unique reads per taxon were considered with a Kraken confidence score >0.50. The upper pie chart shows the proportion of samples positive for each identified viral taxon (family level): bacteriophages were the most represented (e.g., Syphoviridae and Myoviridae in 18.4% and 13.8% of positive samples), followed by Genomoviridae (human eukaryotic 10.3%) and Virgaviridae (6.9%). The lower pie chart shows the relative abundance in number of viral reads among the positive samples: Myoviridae, Siphoviridae, and podoviridae were once again the most detected (70.2% of all the reads covered by the three bacteriophages families), followed by Herpesviridae (13.3%).

When the taxonomy assignment was obtained by supporting each viral taxon by at least two unique reads with a Kraken confidence score >0.50, virome could be retrieved for 47 samples, of which 39 (48.1%) from PWH and 8 (72.7%) from CWH. Bacteriophages accounted again for 71% of total viral reads and were detected in 26 subjects (number of reads 30 [5-86]), and *Siphoviridae* constituted again the most abundant phage community (number of reads per sample 3 [0-32]; Figure 8). In addition to bacteriophages, eukaryotic human DNA and RNA viruses accounted for 16% of total viral reads and were detected in 21 (number of reads 10 [4-33]) subjects. Eukaryotic animal, invertebrate, and plant viruses accounted for 13% of total viral reads and were detected in 18 (number of reads 4 [2-11]) subjects (Figure 8). As for taxonomic classification by contigs, and for the same reason linked to the depth of sequencing, taxonomic classification by reads failed to identify HIV-1, EBV and JCV reads.

Looking at pairs of repeated samples, the number of samples in which CSF virome was retrieved and the number of reads did not differ significantly between the first and second experiments, likewise when the confidence score was applied (number of samples and median number of reads: 7, 42 [2-57] vs 6, 7 [3-44], p=0.176 by Wilcoxon test without applying the confidence score; 4, 1 [0-13] vs 2, 0 [0-4] p= 0.893 by Wilcoxon test applying the confidence score).

2.2.1 Diversity against HIV status and clinical parameters

To determine potential differences in virome composition between PWH and CWH and by detectable and undetectable HIV RNA groups, α and β diversity were examined. In α diversity analysis, the CSF viral communities did not differ between PWH and CWH or between CSF HIV RNA detection and not, when considering either reads without confidence score cut-off or reads with a Kraken confidence score >0.50 (Figures 9 and 10).

Figure 9. Estimating α diversity of the viral communities obtained by CSF samples against HIV status and CSF HIV-RNA detection (two unique reads per taxon).

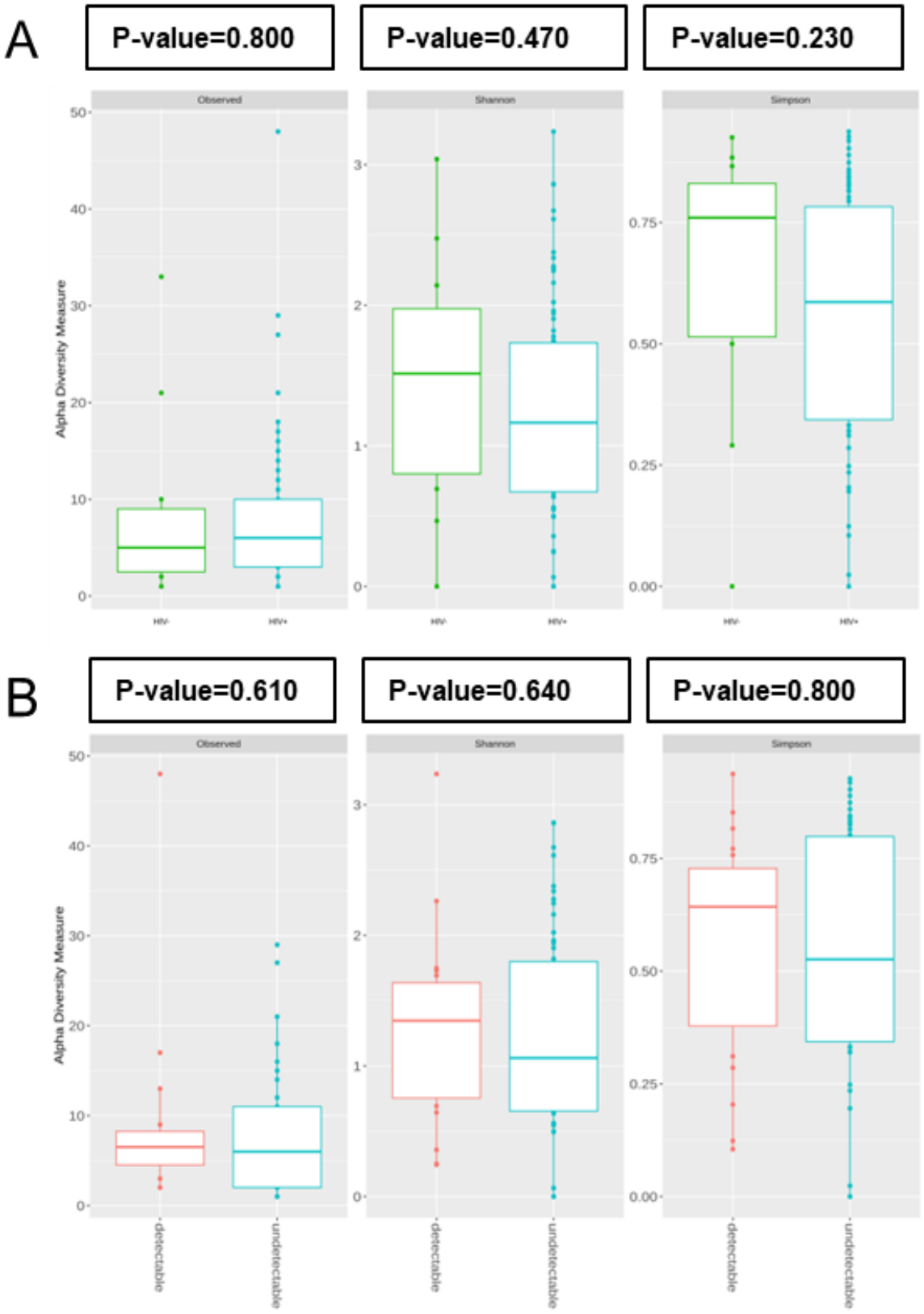

Observed, Shannon and Simpson diversity indexes of the viral communities against HIV status (panel A) and CSF HIV-RNA detection (panel B).

Figure 10. Estimating α diversity of the viral communities obtained by CSF samples against HIV status and CSF HIV-RNA detection (two unique reads per taxon with a confidence score >0.50).

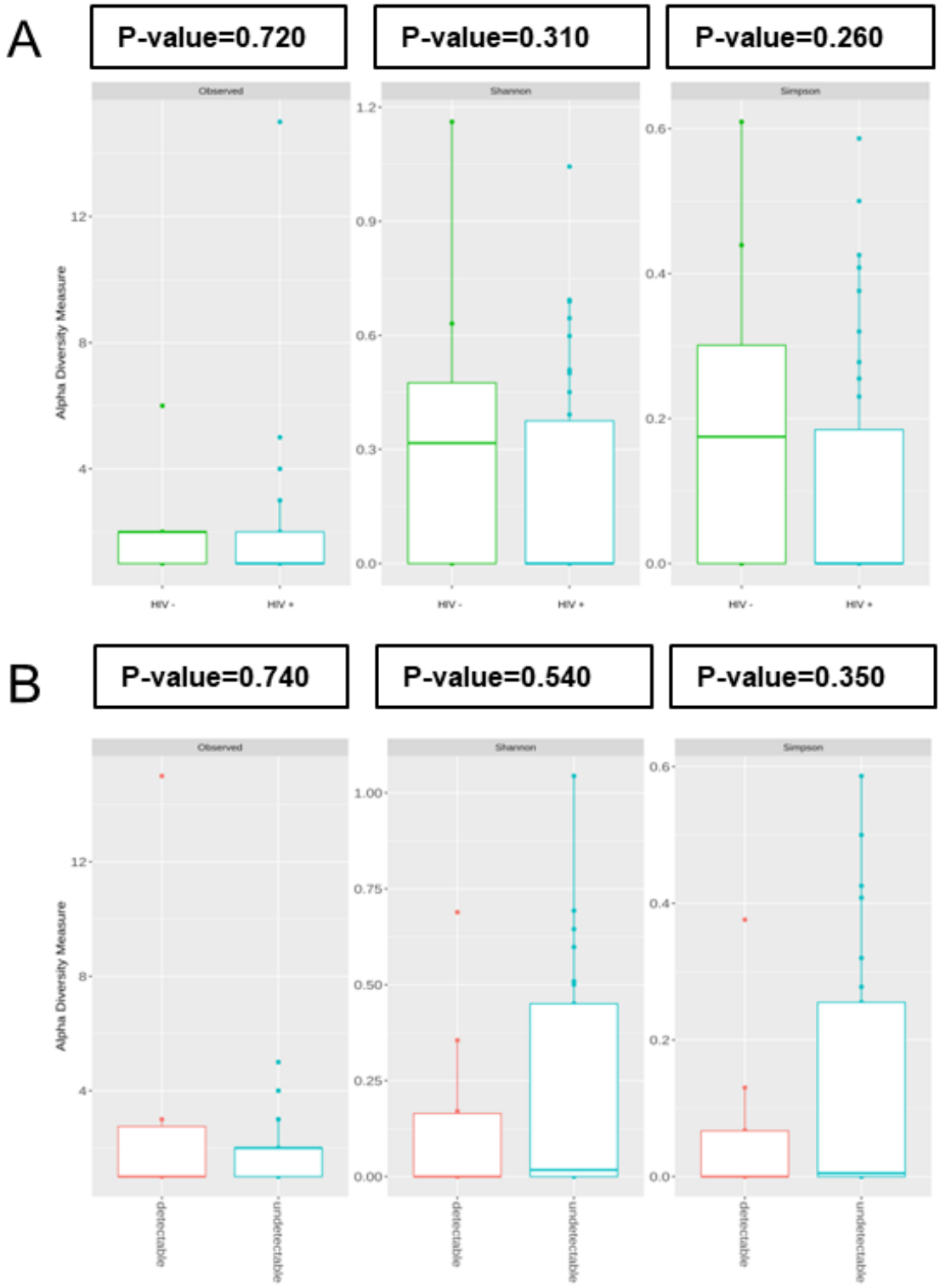

Observed, Shannon and Simpson diversity indexes of the viral communities against HIV status (panel A) and CSF HIV-RNA detection (panel B).

The β diversity analysis between PWH and CWH showed no clear definition of clusters (PCoA, Figure 11). This overlap in community composition was confirmed statistically via Adonis (p=0.218 and 0.333). The same analysis considering CSF HIV RNA detection showed two taxonomic patterns discriminating samples with detectable CSF HIV RNA and samples with undetectable CSF HIV RNA (Figure 11). These different patterns could be explained by the phage *Siphoviridae* family, which was more frequently detected in CSF HIV RNA negative samples than in CSF HIV RNA positive samples (57 [98.3%] vs 15 [75.0%], P=0.004). No other differences were detected (e.g, by CSF proteins above or below 45 mg/dL, CSF biomarkers, or neurocognitive diagnoses; data not shown).

Figure 11. β diversity of the viral communities by HIV status and CSF HIV-RNA detection (considering two unique reads per taxon).

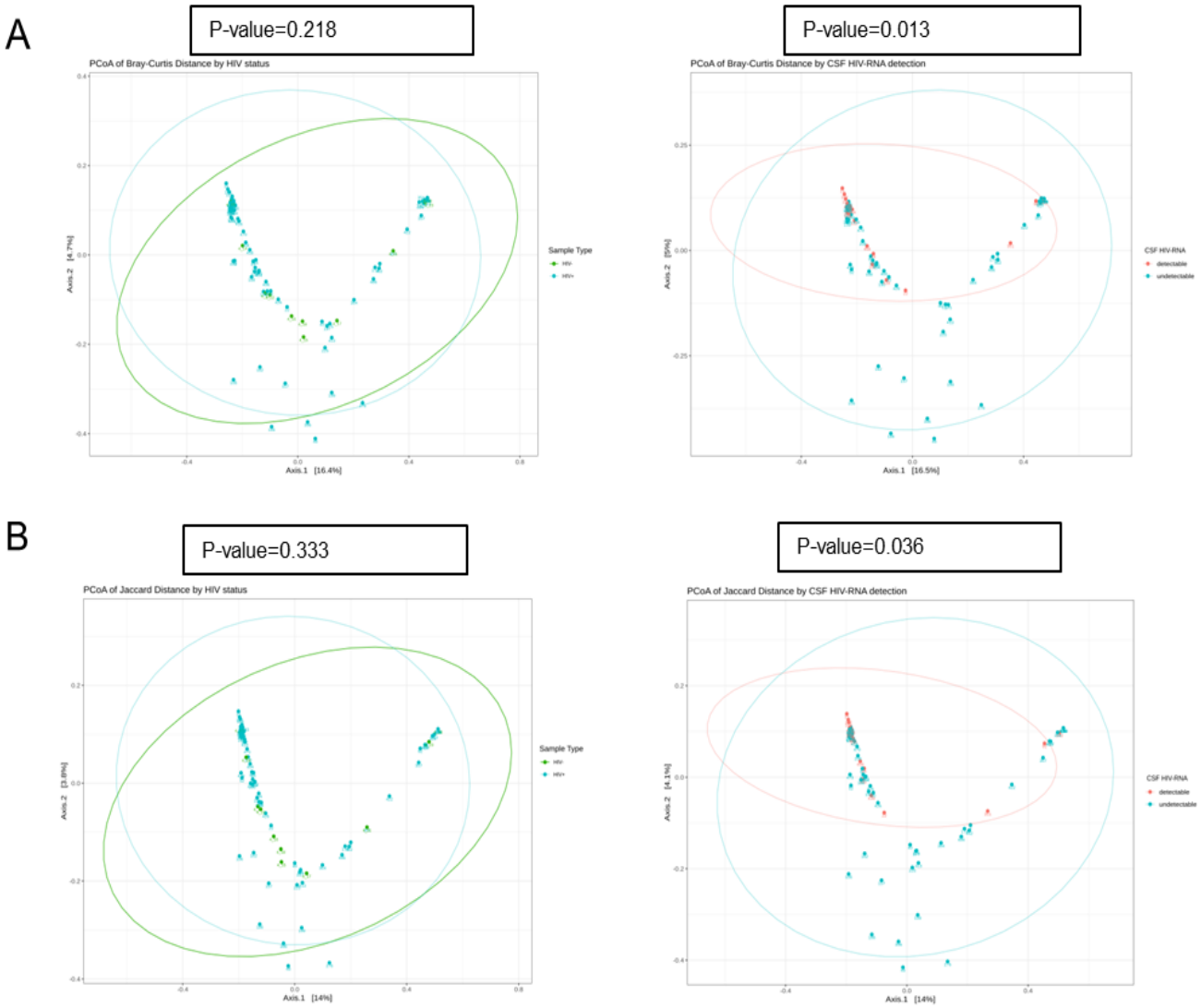

Representation of beta-diversity based on Bray Curtis and Jaccard distances. Each dot represents a sample. For HIV status, green represents HIV-1 negative samples, while blue represents HIV-1 negative samples. For CSF HIV-RNA, red represents CSF samples characterized by episodic detection of HIV-1 RNA in CSF, while blue dots represent CSF samples characterized by the absence of HIV-1 RNA in CSF.

The β diversity analysis with reads and a confidence score >0.50 showed two taxonomic patterns discriminating PWH and CWH (Figure 12). This difference in community composition was confirmed statistically via Adonis (p=0.019 and 0.017). However, when the frequency and abundance of each viral family were compared between PWH and CWH no differences were detected. The same analysis considering CSF HIV RNA detection showed no differences between samples with detectable CSF HIV RNA and samples with undetectable CSF HIV RNA (Figure 12). No differences were detected against clinical parameters (e.g, CSF proteins above or below 45 mg/dL, CSF biomarkers, neurocognitive diagnoses; data not shown).

Figure 12. β diversity of the viral communities by HIV status and CSF HIV-RNA detection (considering two unique reads per taxon with a confidence score >0.50).

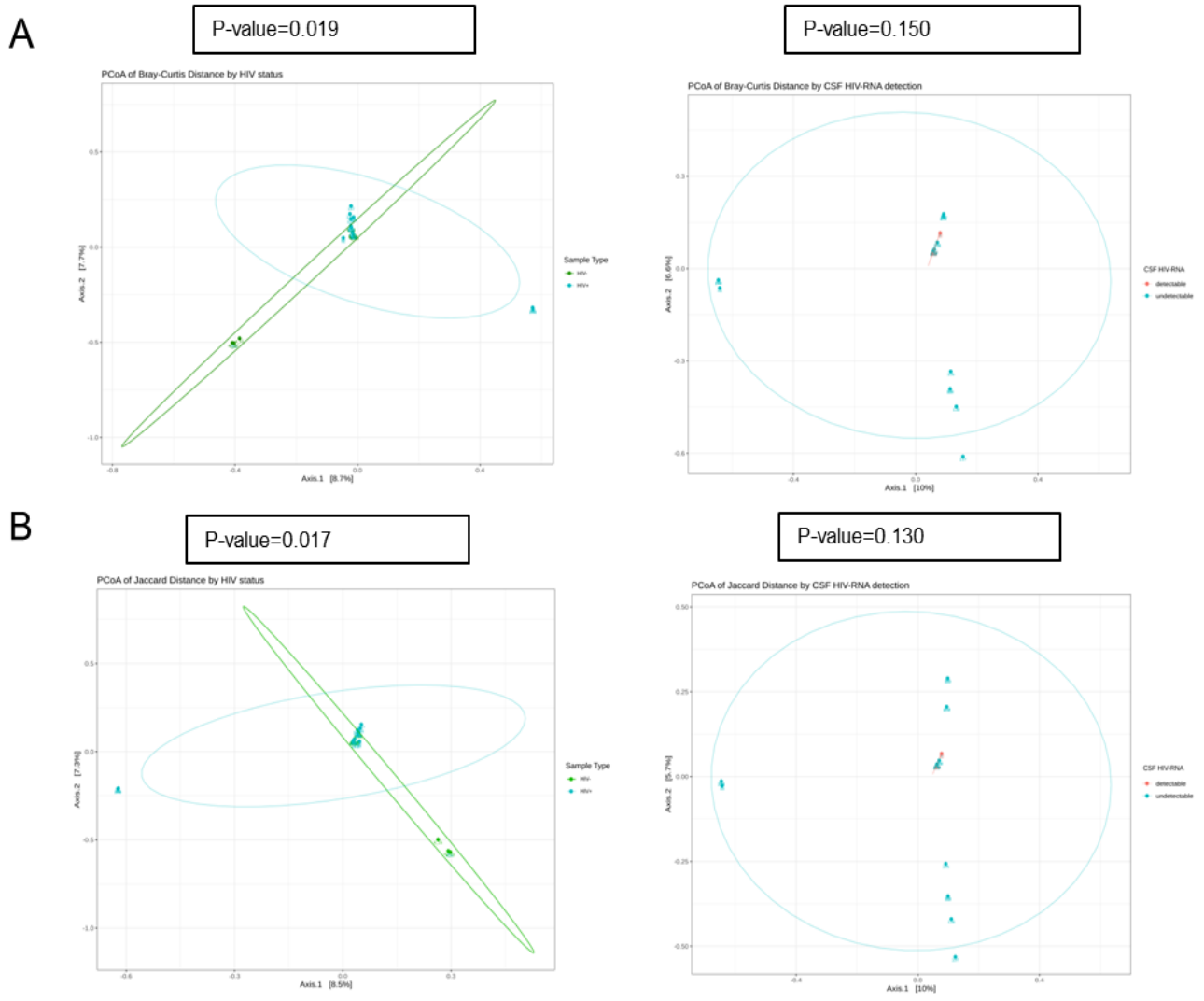

Representation of beta-diversity based on Bray Curtis and Jaccard distances. Each dot represents a sample. For HIV status, green represents HIV-1 negative samples, while blue represents HIV-1 negative samples. For CSF HIV-RNA, red represents CSF samples characterized by episodic detection of HIV-1 RNA in CSF, while blue dots represent CSF samples characterized by the absence of HIV-1 RNA in CSF.

2.2.2 Cluster Analysis

Considering that α and β diversity analyses relied on clinical cut-offs (e.g., normal CSF protein and cells, BDI-II above or below 14) and that these thresholds have never been related to virome composition before, we also performed unsupervised two-step cluster analysis to remove any potential bias introduced by these arbitrary cut-offs.

We hypothesized that participants with sterile CSF compared to CSF milieu harboring viruses have differences in CSF biomarkers and HIV-related parameters. We also hypothesized that the CSF virome composed by viruses evolutionary adapted to be part of it (e.g., *Herpesviridae*) compared to “unusual” viruses (e.g., nonhuman eukaryotic viruses) or to bacteriophages (for which a co-adaptation with human is known, as example within the gut [1,3,5], but no data is useful in confirming co-adaptation in the CNS) is associated with distinct CSF features (measured by CSF biomarkers) and eventually with cognitive performance and depressive mood. Therefore, the clustering was based on the relative abundance of viral reads (after the confidence score cut-off of >0.5) attributed to prokaryotic, human eukaryotic, and nonhuman eukaryotic viruses.

The procedure reported a four-cluster classification as the optimal solution for the data (Figure 13): tightness and separation of the silhouette was extremely high (0.9) with the lowest Bayesian Information Criterion of 118 (vs 140 and 141 of the prior and the next clustering solution), and the highest ratio of distance measures of 12.8 (vs 1.2 and 1.6 of the prior and the next clustering solution). The contribution of predictors in defining clusters was 100% for human eukaryotic, >95% for prokaryotic and >80% for nonhuman eukaryotic viruses.

CWH were included in the clustering but thereafter contributed only to the analyses involving data that were available for this group (e.g., demographics, intrathecal synthesis, CSF cells and protein).

Figure 13. Clustering measures of separation and identified clusters of CSF virome.

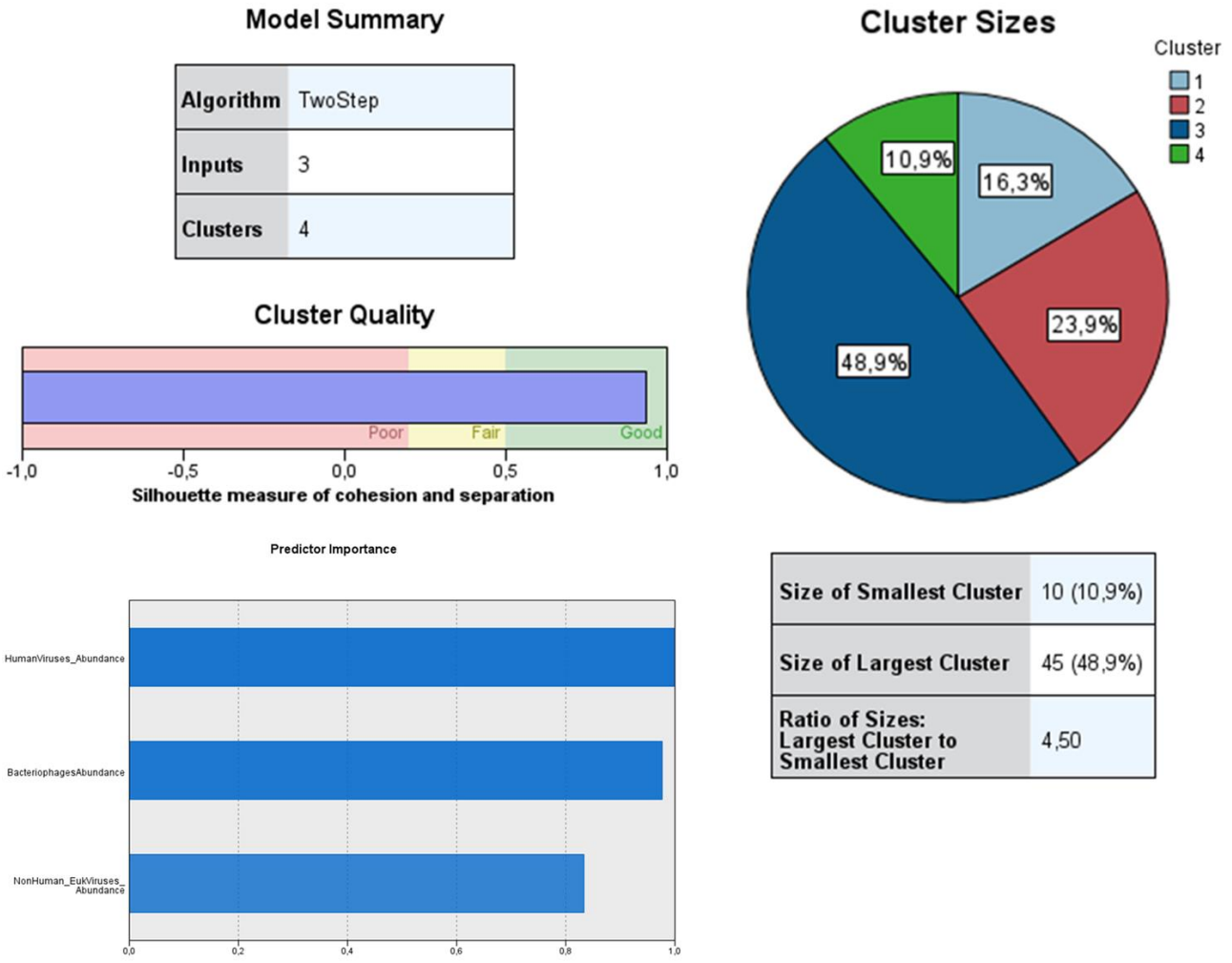

As shown in Figure 14, Cluster 1 (C1) was composed of 15 (16.3%) participants that were characterized by the highest relative abundance of human eukaryotic viruses in their CSF, and low/null contribution of other viral groups. Cluster 2 (C2) was represented by 22 (23.9%) participants with CSF virome mainly composed by bacteriophages, and with milder contribution of eukaryotic (human and nonhuman) viruses. Cluster 3 (C3) was composed of the 45 participants (48.9%) with no ("sterile") CSF virome, and Cluster 4 (C4) grouped 10 (10.9%) participants whose CSF virome was mainly composed by nonhuman eukaryotic viruses. The proportion of CWH did not statistically differ across the clusters (p=0.366), despite higher concentration was observed in C2 and C4: 6.7% of C1, 18.0% of C2, 6.7% of C3, and 20.0% of C4.

Figure 14. Absolute and relative distribution of the cluster predictors within clusters.

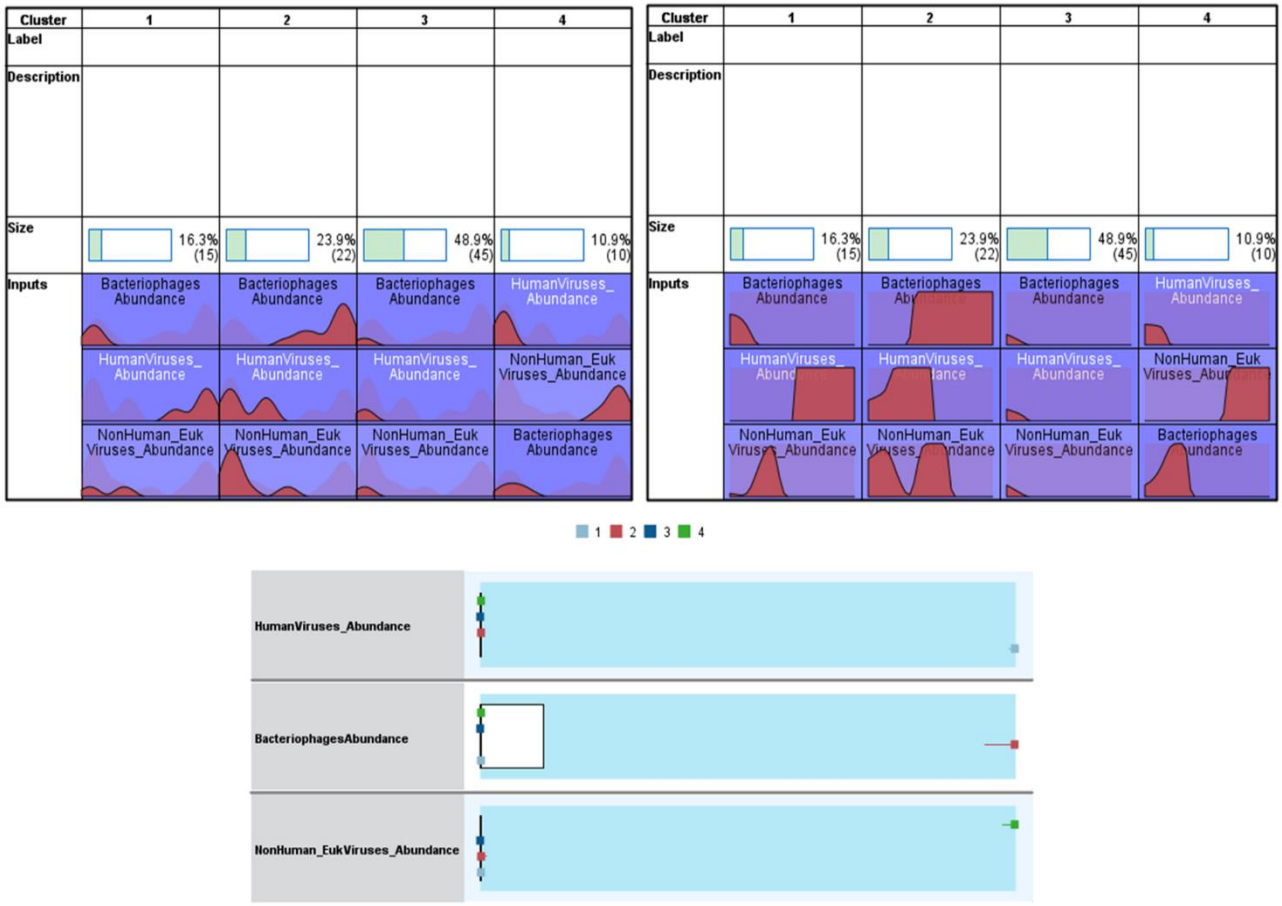

Comparisons between the clusters detected very limited and specific differences in immunological parameters, CSF biomarkers, and neuropsychiatric conditions (as shown in Table 6 and Figures 15-16). No difference in demographics was observed across clusters, as well as in most clinical and HIV-related parameters, nor in depressive mood. Notably, the "sterile" C3 had lower CD4+ T cell count compared to C2 (441 [238-659] vs 702 [485-831] cells/μL), higher CSF protein than C1 (49 [39-56] vs 39 [31-48] mg/dL) and C2 (38 [29-48] mg/dL), higher CSAR than C2 (6.2 [4.8-7.6] vs 4.7 [3.6-5.5]), and higher CSF βA42 levels than C1 (950 [743-1086] pg/mL vs 791 [630-878] pg/mL; Table 6). The "expected CSF virome" C1 had significantly less cognitive impairment compared to all the other clusters and all the cases in the asymptomatic degree (12.5% and 100% asymptomatic vs 61.5% of whom 50% symptomatic in C2, vs 67.6% of whom 16% symptomatic in C3, and vs 66.7% of whom 25.0% symptomatic in C4; see Table 6 and Figure 15). The "nonhuman CSF virome" C4 had higher CSF cells compared to all the other clusters (0 [0-2] vs 0 [0-0] cells/mL for all clusters) and higher CSAR (6.3 [4.5-8.8] vs 4.7 [3.6-5.5] in C2; Table 6). Of note, most of the values of the parameters that differed between clusters were in any case within the

normal range (e.g., CSF cells, CSAR, β amyloid). Figure 16 summarizes the 6 markers in CSF and blood that distinctly differ across the four clusters.

Table 6. Comparison of clinical and viro-immunological variables between the clusters (only significant variables are shown).

	KW p	Comparisons between clusters (direction and p value°)					
		1 vs 2	1 vs 3	1 vs 4	2 vs 3	2 vs 4	3 vs 4
Current CD4+ T cell count, cells/µL	0.008	L 0.002			H 0.019	H 0.011	
Current CD4+ T cell count, %	0.017	L 0.025			H 0.012	H 0.011	
Duration of HIV infection, years	0.018	L 0.002	L 0.032	L 0.049	H 0.024		
CSF leukocytes, cells/mL	0.013			L 0.006		L 0.028	L 0.014
CSF protein, mg/dL	0.026		L 0.050		L 0.017		
CSAR	0.048				L 0.008	L 0.047	
CSF βA42, pg/mL	0.012	L 0.004	L 0.011				
Neurocognitive impairment, n	0.039	L 0.034	L 0.032	L 0.048			

°Only p value≤0.05 are reported. KW, Kruskal Wallis test; L, lower in former cluster versus the latter cluster; H, higher in the former cluster versus the latter cluster; CSF, cerebrospinal fluid; CSAR, CSF to serum albumin ratio; βA42, fragment 1-42 of the amyloid beta.

Figure 15. Prevalence of cognitive impairment among the clusters.

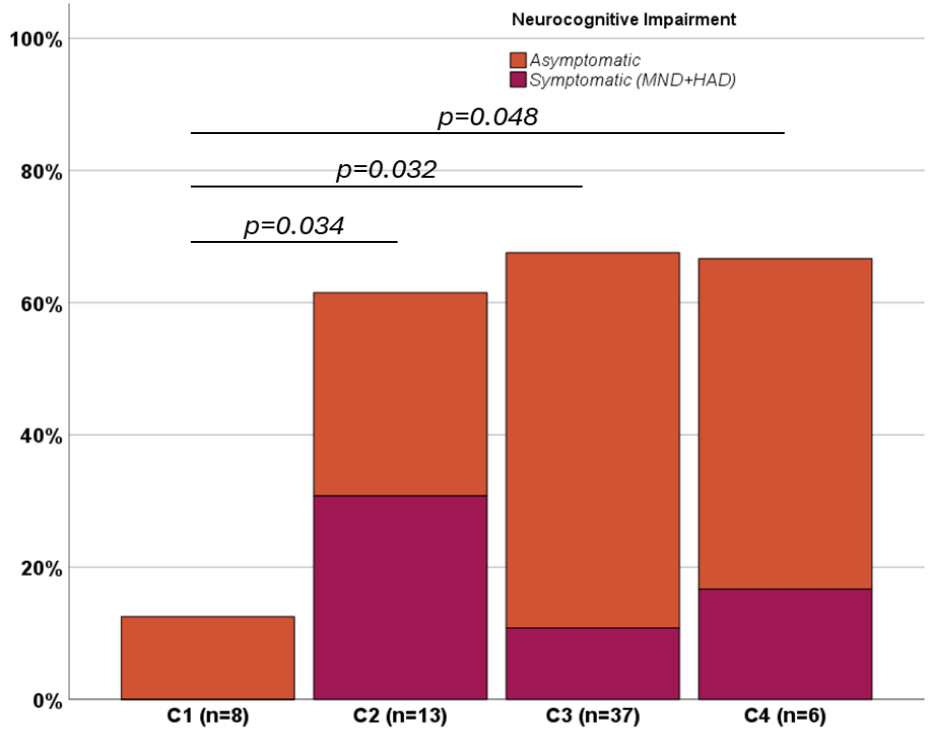

Legend: MND, mild neurocognitive impairment; HAD, HIV-associated dementia.

Figure 16. Box plots of CSF and immune markers differing between the clusters.

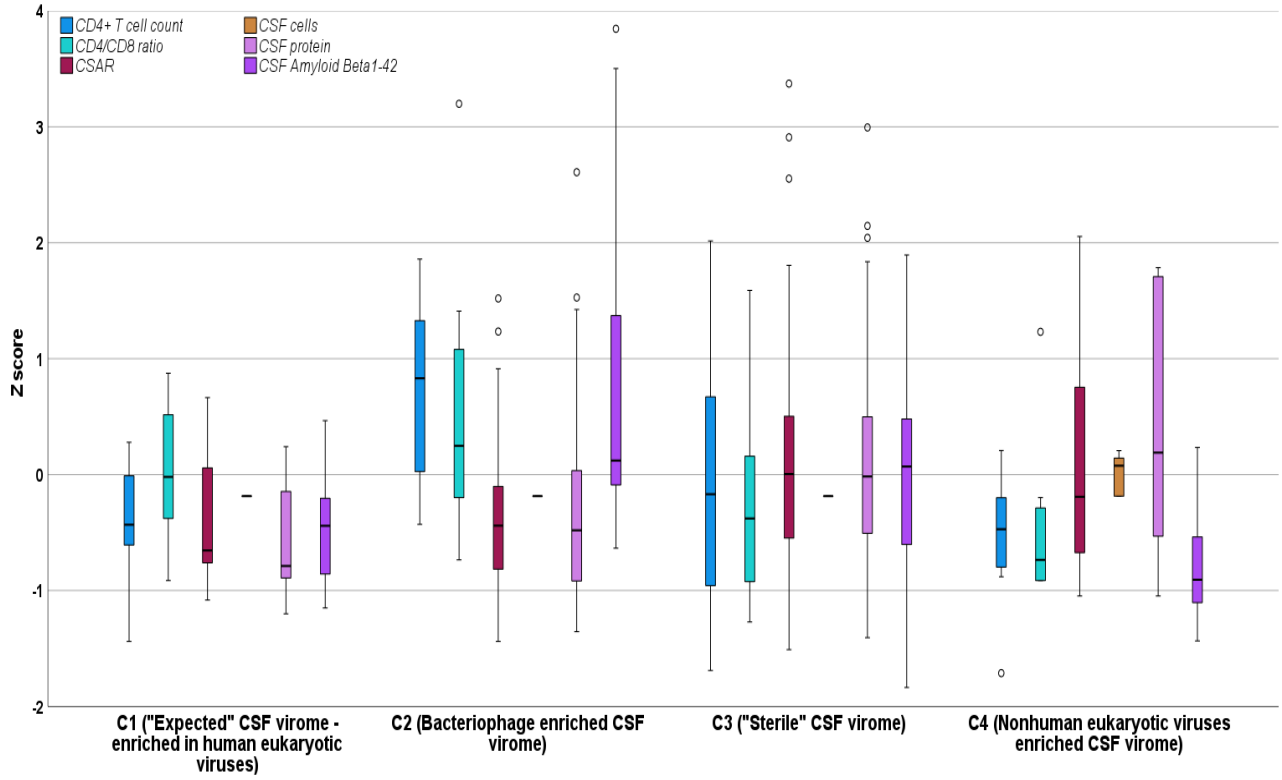

Legend: CSF, cerebrospinal fluid; CSAR, CSF-to-serum albumin ratio.

Univariable analysis observed an association between CSF virome by cluster and neurocognitive impairment: compared to C1, C2 (OR 11.2 [1.1-120.4], p=0.046), C3 (OR 14.6 [1.6-132.3], p=0.017) and C4 (OR 14.0 [0.95-207.6], p=0.055) had each significantly higher prevalence of cognitive impairment (the large confidence intervals are due to the small number per group and the application of Firth penalized method).

In adjusted analysis, the CSF clusters retained the association with different prevalence of cognitive impairment independently from the other parameters that differed between clusters, and from age, depressive mood, and education (the results of entry method for variable retention are shown in Table 7; model's R^2=0.46 and p=0.015; similar results were obtained through backward selection method to address potential overfitting; data not shown).

Table 7. Multivariable logistic regression for neurocognitive impairment (n=64).

	aOR (95%CI)*	P value
CSF virome cluster, C1	Ref.	-
C2	10.1 (0.6-168.6)	0.062
C3	17.1 (1.5-198.6)	0.014
C4	31.3 (1.6-993.7)	0.030
Age, years	1.1 (0.9-1.2)	0.066
CSAR	1.3 (0.6-3.0)	0.538
CD4+ T cell count, cells/μL	1.0 (1.0-1.0)	0.088
CSF amyloid β 1-42, pg/mL	1.0 (0.9-1.0)	0.681
CSF cells, cells/mL	1.0 (0.9-1.1)	0.706
CSF protein, mg/dL	0.9 (0.8-1.1)	0.665
Education, years	0.9 (0.7-1.1)	0.288
BDI-II score	1.1 (1.0-1.2)	0.143
Length of HIV infection, years	0.9 (0.9-1.0)	0.499

*Legend: aOR, adjusted odds ratio; 95%CI, 95% confidence interval; CSF, cerebrospinal fluid virome; C, cluster; CSAR, CSF to serum albumin ratio; BDI-II, Beck Depression Inventory II. *Firth penalized regression method was applied.*

Discussion

We have described the presence and composition of the CSF virome in sample of PWH on effective ART (plasma viral load <200 cp/mL), valid immunological status, and significant prevalence of mild cognitive impairment and depressive mood, as representative of modern cohorts of PWH. In line with our hypothesis and with previous limited evidence in people without HIV [4,5], human CSF cannot be considered anymore a sterile body fluid regardless of HIV status, immune performance, neurological signs or symptoms, and BBB permeability. In fact, communities of eukaryotic (human and nonhuman) and prokaryotic viruses were detected with similar prevalence in both PWH and CWH, participants with intact or altered BBB, and participants with or without neuropsychiatric complaints. Contrary to our hypothesis, the presence and composition of CSF virome did not result to be significantly associated with BBB permeability, immune performance, and CSF levels of inflammation and immune activation. However, in restricted analyses dependent on taxonomic attribution methods and grouping of the participants, the composition of the CSF virome and some of its characteristics (e.g., relative abundance of eukaryotic *versus* prokaryotic viruses, β diversity) were variably associated with HIV status, neurocognitive performance, CD4+ T cells, CSAR, CSF β amyloid, and CSF proteins.

Among the several observations, our findings lead to a primary and concerning one: the large variability in taxonomy attribution, and thereby in the detectability and composition of CSF virome, across the three pipelines that were followed for taxa attribution: one based on contigs reconstruction, and two based on reads with or without Kraken confidence score. The choice between using reads or contigs for taxonomy attribution depends on various factors, and each has its own set of pros and cons: reads-based approaches can detect more diverse genetic material, they have higher sensitivity for microbial diversity and low-abundance species, and they cover a broader range of taxon abundances within the same community [163–170]. From a practical perspective, the computational efficiency of reads-based methods is better than the one provided by contigs reconstruction, being less intensive, faster, and more scalable for large datasets [163–170]. On the contrary, the accuracy in taxonomic attribution can be lower, as genetic fragments may not span the entire length of a long gene or genomic region, which in turn can lead to ambiguity and inaccurate assignments [163–170]. Contigs-based methods use longer sequences of DNA/RNA, enhancing the accuracy in assignments (e.g., in differentiating closely related species), but this improvement comes with the costs of higher computational intensity, of loss in sensitivity, which can lead to miss lower-abundance species and to underestimate viral diversity, and

of greater risk of introducing assembly artifacts through chimeric sequences and taxonomic misinterpretations [163–170]. Based on these and on the very limited previous information on human virome in the CSF [4,5], we were not confident enough in making any assumption to prefer one method instead of the other. Furthermore, and more importantly, we performed these three methods of taxonomic attribution and presented all their results for the following considerations:

1) Current studies having the human virome as a predictor of clinical outcomes have been used either one of the two methods (reads vs contigs) only and drawn conclusions that have never been reinforced or confuted by comparing their results with those obtained by alternative methods within the same dataset (e.g., virome studies in PWH: [37–40,171–175]); this occurs despite the aforementioned relevant differences between the methods and limits data comparability. Furthermore, in most of the studies the choice of the method of taxonomic attribution is never explained and justified by hypotheses or models. Without a consensus on the most reliable method, we opted to present and discuss the findings of all the methods. Plausibly, the choice of the method should also weight study objectives, type of biological samples, and expected richness and diversity of local microbial communities, and it should not be merely based on available computational resources and bioinformatics expertise.
2) Our hypothesis model did not specify *a priori* - and voluntarily - the origin of the viral communities in the CSF. While the routes and mechanisms of entry into the CNS of neurotropic human eukaryotic viruses (e.g., *Herpesviridae*) are well known [176], the detection of nonhuman eukaryotic and prokaryotic viruses in the CSF should be carefully explained with alternative and non-mutually exclusive origins: these viruses could be carried by trafficking cells into the CSF/CNS (e.g., macrophages, bacteria), they could actively cross the BBB (e.g., through receptor bindings, pinocytosis, or leakage through severely impaired barriers), and they could passively overcome the blood filtering at the choroid plexus. Lastly, they could also represent fragments of genetic material rather than intact virions, which have been neutralized by the immune system in periphery (e.g., in the gut or in the blood). These circulating fragments can more easily cross the BBB thanks to their potentially very small size, similarly to what has been described for products of microbial translocation [177,178]. If we do give credit to all these hypotheses, NGS pipelines which use contigs to assign viral taxa could miss most of the genetic fragments of such viruses, as aforementioned. While it is arguable that genetic fragments are not active “living” components of microbial communities such as virions, it is also true

that their immunomodulatory properties may not be null, and their presence in the body, including the CSF, might trigger immune responses and activation of immune cells [3,5], which were the target of our biomarkers and the hypothesized pathogenic mechanism behind the neurocognitive outcomes of our study.

For all these reasons, we also eventually considered that a hybrid method such as the taxonomic attribution based on reads but filtered through a confidence score could be a balanced compromise between the higher sensitivity of reads assignment (not to miss shorter genetic fragments of dead virions) and the need of higher accuracy to avoid false attributions [145,146]. Therefore, we won't discuss the findings coming from the taxonomic attribution based on reads without confidence cut-off. In support of this conclusion and of the hypothesis of the origins of the CSF virome, several observations can be made through our findings:

1) All the human eukaryotic viruses identified by each of the methods have been previously reported in human CSF and neuroinvasive mechanisms have been provided for most of them [153–160,176]. Indeed, for some of them the contamination of CSF through blood or skin during the LP cannot be ruled out with certainty (e.g., HCV, HPV, *Molluscum contagiosum virus*).
2) None of the participants with and without HIV had clinically symptomatic systemic or CNS infections at the time of CSF collection, nor laboratory markers compatible with undiagnosed infections (e.g., no CSF leukocytes, normal CSF protein and CSF glucose). This may suggest that immune or bacterial cells trafficking from periphery into the CSF is not a common mechanism explaining the presence of viral communities in the CSF of individuals without ongoing infections. The absence of CSF cells (including red blood cells) also reduces the possibility of CSF contamination by blood during the LP. Lastly, the lack of cells able to be infected by viruses (either human or bacterial cells) also suggests that at least part of the viral material detected is probably not in the form of virions but fragments.
3) About one fifth of both PWH and CWH had variable degree of BBB impairment (from mild to severe). This data hints to alternative mechanisms of entrance of the virions and their fragments other than the simple crossing of permeable BBB.
4) Many of the non-human eukaryotic viruses and prokaryotic viruses detected in the CSF of our participants by each of the methods have been previously described as components of the human gut and blood virome [7,115,179,180]. Most of the bacteriophages assigned by contigs (*CrAssphage, Corynebacterium, Burkholderia,*

Acinetobacter, and *Pseudomonas* genus) are phages of bacteria that can be found in human gut either as pathogens, commensal symbionts, pathobionts, or persistent or transient bystanders, and similarly, all the phages identified by reads (*Syphoviridae, Podoviridae, Myoviridae, and Autographiviridae)* are phages of *Enterobacteriaceae* and the most common viral species in the human gut virome [7,9,115,179,181–187]. *Cronobacter* spp is an environmental bacteria that contaminates powdered milk, herbal teas, and starches, and its phage can come along in contaminated foods [188]; similarly, the two plant viruses by contigs (*Southern tomato virus* and *Tomato brown rugose fruit virus*) are common viruses that infect tomato seeds and plant, and their pathogenic effects can be slow or null, leading to the possibility that human ingest infected tomatoes that look edible [189,190]. For other viruses the hypothesis of their origin is less straightforward: *Mastadenovirus C* is a pathogenic virus that can cause respiratory tract infections in children, while it is usually asymptomatic in older ages [191]; the fact that it has been previously identified also in human CSF ([192,193]) may suggest either neurotropism or transient blood viremia that could lead to CSF spillage. Similarly, *Gemycircularvirus HV-GcV2* has been identified sporadically as the etiological cause of recurrent pericarditis in human [194], suggesting a possible circulation in blood that can reach CSF too.

We did not perform virome analysis in the blood, feces, or gut samples of our participants. This addition could have significantly improved the interpretation of the possible gut or blood origin of CSF viruses. Future studies should overcome such limitation by performing sequencing in paired samples of CSF, blood, and possibly gut. Of note, in the study of Ghose et al., where CSF, plasma, saliva, urine, feces, breast milk, and other body fluid samples from participants with and without CNS infections were analyzed, the type of sample only moderately affected β diversity [4]. Furthermore, both α and β analyses clustered the CSF virome as closer to the virome in plasma, breast milk, and body fluids, and more distant from the composition and characteristics of the virome in feces, saliva, and urine [4].

Both the α and β diversity analyses by contigs and reads assignment did not support our hypotheses that the characteristics of CSF virome are associated with biomarkers of immunological status (e.g., CD4+ T cell count), inflammation (e.g., intrathecal synthesis, CSF tau), BBB permeability (e.g., CSAR), and immune activation (e.g., CSF neopterin), nor that the characteristics of CSF virome are associated with depressive mood or global cognitive performance.

According to contigs assignment, no demographic, clinical (including HIV status), viroimmunological variables and no biomarker was associated with the presence of CSF virome nor with α and β diversity, apart sex at birth. Female sex was associated with an adjusted significant increase in the probability of detecting viruses in the CSF. Despite we adjusted our model for HIV acquisition routes, several other factors not analyzed herein could explain this finding, which report a sex-based distinction previously observed in human viromes of other body niches [2,195,196]: e.g., differences in dietary and sexual behaviors, different prevalence of comorbidities, hormones levels, and differences in the immune system. Further studies should confirm this data to assess whether, how, and why sex-based differences in CSF virome could have distinct outcomes, as we could not stratify our association analyses by sex.

According to reads assignment with confidence score, no demographic, clinical, viroimmunological variables and no biomarker was associated with the presence of CSF virome nor with α and β diversity, apart HIV status. Interestingly, there was a significant divergence between the virome of PWH and that of CWH, which was however not dependent on the frequency or abundance of specific viral families. Among PWH, neither low-level traces of HIV RNA in CSF (measured through PCR) nor current and past CD4+ T cell count associated with between-samples distance. Furthermore, when participants were clustered by relative abundance of viral categories (human and nonhuman eukaryotic, prokaryotic), HIV status did not change significantly across the clusters. Future studies on larger sample size and that enroll HIV-negative controls should more powerfully assess this finding, and investigate the potential source (e.g., use of antiretrovirals and HIV-induced immunological perturbations [37,129,171,175]).

When CSF virome was investigated by clustering participants according to the relative abundance of the three major categories of viruses (human and nonhuman eukaryotic viruses, and prokaryotic viruses), more clinical variables and biomarkers resulted associated with CSF virome composition under this framework. The most represented cluster was C3 (~50% of participants) which was featured by the lowest/null presence of any viral species, followed by C2 (23.9%, prokaryotic viruses/bacteriophages' predominance), C1 (16.3%, human eukaryotic viruses' predominance), and C4 (10.9%, nonhuman eukaryotic viruses' predominance). Of note, C3 was called "sterile" based on the limit of detection of our NGS pipelines. The very low abundance or apparent total absence of viral species depends on the depth of sequencing and other factors that affect the sensitivity of our NGS methods, and none of the CSF could be considered truly sterile (HIV, EBV, and JCV detected by RT-

PCR were not detected by NGS and other neurotropic viruses highly prevalent in the general population were not detected, but likely present at variable degrees and combinations based on previous estimates [64,132,197]).

Using as reference C1, being primarily populated by human eukaryotic viruses, all the other clusters had longer duration of HIV infection, C4 – at its polarized opposite - had significantly higher CSF cells, while C3 had higher CSF proteins. C1 had also lower levels of CSF βA42 compared to clusters predominantly populated by bacteriophages or “sterile”. Most notably, C1 had extremely lower prevalence of neurocognitive impairment compared to all the others. While some of these findings may lead to conflicting conclusions compared to what previously expected and within our data, some considerations require further discussion. As example, βA42 should be consumed during chronic CNS infections, such those depicted in C1, and its reduced CSF levels as well as chronic CNS viral infections have been associated with cognitive impairment in people with and without HIV infection [71,198–203]. However, the cross-sectional analysis can only provide a snapshot of this population. We cannot establish where our participants sit along the dynamic curve of CSF levels described by βA42 in response to microbial triggers. The lower values of CSF βA42 in C1 associated with better cognitive performance may be explained by the fact that the CSF levels measured in all the clusters are still within the normal range for most of the participants, and increased CSF levels may feature the phase preceding amyloid deposition, in which amyloid is overproduced in response to local microbes (including viruses) [203,204]. The higher value of CSF proteins in C3 may be a sign of greater inflammation that increased the “sterility” of the CSF, rather than a sign of increased inflammation in presence of less rich and abundant viral communities. C2 had the lowest values of CSAR, although the greatest contribution by bacteriophages to the virome composition. In line with our previous hypothesis on the origin of the CSF virome, this can be explained by the fact that bacteriophages may enter the CNS as genetic fragments which do not require impaired BBB.

Not to further complicate our model, we have not commented on the role of the glymphatic system so far [205], but it is worth mentioning that differences in CSF virome composition, as described by our clusters, may depends not only or primarily on mechanisms of viral entry into the CNS, but also on mechanisms of CSF clearance. In this regard, cognitive impairment and neurodegenerative disorders such Alzheimer’s dementia have been attributed to altered functions of the glymphatic system [206–209]. This “CNS sewage” uses a system of perivascular channels formed by astrocytes to drain and eliminate soluble proteins and metabolites from the CNS, and its dysfunction may lead to the accumulation of neurotoxic

products and amyloid [205–208]. From this perspective, C1 and C3 could be grouped together to represent participants with an effective glymphatic system; within this group, the frequency and intensity of exposures and reactivations of neurotropic human eukaryotic viruses can further distinguish C1 from C3. On the opposite, C2 and C4 could be grouped together to represent participants with impaired glymphatic system, where the same amount of nonhuman eukaryotic and prokaryotic viruses that “physiologically” reach the CSF is less efficiently and rapidly drained outside the CNS.

The complexity of the hypotheses and the number of permutative possible interpretations could follow a factorial growth and require further data from longitudinal studies with larger samples and assessments of factors that we did not measure to avoid false rabbit holes. What our data suggest is that there is evidence of a relationship between the composition of CSF virome, immunity, specific biomarkers’ pathways, and cognition, which justify further efforts to better disentangle such intertwined relationships. Of relevance, our data are not in conflict with previous data endorsing an etiologic role of neurotropic viruses in cognitive impairment [63,64,67,210–213]; rather, they complement these and can explain discrepancies among studies with positive and negative findings, as they have been measured only the tip of the ice berg.

Among the other limitations of our study, there is the cross-sectional and retrospective design. This can have affected the detection of genetic material, especially RNA, due to the long-time span of conservation of some of the samples as well as causal inferences and interpretations for the associations detected. Longitudinal studies should address the stability of the CSF virome composition and characteristics overtime and their relationship with mental health outcomes and CSF biomarkers levels overtime. The variability in metagenomic findings does not depend solely on methods of taxonomic attribution, and other steps in our NGS pipelines (from the initial pore micro filtering, that could have retained cells and larger virions, to library preparation) inevitably introduce heterogeneity in the methods that limits data comparison and affects the final characteristics of the viral communities: e.g., the depth of sequencing did not allow us to detect very low-level traces of HIV, EBV and JCV that were detected by the more sensitive RT-PCRs. In this regard, all the viromes described are likely an underestimation of what is the true richness and composition of the samples. The participants without HIV infection were used as controls in only a part of our analyses, as they did not undergo all the testing and collection of clinical data available for PWH. Furthermore, both the groups were limited in number and no calculation of the statistical power could be reliably performed. This could have affected both

type I and II errors and our capacity to address them. This is also the reason why, despite multiple testing, we have not performed adjustments of the threshold of significance (α set at 0.05). However, despite some of the findings found to significantly differ between clusters require confirmation on larger sample, the differential risk of cognitive impairment according to cluster strengthen the significance of its association when adjusted in multivariable models, supporting the robustness of this clinical finding.

Among the strengths of our study, other than the originality of the findings, the comparison of taxonomic attribution methods, the ecological validity of the study population compared to modern cohorts of PWH, the inclusion of blank controls for the sequencing and of HIV-negative controls, and the extensive neurocognitive and CSF assessment of PWH. We will also further exploit the richness of our dataset through post-hoc and subgroup analyses: e.g., the contribution of specific viral taxa in CSF biomarkers, clinical outcomes, and cognitive domains (as suggested by the association between executive functions and memory performance and ratios between dominant viral taxa within consortia in human and other animal spp [14]); alternative cluster solutions based on different parameters (only quantitative to evaluate the “glymphatic hypothesis”, instead of quali-quantitative as the one presented); the longitudinal assessment of participants with stored and available CSF samples at subsequent time points (pending the results of the submitted research grant to the HIV Neurobehavioral Research Center, UCSD).

Conclusions

We have described for the first time the presence, composition, and characteristics of the viral communities that inhabit the CSF of PWH on suppressive ART and valid immunological status. The variability in all these was extremely wide by simply changing the taxonomic assignment approach, with eventually significant differences in the factors that resulted associated with the composition of the viral consortia in the CSF (e.g., sex, neurocognition, HIV status). An international consensus for a shared and reliable metagenomic pipeline for virome studies is therefore essential, and clearer models and *a posteriori* interpretation of findings produced by distinct approaches in parallel may guide better informed decisions. All the methods agreed on that both prokaryotic and eukaryotic viruses, including non-human viruses, inhabit the CSF of ART-treated PWH and of CWH. Most of the detected viruses without known neurotropism has been previously found in human gut and blood, suggesting that a gut-blood-brain route may be the path followed to reach the CSF. Overall, our data indirectly suggest also that most of the CSF virome is composed by genetic fragments rather than replication-competent virions. Several factor can affect or be affected

by the composition of the CSF viral consortia, including cognitive performance, β amyloid metabolism, and, directly or indirectly, HIV infection itself. The relative abundance of eukaryotic (human and nonhuman) and prokaryotic viruses (mainly bacteriophages) in the CSF was able to discriminate PWH that differ for all the above. Our data delineate a further mechanism by which the gut-brain axis can shape neuroinflammation, neurodegeneration, and cognitive performance, and contribute to describe a further piece in the emerging disease models that link brain health to the human microbiota. If confirmed, these data can inform tailored interventions to target the human virome, as already attempted for psychiatric and neurological disorders in the general population [125–128,214–216].

Acknowledgements

Thanks to my family, friends, mentors, and teachers. A special thanks to Prof. Andrea Calcagno, Prof. Claudia Alteri, Dr. Rossana Scutari, Dr. Valeria Fox, and to the participants of the study. The study was supported through fundings by Gilead Sciences (fellowship program 2021).

References

1 Shkoporov AN, Turkington CJ, Hill C. **Mutualistic interplay between bacteriophages and bacteria in the human gut**. *Nat Rev Microbiol* 2022; **20**:737–749.
2 Liang G, Bushman FD. **The human virome: assembly, composition and host interactions**. *Nat Rev Microbiol* 2021; **19**:514–527.
3 Popescu M, Van Belleghem JD, Khosravi A, Bollyky PL. **Bacteriophages and the Immune System**. *Annu Rev Virol* 2021; **8**:415–435.
4 Ghose C, Ly M, Schwanemann LK, Shin JH, Atab K, Barr JJ, *et al.* **The Virome of Cerebrospinal Fluid: Viruses Where We Once Thought There Were None**. *Front Microbiol* 2019; **10**:2061.
5 Blanco-Picazo P, Fernández-Orth D, Brown-Jaque M, Miró E, Espinal P, Rodríguez-Rubio L, *et al.* **Unravelling the consequences of the bacteriophages in human samples**. *Sci Rep* 2020; **10**:6737.
6 Federici S, Nobs SP, Elinav E. **Phages and their potential to modulate the microbiome and immunity**. *Cell Mol Immunol* 2021; **18**:889–904.
7 Cao Z, Sugimura N, Burgermeister E, Ebert MP, Zuo T, Lan P. **The gut virome: A new microbiome component in health and disease**. *eBioMedicine* 2022; **81**. doi:10.1016/j.ebiom.2022.104113
8 Tisza MJ, Buck CB. **A catalog of tens of thousands of viruses from human metagenomes reveals hidden associations with chronic diseases**. *Proc Natl Acad Sci U S A* 2021; **118**:e2023202118.
9 Tomofuji Y, Kishikawa T, Maeda Y, Ogawa K, Nii T, Okuno T, *et al.* **Whole gut virome analysis of 476 Japanese revealed a link between phage and autoimmune disease**. *Ann Rheum Dis* 2022; **81**:278–288.
10 Byrd AL, Segre JA. **Infectious disease. Adapting Koch's postulates**. *Science* 2016; **351**:224–226.
11 Sciascia S, Arbrile M, Trunfio M, Calcagno A, Radin M, Roccatello D, *et al.* **The role of bacteria and viruses in Behçet syndrome: Should we move towards new paradigms?** *Autoimmun Rev* 2023; **22**:103237.
12 Bjornevik K, Cortese M, Healy BC, Kuhle J, Mina MJ, Leng Y, *et al.* **Longitudinal analysis reveals high prevalence of Epstein-Barr virus associated with multiple sclerosis**. *Science* 2022; **375**:296–301.
13 Liu L, Wang H, Chen X, Zhang Y, Zhang H, Xie P. **Gut microbiota and its metabolites in depression: from pathogenesis to treatment**. *eBioMedicine* 2023; **90**. doi:10.1016/j.ebiom.2023.104527
14 Mayneris-Perxachs J, Castells-Nobau A, Arnoriaga-Rodríguez M, Garre-Olmo J, Puig J, Ramos R, *et al.* **Caudovirales bacteriophages are associated with improved executive function and memory in flies, mice, and humans**. *Cell Host Microbe* 2022; **30**:340-356.e8.
15 Rodriguez MT, McLaurin KA, Shtutman M, Kubinak JL, Mactutus CF, Booze RM. **Therapeutically targeting the consequences of HIV-1-associated gastrointestinal dysbiosis: Implications for neurocognitive and affective alterations**. *Pharmacology Biochemistry and Behavior* 2023; **229**:173592.
16 Carrico AW, Cherenack EM, Rubin LH, McIntosh R, Ghanooni D, Chavez JV, *et al.* **Through the Looking-Glass: Psychoneuroimmunology and the Microbiome-Gut-Brain Axis in the Modern Antiretroviral Therapy Era**. *Psychosom Med* 2022; **84**:984–994.

17 Rich S, Klann E, Bryant V, Richards V, Wijayabahu A, Bryant K, *et al.* **A review of potential microbiome-gut-brain axis mediated neurocognitive conditions in persons living with HIV**. *Brain Behav Immun Health* 2020; **9**:100168.
18 Dong R, Lin H, Chen X, Shi R, Yuan S, Li J, *et al.* **Gut Microbiota and Fecal Metabolites Associated With Neurocognitive Impairment in HIV-Infected Population**. *Frontiers in Cellular and Infection Microbiology* 2021; **11**.https://www.frontiersin.org/articles/10.3389/fcimb.2021.723840 (accessed 5 Feb2024).
19 Hua S, Peters BA, Lee S, Fitzgerald K, Wang Z, Sollecito CC, *et al.* **Gut Microbiota and Cognitive Function Among Women Living with HIV**. *J Alzheimers Dis* 2023; **95**:1147–1161.
20 McGuinness AJ, Loughman A, Foster JA, Jacka F. **Mood Disorders: The Gut Bacteriome and Beyond**. *Biol Psychiatry* 2024; **95**:319–328.
21 Tsunoda I. **Lymphatic system and gut microbiota affect immunopathology of neuroinflammatory diseases, including multiple sclerosis, neuromyelitis optica and Alzheimer's disease**. *Clin Exp Neuroimmunol* 2017; **8**:177–179.
22 Bu L, Wang C, Bai J, Song J, Zhang Y, Chen H, *et al.* **Gut microbiome-based therapies for alleviating cognitive impairment: state of the field, limitations, and future perspectives**. *Food Funct* 2024; **15**:1116–1134.
23 Mudaliar SB, Poojary SS, Bharath Prasad AS, Mazumder N. **Probiotics and Paraprobiotics: Effects on Microbiota-Gut-Brain Axis and Their Consequent Potential in Neuropsychiatric Therapy**. *Probiotics Antimicrob Proteins* Published Online First: 31 January 2024. doi:10.1007/s12602-024-10214-6
24 Mhanna A, Martini N, Hmaydoosh G, Hamwi G, Jarjanazi M, Zaifah G, *et al.* **The correlation between gut microbiota and both neurotransmitters and mental disorders: A narrative review**. *Medicine (Baltimore)* 2024; **103**:e37114.
25 Malan-Muller S, Valles-Colomer M, Raes J, Lowry CA, Seedat S, Hemmings SMJ. **The Gut Microbiome and Mental Health: Implications for Anxiety- and Trauma-Related Disorders**. *OMICS* 2018; **22**:90–107.
26 Neil JA, Cadwell K. **The Intestinal Virome and Immunity**. *J Immunol* 2018; **201**:1615–1624.
27 Lv T, Cao W, Li T. **HIV-Related Immune Activation and Inflammation: Current Understanding and Strategies**. *J Immunol Res* 2021; **2021**:7316456.
28 Streeck H, Maestri A, Habermann D, Crowell TA, Esber AL, Son G, *et al.* **Dissecting drivers of immune activation in chronic HIV-1 infection**. *eBioMedicine* 2022; **83**. doi:10.1016/j.ebiom.2022.104182
29 So-Armah K, Benjamin LA, Bloomfield GS, Feinstein MJ, Hsue P, Njuguna B, *et al.* **HIV and cardiovascular disease**. *The Lancet HIV* 2020; **7**:e279–e293.
30 Noël N, Saez-Cirion A, Avettand-Fenoël V, Boufassa F, Lambotte O. **HIV controllers: to treat or not to treat? Is that the right question?** *The Lancet HIV* 2019; **6**:e878–e884.
31 Verheij E, Boyd A, Wit FW, Verboeket SO, Verburgh ML, Valk M van der, *et al.* **Long-term evolution of comorbidities and their disease burden in individuals with and without HIV as they age: analysis of the prospective AGEhIV cohort study**. *The Lancet HIV* 2023; **10**:e164–e174.
32 McArthur JC, Johnson TP. **Chronic inflammation mediates brain injury in HIV infection: relevance for cure strategies**. *Curr Opin Neurol* 2020; **33**:397–404.
33 McIntosh EC, Tureson K, Rotblatt LJ, Singer EJ, Thames AD. **HIV, Vascular Risk Factors, and Cognition in the Combination Antiretroviral Therapy Era: A Systematic Review and Meta-Analysis**. *J Int Neuropsychol Soc* 2021; **27**:365–381.
34 Lisco A, Vanpouille C, Margolis L. **Coinfecting Viruses as Determinants of HIV Disease**. *Curr HIV/AIDS Rep* 2009; **6**:5–12.
35 Lisco A, Vanpouille C, Margolis L. **War and peace between microbes: HIV-1 interactions with coinfecting viruses**. *Cell Host Microbe* 2009; **6**:403–408.
36 Gianella S, Moser C, Vitomirov A, McKhann A, Layman L, Scott B, *et al.* **Presence of Asymptomatic CMV and EBV DNA in Blood of Persons with HIV Starting Antiretroviral Therapy are Associated with Non-AIDS Clinical Events**. *AIDS* 2020; **34**:849–857.
37 Li Y, Altan E, Pilcher C, Hartogensis W, Hecht FM, Deng X, *et al.* **Semen virome of men with HIV on or off antiretroviral treatment**. *AIDS* 2020; **34**:827–832.
38 Li L, Deng X, Linsuwanon P, Bangsberg D, Bwana MB, Hunt P, *et al.* **AIDS Alters the Commensal Plasma Virome**. *Journal of Virology* 2013; **87**:10912–10915.
39 Monaco CL, Gootenberg DB, Zhao G, Handley SA, Ghebremichael MS, Lim ES, *et al.* **Altered Virome and Bacterial Microbiome in Human Immunodeficiency Virus-Associated Acquired Immunodeficiency Syndrome**. *Cell Host Microbe* 2016; **19**:311–322.
40 Siqueira JD, Curty G, Xutao D, Hofer CB, Machado ES, Seuánez HN, *et al.* **Composite Analysis of the Virome and Bacteriome of HIV/HPV Co-Infected Women Reveals Proxies for Immunodeficiency**. *Viruses* 2019; **11**:422.
41 Mateen FJ, Shinohara RT, Carone M, Miller EN, McArthur JC, Jacobson LP, *et al.* **Neurologic disorders incidence in HIV+ vs HIV− men**. *Neurology* 2012; **79**:1873–1880.
42 Wang Y, Liu M, Lu Q, Farrell M, Lappin JM, Shi J, *et al.* **Global prevalence and burden of HIV-associated neurocognitive disorder: A meta-analysis**. *Neurology* 2020; **95**:e2610–e2621.
43 Bobrow K, Xia F, Hoang T, Valcour V, Yaffe K. **HIV and risk of dementia in older veterans**. *AIDS* 2020; **34**:1673–1679.
44 Lam JO, Hou CE, Hojilla JC, Anderson AN, Gilsanz P, Alexeeff SE, *et al.* **Comparison of dementia risk after age 50 between individuals with and without HIV infection**. *AIDS* 2021; **35**:821–828.
45 Yu X, Kuo Y-F, Raji MA, Berenson AB, Baillargeon J, Giordano TP. **Dementias Among Older Males and Females in the U.S. Medicare System With and Without HIV**. *J Acquir Immune Defic Syndr* 2023; **93**:107–115.
46 Nightingale S, Winsto A, Letendre S, Michael BD, McArthur JC, Khoo S, *et al.* **Controversies in HIV-associated neurocognitive disorders**. *Lancet Neurol* 2014; **13**:1139–1151.
47 Cole JH, Caan MWA, Underwood J, De Francesco D, van Zoest RA, Wit FWNM, *et al.* **No Evidence for Accelerated Aging-Related Brain Pathology in Treated Human Immunodeficiency Virus: Longitudinal Neuroimaging Results From the Comorbidity in Relation to AIDS (COBRA) Project**. *Clin Infect Dis* 2018; **66**:1899–1909.

48 Qu Y, Weinstein A, Wang Z, Cheng Y, Kingsley L, Levine A, *et al.* **Legacy effect on neuropsychological function in HIV-infected men on combination antiretroviral therapy**. *AIDS* 2022; **36**:19–27.
49 Hategan A, Bianchet MA, Steiner J, Karnaukhova E, Masliah E, Fields A, *et al.* **HIV-Tat protein and amyloid β peptide form multifibrillar structures that cause neurotoxicity**. *Nat Struct Mol Biol* 2017; **24**:379–386.
50 Calcagno A, Celani L, Trunfio M, Orofino G, Imperiale D, Atzori C, *et al.* **Alzheimer Dementia in People Living With HIV**. *Neurol Clin Pract* 2021; **11**:e627–e633.
51 Trunfio M, Atzori C, Pasquero M, Di Stefano A, Vai D, Nigra M, *et al.* **Patterns of Cerebrospinal Fluid Alzheimer's Dementia Biomarkers in People Living with HIV: Cross-Sectional Study on Associated Factors According to Viral Control, Neurological Confounders and Neurocognition**. *Viruses* 2022; **14**:753.
52 Haddow LJ, Dudau C, Chandrashekar H, Cartledge JD, Hyare H, Miller RF, *et al.* **Cross-Sectional Study of Unexplained White Matter Lesions in HIV Positive Individuals Undergoing Brain Magnetic Resonance Imaging**. *AIDS Patient Care STDS* 2014; **28**:341–349.
53 Gutierrez J, Byrd D, Yin MT, Morgello S. **Relationship Between Brain Arterial Pathology and Neurocognitive Performance Among Individuals With Human Immunodeficiency Virus**. *Clin Infect Dis* 2019; **68**:490–497.
54 Siddiqui A, He C, Lee G, Figueroa A, Slaughter A, Robinson-Papp J. **Neuropathogenesis of HIV and emerging therapeutic targets**. *Expert Opin Ther Targets* 2022; **26**:603–615.
55 Ntsekhe M, Baker JV. **Cardiovascular Disease Among Persons Living With HIV: New Insights Into Pathogenesis and Clinical Manifestations in a Global Context**. *Circulation* 2023; **147**:83–100.
56 Caligaris G, Trunfio M, Ghisetti V, Cusato J, Nigra M, Atzori C, *et al.* **Blood-Brain Barrier Impairment in Patients Living with HIV: Predictors and Associated Biomarkers**. *Diagnostics (Basel)* 2021; **11**:867.
57 Nottet HS. **Interactions between macrophages and brain microvascular endothelial cells: role in pathogenesis of HIV-1 infection and blood - brain barrier function**. *J Neurovirol* 1999; **5**:659–669.
58 Lee C-H, Giuliani F. **The Role of Inflammation in Depression and Fatigue**. *Front Immunol* 2019; **10**:1696.
59 Han K-M, Ham B-J. **How Inflammation Affects the Brain in Depression: A Review of Functional and Structural MRI Studies**. *J Clin Neurol* 2021; **17**:503–515.
60 Berk M, Williams LJ, Jacka FN, O'Neil A, Pasco JA, Moylan S, *et al.* **So depression is an inflammatory disease, but where does the inflammation come from?** *BMC Medicine* 2013; **11**:200.
61 Mudra Rakshasa-Loots A, Whalley HC, Vera JH, Cox SR. **Neuroinflammation in HIV-associated depression: evidence and future perspectives**. *Mol Psychiatry* 2022; **27**:3619–3632.
62 Bonnan M, Barroso B, Demasles S, Krim E, Marasescu R, Miquel M. **Compartmentalized intrathecal immunoglobulin synthesis during HIV infection — A model of chronic CNS inflammation?** *J Neuroimmunol* 2015; **285**:41–52.
63 Letendre S, Bharti A, Perez-Valero I, Hanson B, Franklin D, Woods SP, *et al.* **Higher Anti-Cytomegalovirus Immunoglobulin G Concentrations Are Associated With Worse Neurocognitive Performance During Suppressive Antiretroviral Therapy**. *Clin Infect Dis* 2018; **67**:770–777.
64 Trunfio M, Sacchi A, Vai D, Pittaluga F, Croce M, Cavallo R, *et al.* **Intrathecal production of anti-EBV Viral Capsid Antigen IgG is associated with Neurocognition and tau pathology in people with HIV**. *AIDS* Published Online First: 8 November 2023. doi:10.1097/QAD.0000000000003775
65 Trunfio M, Mighetto L, Napoli L, Atzori C, Nigra M, Guastamacchia G, *et al.* **Cerebrospinal Fluid CXCL13 as Candidate Biomarker of Intrathecal Immune Activation, IgG Synthesis and Neurocognitive Impairment in People with HIV**. *J Neuroimmune Pharmacol* Published Online First: 11 May 2023. doi:10.1007/s11481-023-10066-x
66 Magaki SD, Vinters HV, Williams CK, Mareninov S, Khanlou N, Said J, *et al.* **Neuropathologic Findings in Elderly HIV-Positive Individuals**. *J Neuropathol Exp Neurol* 2022; **81**:565–576.
67 Itzhaki RF. **Overwhelming Evidence for a Major Role for Herpes Simplex Virus Type 1 (HSV1) in Alzheimer's Disease (AD); Underwhelming Evidence against**. *Vaccines (Basel)* 2021; **9**:679.
68 Adinolfi LE, Nevola R, Rinaldi L, Romano C, Giordano M. **Chronic Hepatitis C Virus Infection and Depression**. *Clin Liver Dis* 2017; **21**:517–534.
69 O'Leary K. **Viruses linked to neurodegenerative disease**. *Nature Medicine* Published Online First: 9 February 2023. doi:10.1038/d41591-023-00016-8
70 Bjornevik K, Münz C, Cohen JI, Ascherio A. **Epstein–Barr virus as a leading cause of multiple sclerosis: mechanisms and implications**. *Nat Rev Neurol* 2023; **19**:160–171.
71 Trunfio M, Di Girolamo L, Ponzetta L, Russo M, Burdino E, Imperiale D, *et al.* **Seropositivity and reactivations of HSV-1, but not of HSV-2 nor VZV, associate with altered blood–brain barrier, beta amyloid, and tau proteins in people living with HIV**. *J Neurovirol* Published Online First: 9 November 2022. doi:10.1007/s13365-022-01105-z
72 Gianella S, Anderson CM, Var SR, Oliveira MF, Lada SM, Vargas MV, *et al.* **Replication of Human Herpesviruses Is Associated with Higher HIV DNA Levels during Antiretroviral Therapy Started at Early Phases of HIV Infection**. *J Virol* 2016; **90**:3944–3952.
73 Simonetti FR, Zhang H, Soroosh GP, Duan J, Rhodehouse K, Hill AL, *et al.* **Antigen-driven clonal selection shapes the persistence of HIV-1–infected CD4+ T cells in vivo**. *J Clin Invest*; **131**:e145254.
74 Martinsen JT, Gunst JD, Højen JF, Tolstrup M, Søgaard OS. **The Use of Toll-Like Receptor Agonists in HIV-1 Cure Strategies**. *Front Immunol* 2020; **11**:1112.
75 Li SX, Sen S, Schneider JM, Xiong K-N, Nusbacher NM, Moreno-Huizar N, *et al.* **Gut microbiota from high-risk men who have sex with men drive immune activation in gnotobiotic mice and in vitro HIV infection**. *PLOS Pathogens* 2019; **15**:e1007611.
76 Sui Y, Dzutsev A, Venzon D, Frey B, Thovarai V, Trinchieri G, *et al.* **Influence of gut microbiome on mucosal immune activation and SHIV viral transmission in naive macaques**. *Mucosal Immunol* 2018; **11**:1219–1229.
77 Jiang J, Hu X, Li W, Liu J, Liang B, Chen H, *et al.* **Enhanced Signaling Through the TLR9 Pathway Is Associated With Resistance to HIV-1 Infection in Chinese HIV-1–Exposed Seronegative Individuals**. *Front Immunol* 2020; **11**:1050.

78 Immonen TT, Conway JM, Romero-Severson EO, Perelson AS, Leitner T. **Recombination Enhances HIV-1 Envelope Diversity by Facilitating the Survival of Latent Genomic Fragments in the Plasma Virus Population**. *PLOS Computational Biology* 2015; **11**:e1004625.
79 Solé RV, Ferrer R, González-García I, Quer J, Domingo E. **Red queen dynamics, competition and critical points in a model of RNA virus quasispecies**. *J Theor Biol* 1999; **198**:47–59.
80 Rambaut A, Posada D, Crandall KA, Holmes EC. **The causes and consequences of HIV evolution**. *Nat Rev Genet* 2004; **5**:52–61.
81 Strotz LC, Simões M, Girard MG, Breitkreuz L, Kimmig J, Lieberman BS. **Getting somewhere with the Red Queen: chasing a biologically modern definition of the hypothesis**. *Biol Lett* 2018; **14**:20170734.
82 Brockhurst MA, Chapman T, King KC, Mank JE, Paterson S, Hurst GDD. **Running with the Red Queen: the role of biotic conflicts in evolution**. *Proc Biol Sci* 2014; **281**:20141382.
83 Muraille E. **Diversity Generator Mechanisms Are Essential Components of Biological Systems: The Two Queen Hypothesis**. *Frontiers in Microbiology* 2018; **9**.https://www.frontiersin.org/articles/10.3389/fmicb.2018.00223 (accessed 10 Apr2023).
84 Gaube G, Armero A, Salmona M, Néré M-L, Mahjoub N, Lascoux-Combe C, *et al.* **Characterization of HIV-1 diversity in various compartments at the time of primary infection by ultradeep sequencing**. *Sci Rep* 2020; **10**:2409.
85 Tovanabutra S, Sirijatuphat R, Pham PT, Bonar L, Harbolick EA, Bose M, *et al.* **Deep Sequencing Reveals Central Nervous System Compartmentalization in Multiple Transmitted/Founder Virus Acute HIV-1 Infection**. *Cells* 2019; **8**:902.
86 Chaillon A, Gianella S, Dellicour S, Rawlings SA, Schlub TE, Oliveira MFD, *et al.* **HIV persists throughout deep tissues with repopulation from multiple anatomical sources**. *J Clin Invest* 2020; **130**:1699–1712.
87 Giatsou E, Abdi B, Plu I, Desire N, Palich R, Calvez V, *et al.* **Ultradeep sequencing reveals HIV-1 diversity and resistance compartmentalization during HIV-encephalopathy**. *AIDS* 2020; **34**:1609–1614.
88 Ferrara M, Bumpus NN, Ma Q, Ellis RJ, Soontornniyomkij V, Fields JA, *et al.* **Antiretroviral drug concentrations in brain tissue of adult decedents**. *AIDS* 2020; **34**:1907–1914.
89 Domínguez-Rodríguez S, Rojas P, Fernández McPhee C, Pagán I, Navarro ML, Ramos JT, *et al.* **Effect of HIV/HCV Co-Infection on the Protease Evolution of HIV-1B: A Pilot Study in a Pediatric Population**. *Sci Rep* 2018; **8**:2347.
90 Rojas Sánchez P, Cobos A, Navaro M, Ramos JT, Pagán I, Holguín Á. **Impact of Clinical Parameters in the Intrahost Evolution of HIV-1 Subtype B in Pediatric Patients: A Machine Learning Approach**. *Genome Biology and Evolution* 2017; **9**:2715–2726.
91 Xu C-H, Shen T, Zheng J-J, Tu J, Zhang W-D, Lu F-M. **Higher dN/dS ratios in the HCV core gene, but not in the E1/HVR1 gene, are associated with human immunodeficiency virus-associated immunosuppression**. *Arch Virol* 2012; **157**:2153–2162.
92 Quadeer AA, Morales-Jimenez D, McKay MR. **Co-evolution networks of HIV/HCV are modular with direct association to structure and function**. *PLoS Comput Biol* 2018; **14**:e1006409.
93 Nie Y, Deng X, Lan Y, Li L, Li F, Hu F. **Comparison and Correlation of Genetic Variability of the HBV Pre-S Region in HIV/HBV Co-Infected Patients: Quasispecies Perspective**. *Infect Drug Resist* 2020; **13**:4327–4334.
94 Chiu CY, Miller SA. **Clinical metagenomics**. *Nat Rev Genet* 2019; **20**:341–355.
95 Miller S, Naccache SN, Samayoa E, Messacar K, Arevalo S, Federman S, *et al.* **Laboratory validation of a clinical metagenomic sequencing assay for pathogen detection in cerebrospinal fluid**. *Genome Res* 2019; **29**:831–842.
96 Kang Y, Ji X, Guo L, Xia H, Yang X, Xie Z, *et al.* **Cerebrospinal Fluid from Healthy Pregnant Women Does Not Harbor a Detectable Microbial Community**. *Microbiol Spectr* 2021; **9**:e0076921.
97 L B, E L, V M, S T, G P. **Applications of next-generation sequencing technologies to diagnostic virology**. *International journal of molecular sciences* 2011; **12**. doi:10.3390/ijms12117861
98 Rascovan N, Duraisamy R, Desnues C. **Metagenomics and the Human Virome in Asymptomatic Individuals**. *Annu Rev Microbiol* 2016; **70**:125–141.
99 Ramachandran PS, Wilson MR. **Metagenomics for neurological infections - expanding our imagination**. *Nat Rev Neurol* 2020; **16**:547–556.
100 Sims D, Sudbery I, Ilott NE, Heger A, Ponting CP. **Sequencing depth and coverage: key considerations in genomic analyses**. *Nat Rev Genet* 2014; **15**:121–132.
101 Nelson MT, Pope CE, Marsh RL, Wolter DJ, Weiss EJ, Hager KR, *et al.* **Human and Extracellular DNA Depletion for Metagenomic Analysis of Complex Clinical Infection Samples Yields Optimized Viable Microbiome Profiles**. *Cell Rep* 2019; **26**:2227-2240.e5.
102 Marotz CA, Sanders JG, Zuniga C, Zaramela LS, Knight R, Zengler K. **Improving saliva shotgun metagenomics by chemical host DNA depletion**. *Microbiome* 2018; **6**:42.
103 Yap M, Feehily C, Walsh CJ, Fenelon M, Murphy EF, McAuliffe FM, *et al.* **Evaluation of methods for the reduction of contaminating host reads when performing shotgun metagenomic sequencing of the milk microbiome**. *Sci Rep* 2020; **10**:21665.
104 O'Flaherty BM, Li Y, Tao Y, Paden CR, Queen K, Zhang J, *et al.* **Comprehensive viral enrichment enables sensitive respiratory virus genomic identification and analysis by next generation sequencing**. *Genome Res* 2018; **28**:869–877.
105 Gaudin M, Desnues C. **Hybrid Capture-Based Next Generation Sequencing and Its Application to Human Infectious Diseases**. *Front Microbiol* 2018; **9**:2924.
106 Briese T, Kapoor A, Mishra N, Jain K, Kumar A, Jabado OJ, *et al.* **Virome Capture Sequencing Enables Sensitive Viral Diagnosis and Comprehensive Virome Analysis**. *mBio* 2015; **6**:e01491-01415.
107 Hasan MR, Rawat A, Tang P, Jithesh PV, Thomas E, Tan R, *et al.* **Depletion of Human DNA in Spiked Clinical Specimens for Improvement of Sensitivity of Pathogen Detection by Next-Generation Sequencing**. *J Clin Microbiol* 2016; **54**:919–927.

108 Ye SH, Siddle KJ, Park DJ, Sabeti PC. **Benchmarking Metagenomics Tools for Taxonomic Classification**. *Cell* 2019; **178**:779–794.
109 Wood DE, Lu J, Langmead B. **Improved metagenomic analysis with Kraken 2**. *Genome Biol* 2019; **20**:257.
110 Rose R, Constantinides B, Tapinos A, Robertson DL, Prosperi M. **Challenges in the analysis of viral metagenomes**. *Virus Evol* 2016; **2**:vew022.
111 Sayers EW, Bolton EE, Brister JR, Canese K, Chan J, Comeau DC, *et al.* **Database resources of the national center for biotechnology information**. *Nucleic Acids Res* 2022; **50**:D20–D26.
112 Paez-Espino D, Roux S, Chen I-MA, Palaniappan K, Ratner A, Chu K, *et al.* **IMG/VR v.2.0: an integrated data management and analysis system for cultivated and environmental viral genomes**. *Nucleic Acids Res* 2019; **47**:D678–D686.
113 Garcia BJ, Simha R, Garvin M, Furches A, Jones P, Gazolla JGFM, *et al.* **A k-mer based approach for classifying viruses without taxonomy identifies viral associations in human autism and plant microbiomes**. *Comput Struct Biotechnol J* 2021; **19**:5911–5919.
114 Nayfach S, Páez-Espino D, Call L, Low SJ, Sberro H, Ivanova NN, *et al.* **Metagenomic compendium of 189,680 DNA viruses from the human gut microbiome**. *Nat Microbiol* 2021; **6**:960–970.
115 Gregory AC, Zablocki O, Zayed AA, Howell A, Bolduc B, Sullivan MB. **The Gut Virome Database Reveals Age-Dependent Patterns of Virome Diversity in the Human Gut**. *Cell Host Microbe* 2020; **28**:724-740.e8.
116 Parks DH, Rinke C, Chuvochina M, Chaumeil P-A, Woodcroft BJ, Evans PN, *et al.* **Recovery of nearly 8,000 metagenome-assembled genomes substantially expands the tree of life**. *Nat Microbiol* 2017; **2**:1533–1542.
117 Singleton CM, Petriglieri F, Kristensen JM, Kirkegaard RH, Michaelsen TY, Andersen MH, *et al.* **Connecting structure to function with the recovery of over 1000 high-quality metagenome-assembled genomes from activated sludge using long-read sequencing**. *Nat Commun* 2021; **12**:2009.
118 Massana R, López-Escardó D. **Metagenome assembled genomes are for eukaryotes too**. *Cell Genom* 2022; **2**:100130.
119 Ayling M, Clark MD, Leggett RM. **New approaches for metagenome assembly with short reads**. *Brief Bioinform* 2020; **21**:584–594.
120 Kuleshov V, Jiang C, Zhou W, Jahanbani F, Batzoglou S, Snyder M. **Synthetic long-read sequencing reveals intraspecies diversity in the human microbiome**. *Nat Biotechnol* 2016; **34**:64–69.
121 Sandybayev N, Beloussov V, Strochkov V, Solomadin M, Granica J, Yegorov S. **Next Generation Sequencing Approaches to Characterize the Respiratory Tract Virome**. *Microorganisms* 2022; **10**:2327.
122 Lou YC, Hoff J, Olm MR, West-Roberts J, Diamond S, Firek BA, *et al.* **Using strain-resolved analysis to identify contamination in metagenomics data**. *Microbiome* 2023; **11**:36.
123 Jurasz H, Pawłowski T, Perlejewski K. **Contamination Issue in Viral Metagenomics: Problems, Solutions, and Clinical Perspectives**. *Front Microbiol* 2021; **12**:745076.
124 Strong MJ, Xu G, Morici L, Splinter Bon-Durant S, Baddoo M, Lin Z, *et al.* **Microbial contamination in next generation sequencing: implications for sequence-based analysis of clinical samples**. *PLoS Pathog* 2014; **10**:e1004437.
125 Manivannan AC, Dhandapani R, Velmurugan P, Thangavelu S, Paramasivam R, Ragunathan L, *et al.* **Phage in cancer treatment - Biology of therapeutic phage and screening of tumor targeting peptide**. *Expert Opin Drug Deliv* 2022; **19**:873–882.
126 Strathdee SA, Hatfull GF, Mutalik VK, Schooley RT. **Phage therapy: From biological mechanisms to future directions**. *Cell* 2023; **186**:17–31.
127 Solomon B. **Filamentous bacteriophage as a novel therapeutic tool for Alzheimer's disease treatment**. *J Alzheimers Dis* 2008; **15**:193–198.
128 Messing J. **Phage M13 for the treatment of Alzheimer and Parkinson disease**. *Gene* 2016; **583**:85–89.
129 Monaco CL. **HIV, AIDS, and the virome: Gut reactions**. *Cell Host Microbe* 2022; **30**:466–470.
130 RUBIN LH, MAKI PM. **HIV, depression, and cognitive impairment in the era of effective antiretroviral therapy**. *Curr HIV/AIDS Rep* 2019; **16**:82–95.
131 Alford K, Vera JH. **Cognitive Impairment in people living with HIV in the ART era: A Review**. *British Medical Bulletin* 2018; **127**:55–68.
132 Lupia T, Milia MG, Atzori C, Gianella S, Audagnotto S, Imperiale D, *et al.* **Presence of Epstein-Barr virus DNA in cerebrospinal fluid is associated with greater HIV RNA and inflammation**. *AIDS* 2020; **34**:373–380.
133 Reiber H. **External quality assessment in clinical neurochemistry: survey of analysis for cerebrospinal fluid (CSF) proteins based on CSF/serum quotients**. *Clin Chem* 1995; **41**:256–263.
134 Antinori A, Arendt G, Becker JT, Brew BJ, Byrd DA, Cherner M, *et al.* **Updated research nosology for HIV-associated neurocognitive disorders**. *Neurology* 2007; **69**:1789–1799.
135 Lawton MP, Brody EM. **Assessment of older people: self-maintaining and instrumental activities of daily living**. *Gerontologist* 1969; **9**:179–186.
136 Beck AT, Steer RA, Brown G. Beck Depression Inventory–II. 2011. doi:10.1037/t00742-000
137 Beck AT, Steer RA, Ball R, Ranieri W. **Comparison of Beck Depression Inventories -IA and -II in psychiatric outpatients**. *J Pers Assess* 1996; **67**:588–597.
138 Petersen KJ, Yu X, Masters MC, Lobo JD, Lu T, Letendre S, *et al.* **Sex-specific associations between plasma interleukin-6 and depression in persons with and without HIV**. *Brain Behav Immun Health* 2023; **30**:100644.
139 Hobkirk AL, Starosta AJ, De Leo JA, Marra CM, Heaton RK, Earleywine M. **Psychometric Validation of the BDI-II Among HIV-Positive CHARTER Study Participants**. *Psychol Assess* 2015; **27**:457–466.
140 Chen S, Zhou Y, Chen Y, Gu J. **fastp: an ultra-fast all-in-one FASTQ preprocessor**. *Bioinformatics* 2018; **34**:i884–i890.
141 Babraham Bioinformatics - FastQC A Quality Control tool for High Throughput Sequence Data. https://www.bioinformatics.babraham.ac.uk/projects/fastqc/ (accessed 12 Jun2023).

142 Ewels P, Magnusson M, Lundin S, Käller M. **MultiQC: summarize analysis results for multiple tools and samples in a single report**. *Bioinformatics* 2016; **32**:3047–3048.
143 Ondov BD, Bergman NH, Phillippy AM. **Interactive metagenomic visualization in a Web browser**. *BMC Bioinformatics* 2011; **12**:385.
144 Lu J, Breitwieser FP, Thielen P, Salzberg SL. **Bracken: estimating species abundance in metagenomics data**. *PeerJ Comput Sci* 2017; **3**:e104.
145 Madison JD, LaBumbard BC, Woodhams DC. **Shotgun metagenomics captures more microbial diversity than targeted 16S rRNA gene sequencing for field specimens and preserved museum specimens**. *PLoS One* 2023; **18**:e0291540.
146 Wright RJ, Comeau AM, Langille MGI. **From defaults to databases: parameter and database choice dramatically impact the performance of metagenomic taxonomic classification tools**. *Microb Genom* 2023; **9**:mgen000949.
147 Nurk S, Meleshko D, Korobeynikov A, Pevzner PA. **metaSPAdes: a new versatile metagenomic assembler**. *Genome Res* 2017; **27**:824–834.
148 Wickham H. Data Analysis. In: *ggplot2: Elegant Graphics for Data Analysis*. Wickham H (editor). . Cham: Springer International Publishing; 2016. pp. 189–201.
149 McDonald D, Clemente JC, Kuczynski J, Rideout JR, Stombaugh J, Wendel D, *et al.* **The Biological Observation Matrix (BIOM) format or: how I learned to stop worrying and love the ome-ome**. *Gigascience* 2012; **1**:7.
150 McMurdie PJ, Holmes S. **phyloseq: an R package for reproducible interactive analysis and graphics of microbiome census data**. *PLoS One* 2013; **8**:e61217.
151 Marcoulides KM, Raykov T. **Evaluation of Variance Inflation Factors in Regression Models Using Latent Variable Modeling Methods**. *Educ Psychol Meas* 2019; **79**:874–882.
152 Yang Y, Chen B, Zhang H, Huang P, Qian J, Lin L, *et al.* **Global prevalence of depressive symptoms among people living with HIV/AIDS: a systematic review and meta-analysis of the past five years**. *AIDS Care* 2023; **0**:1–12.
153 Neri L, Spezia PG, Suraci S, Macera L, Scribano S, Giusti B, *et al.* **Torque teno virus microRNA detection in cerebrospinal fluids of patients with neurological pathologies**. *J Clin Virol* 2020; **133**:104687.
154 Maggi F, Fornai C, Vatteroni ML, Siciliano G, Menichetti F, Tascini C, *et al.* **Low prevalence of TT virus in the cerebrospinal fluid of viremic patients with central nervous system disorders**. *J Med Virol* 2001; **65**:418–422.
155 Edridge AWD, Deijs M, van Zeggeren IE, Kinsella CM, Jebbink MF, Bakker M, *et al.* **Viral Metagenomics on Cerebrospinal Fluid**. *Genes (Basel)* 2019; **10**:332.
156 Erdem G, Kaptsan I, Sharma H, Kumar A, Aylward SC, Kapoor A, *et al.* **Cerebrospinal Fluid Analysis for Viruses by Metagenomic Next-Generation Sequencing in Pediatric Encephalitis: Not Yet Ready for Prime Time?** *J Child Neurol* 2021; **36**:350–356.
157 Laskus T, Radkowski M, Bednarska A, Wilkinson J, Adair D, Nowicki M, *et al.* **Detection and analysis of hepatitis C virus sequences in cerebrospinal fluid**. *J Virol* 2002; **76**:10064–10068.
158 Anh NT, Hong NTT, Nhu LNT, Thanh TT, Lau C-Y, Limmathurotsakul D, *et al.* **Viruses in Vietnamese Patients Presenting with Community-Acquired Sepsis of Unknown Cause**. *J Clin Microbiol* 2019; **57**:e00386-19.
159 Huang M, Peng M, Gan CH, Ma J, Liu R, Li M, *et al.* **A case of intracranial molluscum contagiosum virus infection diagnosed by metagenomic sequencing of cerebrospinal fluid**. *Acta Virol* 2019; **63**:333–337.
160 Krupovic M, Ghabrial SA, Jiang D, Varsani A. **Genomoviridae: a new family of widespread single-stranded DNA viruses**. *Arch Virol* 2016; **161**:2633–2643.
161 Bukowska-Ośko I, Perlejewski K, Nakamura S, Motooka D, Stokowy T, Kosińska J, *et al.* **Sensitivity of Next-Generation Sequencing Metagenomic Analysis for Detection of RNA and DNA Viruses in Cerebrospinal Fluid: The Confounding Effect of Background Contamination.** *Adv Exp Med Biol* Published Online First: 1 July 2016. doi:10.1007/5584_2016_42
162 Schlaberg R, Chiu CY, Miller S, Procop GW, Weinstock G, Professional Practice Committee and Committee on Laboratory Practices of the American Society for Microbiology, *et al.* **Validation of Metagenomic Next-Generation Sequencing Tests for Universal Pathogen Detection**. *Arch Pathol Lab Med* 2017; **141**:776–786.
163 Narzisi G, Mishra B. **Comparing De Novo Genome Assembly: The Long and Short of It**. *PLOS ONE* 2011; **6**:e19175.
164 Roux S, Tournayre J, Mahul A, Debroas D, Enault F. **Metavir 2: new tools for viral metagenome comparison and assembled virome analysis**. *BMC Bioinformatics* 2014; **15**:76.
165 Vázquez-Castellanos JF, García-López R, Pérez-Brocal V, Pignatelli M, Moya A. **Comparison of different assembly and annotation tools on analysis of simulated viral metagenomic communities in the gut**. *BMC Genomics* 2014; **15**:37.
166 Sutton TDS, Clooney AG, Ryan FJ, Ross RP, Hill C. **Choice of assembly software has a critical impact on virome characterisation**. *Microbiome* 2019; **7**:12.
167 Ibañez-Lligoña M, Colomer-Castell S, González-Sánchez A, Gregori J, Campos C, Garcia-Cehic D, *et al.* **Bioinformatic Tools for NGS-Based Metagenomics to Improve the Clinical Diagnosis of Emerging, Re-Emerging and New Viruses**. *Viruses* 2023; **15**:587.
168 Tran Q, Phan V. **Assembling Reads Improves Taxonomic Classification of Species**. *Genes (Basel)* 2020; **11**:946.
169 Portik DM, Brown CT, Pierce-Ward NT. **Evaluation of taxonomic classification and profiling methods for long-read shotgun metagenomic sequencing datasets**. *BMC Bioinformatics* 2022; **23**:541.
170 Tamames J, Cobo-Simón M, Puente-Sánchez F. **Assessing the performance of different approaches for functional and taxonomic annotation of metagenomes**. *BMC Genomics* 2019; **20**:960.

171 Handley SA, Desai C, Zhao G, Droit L, Monaco CL, Schroeder AC, *et al.* **SIV Infection-mediated Changes in Gastrointestinal Bacterial Microbiome and Virome are Associated With Immunodeficiency and Prevented by Vaccination**. *Cell Host Microbe* 2016; **19**:323–335.

172 Abbate I, Rozera G, Cimini E, Carletti F, Tartaglia E, Rubino M, *et al.* **Kinetics of TTV Loads in Peripheral Blood Mononuclear Cells of Early Treated Acute HIV Infections**. *Viruses* 2023; **15**:1931.

173 Li Y, Cao L, Ye M, Xu R, Chen X, Ma Y, *et al.* **Plasma Virome Reveals Blooms and Transmission of Anellovirus in Intravenous Drug Users with HIV-1, HCV, and/or HBV Infections**. *Microbiol Spectr* 2022; **10**:e0144722.

174 Li L, Deng X, Da Costa AC, Bruhn R, Deeks SG, Delwart E. **Virome analysis of antiretroviral-treated HIV patients shows no correlation between T-cell activation and anelloviruses levels**. *J Clin Virol* 2015; **72**:106–113.

175 Villoslada-Blanco P, Pérez-Matute P, Íñiguez M, Recio-Fernández E, Jansen D, De Coninck L, *et al.* **Impact of HIV infection and integrase strand transfer inhibitors-based treatment on the gut virome**. *Sci Rep* 2022; **12**:21658.

176 Ludlow M, Kortekaas J, Herden C, Hoffmann B, Tappe D, Trebst C, *et al.* **Neurotropic virus infections as the cause of immediate and delayed neuropathology**. *Acta Neuropathol* 2016; **131**:159–184.

177 Jiang W, Luo Z, Stephenson S, Li H, Di Germanio C, Norris PJ, *et al.* **Cerebrospinal Fluid and Plasma Lipopolysaccharide Levels in Human Immunodeficiency Virus Type 1 Infection and Associations With Inflammation, Blood-Brain Barrier Permeability, and Neuronal Injury**. *J Infect Dis* 2020; **223**:1612–1620.

178 Branton WG, Fernandes JP, Mohammadzadeh N, Doan MAL, Laman JD, Gelman BB, *et al.* **Microbial molecule ingress promotes neuroinflammation and brain CCR5 expression in persons with HIV-associated neurocognitive disorders**. *Brain, Behavior, and Immunity* 2023; **107**:110–123.

179 Minot S, Sinha R, Chen J, Li H, Keilbaugh SA, Wu GD, *et al.* **The human gut virome: inter-individual variation and dynamic response to diet**. *Genome Res* 2011; **21**:1616–1625.

180 Moustafa A, Xie C, Kirkness E, Biggs W, Wong E, Turpaz Y, *et al.* **The blood DNA virome in 8,000 humans**. *PLoS Pathog* 2017; **13**:e1006292.

181 Yutin N, Benler S, Shmakov SA, Wolf YI, Tolstoy I, Rayko M, *et al.* **Analysis of metagenome-assembled viral genomes from the human gut reveals diverse putative CrAss-like phages with unique genomic features**. *Nat Commun* 2021; **12**:1044.

182 Ye J, Li Y, Wang X, Yu M, Liu X, Zhang H, *et al.* **Positive interactions among Corynebacterium glutamicum and keystone bacteria producing SCFAs benefited T2D mice to rebuild gut eubiosis**. *Food Res Int* 2023; **172**:113163.

183 Shuwen H, Kefeng D. **Intestinal phages interact with bacteria and are involved in human diseases**. *Gut Microbes*; **14**:2113717.

184 Łusiak-Szelachowska M, Weber-Dąbrowska B, Żaczek M, Borysowski J, Górski A. **The Presence of Bacteriophages in the Human Body: Good, Bad or Neutral?** *Microorganisms* 2020; **8**:2012.

185 Okuda J, Hayashi N, Okamoto M, Sawada S, Minagawa S, Yano Y, *et al.* **Translocation of Pseudomonas aeruginosa from the Intestinal Tract Is Mediated by the Binding of ExoS to an Na,K-ATPase Regulator, FXYD3**. *Infection and Immunity* 2010; **78**:4511–4522.

186 Glover JS, Browning BD, Ticer TD, Engevik AC, Engevik MA. **Acinetobacter calcoaceticus is Well Adapted to Withstand Intestinal Stressors and Modulate the Gut Epithelium**. *Frontiers in Physiology* 2022; **13**.https://www.frontiersin.org/articles/10.3389/fphys.2022.880024 (accessed 4 Feb2024).

187 Coenye T, Vandamme P. **Diversity and significance of Burkholderia species occupying diverse ecological niches**. *Environmental Microbiology* 2003; **5**:719–729.

188 CDC. Cronobacter Infection and Infants. Centers for Disease Control and Prevention. 2023.https://www.cdc.gov/cronobacter/index.html (accessed 4 Feb2024).

189 James A, Andronis C, Kryovrysanaki N, Goumenaki E, Kalantidis K, Katsarou K. **First Report of Southern Tomato Virus from Tomato (Solanum lycopersicum) in Greece**. *Plant Disease* 2023; **107**:237.

190 Zhang S, Griffiths JS, Marchand G, Bernards MA, Wang A. **Tomato brown rugose fruit virus: An emerging and rapidly spreading plant RNA virus that threatens tomato production worldwide**. *Mol Plant Pathol* 2022; **23**:1262–1277.

191 Takahashi K, Gonzalez G, Kobayashi M, Hanaoka N, Carr MJ, Konagaya M, *et al.* **Pediatric Infections by Human mastadenovirus C Types 2, 89, and a Recombinant Type Detected in Japan between 2011 and 2018**. *Viruses* 2019; **11**:1131.

192 van Zeggeren IE, Edridge AWD, van de Beek D, Deijs M, Koekkoek SM, Wolthers KC, *et al.* **Diagnostic accuracy of VIDISCA-NGS in patients with suspected central nervous system infections**. *Clin Microbiol Infect* 2021; **27**:631.e7-631.e12.

193 Olausson J, Brunet S, Vracar D, Tian Y, Abrahamsson S, Meghadri SH, *et al.* **Optimization of cerebrospinal fluid microbial DNA metagenomic sequencing diagnostics**. *Sci Rep* 2022; **12**:3378.

194 Halary S, Duraisamy R, Fancello L, Monteil-Bouchard S, Jardot P, Biagini P, *et al.* **Novel Single-Stranded DNA Circular Viruses in Pericardial Fluid of Patient with Recurrent Pericarditis**. *Emerg Infect Dis* 2016; **22**:1839–1841.

195 Abeles SR, Robles-Sikisaka R, Ly M, Lum AG, Salzman J, Boehm TK, *et al.* **Human oral viruses are personal, persistent and gender-consistent**. *ISME J* 2014; **8**:1753–1767.

196 Stefanaki C, Bacopoulou F, Chrousos GP. **Gut Microsex/Genderome, Immunity and the Stress Response in the Sexes: An Updated Review**. *Sexes* 2022; **3**:533–545.

197 Henderson M, Pepper N, Bawa M, Muir D, Everitt A, Mackie NE, *et al.* **Cerebrospinal fluid virology in people with HIV**. *HIV Med* 2023; **24**:838–844.

198 Stroffolini G, Guastamacchia G, Audagnotto S, Atzori C, Trunfio M, Nigra M, *et al.* **Low cerebrospinal fluid Amyloid-βeta 1–42 in patients with tuberculous meningitis**. *BMC Neurol* 2021; **21**:449.

199 van der Kall LM, Truong T, Burnham SC, Doré V, Mulligan RS, Bozinovski S, *et al.* **Association of β-Amyloid Level, Clinical Progression, and Longitudinal Cognitive Change in Normal Older Individuals**. *Neurology* 2021; **96**:e662–e670.

200 Mormino EC, Papp KV. **Amyloid accumulation and cognitive decline in clinically normal older individuals: implications for aging and early Alzheimer's disease**. *J Alzheimers Dis* 2018; **64**:S633–S646.

201 Stevens DA, Workman CI, Kuwabara H, Butters MA, Savonenko A, Nassery N, *et al.* **Regional amyloid correlates of cognitive performance in ageing and mild cognitive impairment**. *Brain Commun* 2022; **4**:fcac016.

202 Vojtechova I, Machacek T, Kristofikova Z, Stuchlik A, Petrasek T. **Infectious origin of Alzheimer's disease: Amyloid beta as a component of brain antimicrobial immunity**. *PLoS Pathog* 2022; **18**:e1010929.

203 Mawuenyega KG, Sigurdson W, Ovod V, Munsell L, Kasten T, Morris JC, *et al.* **Decreased clearance of CNS beta-amyloid in Alzheimer's disease**. *Science* 2010; **330**:1774.

204 Vijaya Kumar DK, Choi SH, Washicosky KJ, Eimer WA, Tucker S, Ghofrani J, *et al.* **Amyloid-β Peptide Protects Against Microbial Infection In Mouse and Worm Models of Alzheimer's Disease**. *Sci Transl Med* 2016; **8**:340ra72.

205 Jessen NA, Munk ASF, Lundgaard I, Nedergaard M. **The Glymphatic System – A Beginner's Guide**. *Neurochem Res* 2015; **40**:2583–2599.

206 Kamagata K, Andica C, Takabayashi K, Saito Y, Taoka T, Nozaki H, *et al.* **Association of MRI Indices of Glymphatic System With Amyloid Deposition and Cognition in Mild Cognitive Impairment and Alzheimer Disease**. *Neurology* 2022; **99**:e2648–e2660.

207 Buccellato FR, D'Anca M, Serpente M, Arighi A, Galimberti D. **The Role of Glymphatic System in Alzheimer's and Parkinson's Disease Pathogenesis**. *Biomedicines* 2022; **10**:2261.

208 Reeves BC, Karimy JK, Kundishora AJ, Mestre H, Cerci HM, Matouk C, *et al.* **Glymphatic System Impairment in Alzheimer's Disease and Idiopathic Normal Pressure Hydrocephalus**. *Trends Mol Med* 2020; **26**:285–295.

209 Silva I, Silva J, Ferreira R, Trigo D. **Glymphatic system, AQP4, and their implications in Alzheimer's disease**. *Neurological Research and Practice* 2021; **3**:5.

210 Pedersen EMJ, Köhler-Forsberg O, Nordentoft M, Christensen RHB, Mortensen PB, Petersen L, *et al.* **Infections of the central nervous system as a risk factor for mental disorders and cognitive impairment: A nationwide register-based study**. *Brain, Behavior, and Immunity* 2020; **88**:668–674.

211 Reis PA, Castro-Faria-Neto HC. **Systemic Response to Infection Induces Long-Term Cognitive Decline: Neuroinflammation and Oxidative Stress as Therapeutical Targets**. *Frontiers in Neuroscience* 2022; **15**.https://www.frontiersin.org/articles/10.3389/fnins.2021.742158 (accessed 4 Feb2024).

212 Rizvi ST, Shah JS, Shaaya S, Mollayeva T. **Treating cognitive impairments in primary central nervous system infections: A systematic review of pharmacological interventions**. *Medicine (Baltimore)* 2023; **102**:e34151.

213 Acuña-Hinrichsen F, Covarrubias-Pinto A, Ishizuka Y, Stolzenbach MF, Martin C, Salazar P, *et al.* **Herpes Simplex Virus Type 1 Neuronal Infection Triggers the Disassembly of Key Structural Components of Dendritic Spines**. *Frontiers in Cellular Neuroscience* 2021; **15**.https://www.frontiersin.org/articles/10.3389/fncel.2021.580717 (accessed 16 Aug2023).

214 Boehme M, Guzzetta KE, Wasén C, Cox LM. **The gut microbiota is an emerging target for improving brain health during ageing**. *Gut Microbiome (Camb)* 2023; **4**:E2.

215 Lopatko Lindman K, Hemmingsson E, Weidung B, Brännström J, Josefsson M, Olsson J, *et al.* **Herpesvirus infections, antiviral treatment, and the risk of dementia—a registry-based cohort study in Sweden**. *Alzheimers Dement (N Y)* 2021; **7**:e12119.

216 Devanand DP, Andrews H, Kreisl WC, Razlighi Q, Gershon A, Stern Y, *et al.* **Antiviral therapy: Valacyclovir Treatment of Alzheimer's Disease (VALAD) Trial: protocol for a randomised, double-blind, placebo-controlled, treatment trial**. *BMJ Open* 2020; **10**:e032112.